LUANA MORAES DA LUZ

ON THE FUNCTION OF GUARD CELL TRANSPORTERS IN THE RESPONSE OF *Arabidopsis thaliana* TO CHANGES IN CO_2 AND WATER AVAILABILITY

Thesis presented to the Universidade Federal de Viçosa as part of the requirement of the Plant Physiology Graduate Program for the obtention of the degree of *Doctor Scientiae*.

VIÇOSA
MINAS GERAIS – BRAZIL
2019

Ficha catalográfica preparada pela Biblioteca Central da Universidade Federal de Viçosa - Câmpus Viçosa

T
Luz, Luana Moraes da, 1986-
L978f On the function of guard cell transporters in the response of
2019 *Arabidopsis thaliana* to changes in CO 2 and water availability / Luana Moraes da Luz. – Viçosa, MG, 2019.
viii, 108 f. : il. (algumas color.) ; 29 cm.

Texto em inglês.
Orientador: Wagner Luiz Araújo.
Tese (doutorado) - Universidade Federal de Viçosa.
Inclui bibliografia.

1. *Arabidopsis thaliana. 2.* Estômatos. 3. Água - Uso eficiente. 4. Células - Metabolismo . I. Universidade Federal de Viçosa. Departamento de Biologia Vegetal. Programa de Pós-Graduação em Fisiologia Vegetal. II. Título.

CDD 22. ed. 583.64

LUANA MORAES DA LUZ

ON THE FUNCTION OF GUARD CELL TRANSPORTERS IN THE RESPONSE OF *Arabidopsis thaliana* TO CHANGES IN CO_2 AND WATER AVAILABILITY

Thesis presented to the Universidade Federal de Viçosa as part of the requirement of the Plant Physiology Graduate Program for the obtention of the degree of *Doctor Scientiae*.

APPROVED: February 25th, 2019.

Paula F. Pereira
Paula da Fonseca Pereira

Dimas Mendes Ribeiro
Dimas Mendes Ribeiro

David Barbosa Medeiros

Samuel Cordeiro Vitor Martins
(Co-advisor)

Wagner Luiz Araújo
(Advisor)

ACKNOWLEDGMENTS

Firstly, I am very grateful to God for the strength which made me not give up.

I would like to express my special thanks to my mom Edna, for love, affection, and for your dedication to always helping me. Thank you for the education, especially for the hard wrist and for having forced me to study. And to my father Antonio, by the wise conversations that we have always had and guided me through life, my thank you very much.

I am also grateful to my brother Leandro, for the great protection given to our family and for having given me a pleasant surprise of having my nephew Tayler. I do not know him yet, but my love for him already overflows.

To all my grandparents, uncles, aunts, cousins who together helped me to follow this path.

I would like thanks to the Universidade Federal Rural da Amazônia (UFRA) for the financial support and for having provided my qualification. I am also grateful CAPES for scholarships granting the “Prodoutoral” grant.

I would especially like to thank the Universidade Federal de Viçosa (UFV), mainly to the Plant Physiology Program, for the infrastructure and for all support to carry out my research and extracurricular activities.

Thanks to my great friend Williams Macêdo and Rafaelle Fazzi for having replaced me in the classes. Without the generosity of these people, so soon I would not be here.

Likewise, I would like also to express my deepest thanks to my advisor Wagner Araújo for all the help and patience in carrying out this project together. Thank you for the generosity in listening and for your optimism that always calmed me down. This gave me strength and made me believe that everything would work out. Thank you very much for all your teaching and guidance that made me today conclude this work.

Thanks to the professors that contributed to my knowledge in the classes, especially professors Fabio DaMatta, Marília Ventrella, Elizabeth Fontes, Humberto Ramos, Dimas Ribeiro, Adriano Nunes-Nesi, Juliana Fieto, Claudio Mafra and especially to my co-advisor Prof. Samuel Martins for all contributions to my thesis.

I am also grateful to David Medeiros for the collaboration and assistance in several analyses and data outputs.

Thanks to the "chubbies anonymous" and best friends, Franciele Oliveira Jessica Barros, and Jonas Vargas. I will be eternally grateful for the collaboration and willingness in the days of working as well as so many other better moments together, especially those involving food and games. Friendship is a million little things. Here, you were my family. Thanks a lot!

Thanks to the Technician Rogério Gomide, Robert, and Prof. Adriano Nunes-Nesi for giving me all the support to build my experiments.

I also thank William Batista, Auxiliadora Martins, Jorge Condori and Pablo Nunes for the help in the analyses and for always being willing to help. Thanks to the undergraduate students, Tais, Ana, and Carlinha who helped me in the overwork demanding moments, and especially to Luiz Valente who is also a co-author in the manuscripts from this work. Thanks to Paulete and Elias for facing together the moments of despair in the CO_2 room. Also, to the other colleagues of the “UCP partner Group” for all coexistence and mutual aid, my thank you.

Thanks to my friends from the study moments, Wellington, Franciele, Mirele, James, Raquel, Janaina and Valquiria.

Likewise, I could not forgive to express my thanks to my best friends, Alinne, Iolanda, Tathianne and Valena, who even from away, participated in my life.

I would also like to apologize to all the other people who were not mentioned and who at some point helped me or did me some good. Thank you!

And finally, to Lucas Cavalcante for all love and companionship during these four years. I am deeply grateful for your enormous patience, help, and contributions given to my study. Thank you very much!

TABLE OF CONTENT

ABSTRACT

LUZ, Luana Moraes da, D.Sc., Universidade Federal de Viçosa, February, 2019. **On the function of guard cell transporters in the response of *Arabidopsis thaliana* to changes in CO_2 and water availability**. Advisor: Wagner Luiz Araújo. Co-advisor: Samuel Cordeiro Vitor Martins.

Plants represent the major sources worldwide of human foods and livestock feeds. Thus, future food security will clearly depend on how plant species respond to global environmental changes. Increases in carbon dioxide concentration [CO_2] in the atmosphere and fluctuations in rain patterns are amongst the main climate changes affecting crop yield. Notably, crop yield decreases under drought, yet elevated [CO_2], when associated with drought, may mitigate the negative effects of drought. Among the physiological effects of elevated [CO_2], partial stomatal closure and synergistically increased water use efficiency (*WUE*), leading to higher growth, are usually observed. However, either higher growth or survival of plants under high [CO_2] will directly depend on the degree of water availability into the soil. Water losses are controlled directly by the stomata, functionally specialized microscopic pores in leaf surface, that regulates the flow of gases between plants and atmosphere. Accordingly, stomata are the key entry point for CO_2 assimilation and water losses, controlling the essential exchange of CO_2 and H_2O with the environment in land plants. Stomatal movements occur in response to the activation and inactivation of membrane proteins present in the guard cells. The relationship between stomatal aperture and photosynthesis/transpiration is linear over a wide range of environmental conditions. Thus, a better understanding of stomatal regulation by environmental stimuli represents an important step for developing plants in which *WUE* and photosynthesis capacity are optimized, once the maintenance of photosynthesis, one of the main events of the primary metabolism, and its capacity may directly influence crop yield. This thesis is largely focused on the role of proteins involved in the stomatal movements in response to changes in both [CO_2] and water availability. To this end, two stomatal proteins in *Arabidopsis thaliana*, namely the slow-type anion channel (SLAC1) and the ATP-binding cassette B14 transporter (ABCB14) were used to further investigate the duality of the efficiency between the CO_2 influx and the water efflux by the stomata under elevated [CO_2] and water limitation. SLAC1 is considered a key protein for stomatal closure in response to drought and [CO_2], while ABCB14 is the sole influx transporter of malate of the guard cell and is only responsive to increased CO_2. The main goal of this study is to increase our understanding of the stomatal regulation in response to a realistic future climate change scenario using a metabolic, physiological, anatomical and molecular characterization of mutant plants with opposite stomatal responses. First, our results demonstrated that *slac1* mutant plants are seemingly constantly under stress effect, regardless of the water restriction, since to sustain the increased stomatal conductance (g_s) *slac-1* mutant plants display an elegant metabolic reprogramming that is apparently crucial for growth survival under moderate water limitation. Here we further hypothesized that ABCB14 may play an important role while allowing a modest stomatal opening that may be essential for continuity of gas exchanges under high [CO_2] conditions. In the second part, it was demonstrated that despite the reductions in the stomatal opening, the absence of a functional guard cell ABCB14 protein does not compromise overall photosynthetic activity and growth and that an exquisite metabolic and genetic regulation occurs in guard cells likely compensating, at least partially, the functional lack of *abcb14*. The data obtained here are discussed in the context of the role of each guard cell transport both generally to guard cell and photosynthetic metabolism and specifically with respect to its function in the regulation of stomatal aperture.

RESUMO

LUZ, Luana Moraes da, D.Sc., Universidade Federal de Viçosa, fevereiro de 2019.
Função de transportadores de células-guarda na resposta de *Arabidopsis thaliana* às mudanças na concentração de CO_2 e disponibilidade de água. Orientador: Wagner Luiz Araújo. Coorientador: Samuel Cordeiro Vitor Martins.

As plantas representam as principais fontes mundiais de alimentos e rações para animais. Assim, a segurança alimentar futura dependerá claramente de como as espécies de plantas respondem às mudanças ambientais globais. O aumento da concentração de CO_2 [CO_2] na atmosfera e as flutuações nos padrões de chuva estão entre as principais mudanças climáticas que afetam o rendimento das culturas. Notavelmente, o rendimento das culturas diminui sob a seca, ainda que a elevada [CO_2], quando associado à seca, pode mitigar os efeitos negativos da seca. Entre os efeitos fisiológicos do elevado [CO_2], o fechamento parcial dos estômatos e o aumento sinérgico da eficiência do uso da água (*WUE*), levando a um maior crescimento, são geralmente observados. No entanto, o crescimento mais alto ou a sobrevivência de plantas sob alta [CO_2] dependerão diretamente do grau de disponibilidade de água no solo. As perdas de água são controladas diretamente pelos estômatos, poros microscópicos funcionalmente especializados na superfície foliar, que regulam o fluxo de gases entre as plantas e a atmosfera. Assim, os estômatos são o principal ponto de entrada para a assimilação de CO_2 e as perdas de água, controlando as trocas essenciais de CO_2 e H_2O com o meio ambiente nas plantas terrestres. Os movimentos estomáticos ocorrem em resposta à ativação e inativação de proteínas de membrana presentes nas células-guarda. A relação entre a abertura estomática e a fotossíntese / transpiração é linear em uma ampla gama de condições ambientais. Assim, uma melhor compreensão da regulação estomática por meio de estímulos ambientais representa um passo importante para o desenvolvimento de plantas em que a capacidade de fotossíntese e *WUE* é otimizada, uma vez que a manutenção da fotossíntese, um dos principais eventos do metabolismo primário, e sua capacidade pode influenciar diretamente a produção de cultura agrícolas. Esta tese está amplamente focada no papel das proteínas envolvidas nos movimentos estomáticos em resposta a mudanças na disponibilidade de [CO_2] e na disponibilidade de água. Para este fim, duas proteínas estomáticas de *Arabidopsis thaliana*, nomeadamente slow-type anion channel (SLAC1) e o transportador ATP-binding cassette B14 (ABCB14) foram utilizadas para investigar a dualidade da eficiência entre o influxo de CO_2 e o efluxo de água pelos estômatos sob elevado [CO_2] e limitação de água. O SLAC1 é considerado uma proteína chave para o fechamento estomático em resposta à seca e [CO_2], enquanto o ABCB14 é o único transportador de influxo de malato das células-guarda e responde apenas ao aumento de CO_2. O principal objetivo deste estudo é aumentar nossa compreensão da regulação estomática em resposta a um cenário realista de mudanças climáticas futuro, utilizando uma caracterização metabólica, fisiológica, anatômica e molecular de plantas mutantes com respostas estomaticas opostas. Primeiro, nossos resultados demonstraram que as plantas mutantes de *slac1* aparentemente estão constantemente sob efeito de estresse, independentemente da restrição hídrica, pois as plantas mutantes *slac1* ao sustentar maiores condutâncias estomáticas (g_s), exibem uma elegante reprogramação metabólica que é aparentemente crucial para a sobrevivência do crescimento sob moderada limitação hídrica. Aqui, hipotetizamos ainda que o ABCB14 pode desempenhar um papel importante, ao mesmo tempo em que permite uma modesta abertura estomática que pode ser essencial para a continuidade das trocas gasosas sob condições de elevada [CO_2]. Segundo, demonstrou-se que, apesar das reduções na abertura estomática, a ausência da proteína ABCB14 de célula guarda não compromete a atividade fotossintética geral e o crescimento e que uma regulação genética e metabólica ocorre em células-guarda provavelmente compensando, pelo menos parcialmente, a falta funcional de ABCB14. Os dados obtidos são discutidos no contexto do papel de cada transporte de células de guarda, tanto emcélulas-guarda e metabolismo fotossintético e, especificamente, em relação à sua função na regulação da abertura estomática.

GENERAL INTRODUCTION

Plants represent the major sources worldwide of human foods and livestock feeds. Thus, future food security will clearly depend on how plant species respond to global environmental changes. Therefore, it is not surprising, that the acclimation mechanisms of plants under future realistic climate scenarios, such as increased climatic atmospheric [CO_2] and water limitation, are currently intensively investigated. Increased [CO_2] in the atmosphere and fluctuations in rain patterns are amongst the main climatic changes affecting crop yield (Lobell et al., 2011; Peñuelas et al., 2013; Ruiz-Vera et al., 2013; IPCC, 2014; Bagley et al., 2015). In this context, it is estimated that, due to current human activities, the current concentration of CO_2 (~400 ppm) could reach ~ 900 ppm by the end of the 21st century in parallel with increases in temperature of up to 5.0 °C if global greenhouse gas emissions continue (IPCC, 2013).

Stomata, functionally specialized microscopic pores surrounded by two guard cells in the leaf epidermis, regulates the flow of gases between plants and atmosphere. Accordingly, stomata are the key entry point for CO_2 assimilation and water losses, controlling the essential exchange of CO_2 and H_2O with the environment in land plants. Several environmental cues such as light quantity/ quality, CO_2 concentration, relative humidity and vapour pressure deficit induce changes in stomatal aperture throughout the diel course (Merilo et al., 2013, 2015; Aliniaeifard and van Meeteren, 2013; Creese et al., 2014; Wang et al., 2017).

The relationship between stomatal aperture and photosynthesis/transpiration is linear over a wide range of environment conditions (Gago et al, 2016). Indeed, it seems reasonable to assume that C3 photosynthesis improvements can be achieved by modifying stomatal behaviour (Lawson et al., 2014; Flexas, 2016). That being said, a better understanding of stomatal regulation and how it is influenced by the surrounding mesophyll cells and environmental stimuli represents an important step for developing plants with enhanced water use efficiency (*WUE*) (Gago et al., 2016; Lawson et al., 2014; Flexas, 2016). Since stomata movements are of pivotal significance for the overall crop yield, their genetic manipulation may allow enhanced *WUE* and soil moisture conservation (Leakey et al., 2006; Bernacchi et al., 2007).

It is widely accepted that elevated [CO_2] not only promotes reductions in g_s (Ainsworth et al., 2002; Rogers et al., 2004; Bernacchi et al., 2006, 2007), but also increases net photosynthesis rate (*A*$_N$), growth rate and biomass in several species (Curtis e Wang, 1998; Long et al., 2004; Nowak et al., 2004; Ainsworth e Long, 2005; Ainsworth e Rogers, 2007), a fact that only not occurs when there is an acclimation response. It has been reported that the enhancement of *A*$_N$ does not persist and it declines below its maximum potential after a long time under high CO_2, in a process described as acclimatization (Jifon and Wolfe, 2002; Long et al., 2004; Rosenthal et al., 2014). During this process, in response to the reduction of V_{cmax}, J_{max} (Ainsworth and Long, 2005; Bernacchi et al., 2005), decreased leaf rubisco content and total nitrogen concentration (Stitt and Krapp, 1999, Long et al., 2004; Gutierrez et al., 2013) are also observed. Notwithstanding, elevated [CO_2], when associated with drought episodes, may mitigate the negative effects in plants (Araus et al, 2002; Zinta et al., 2014). It is important to mention that crop yield may decrease under a combination of high [CO_2] and severe drought (Leakey et al., 2012). Thus, either higher growth or survival of plants under elevated [CO_2] will be directly dependent on the degree of water limitation (Poorter and Perez-Soba, 2001; Ameye et al., 2012; Bauweraerts et al., 2013; Naudts et al., 2013).

It has been recently demonstrated that in response to soil drying stomatal closure is one of the initial events (Osakabe et al., 2014, Pustovoitova et al., 2003; Antonio et al., 2008; Maurel et al., 2016; Pinheiro et al., 2019), but it is reasonable to suggest that many other metabolic adjustments may also occur. For instance, under moderate water limitation, carbon metabolism is altered, as depicted by changes in CO_2 assimilation as well as in sucrose and starch synthesis and allocation (Pinheiro et al., 2011; Bechtold et al., 2016). In addition, water deficit is usually associated with increases in the content of sucrose, glucose, fructose (Rizhsky et al., 2004; Mane et al., 2008; Fumagalli et al., 2009), proline (Rizhsky et al., 2004; Lugan et al., 2009), phenolic compounds (Rivas-Ubach et al., 2012), and organic acids (Naya et al., 2007; Fumagalli et al., 2009; Sanchez et al., 2012). Moreover, water limitation is also accompanied by increased levels of sulfate transporter proteins and the expression of genes related to stomatal control (Cuming et al., 2007; Foito et al., 2009; Aubert et al., 2010; Cohen et al., 2010; Batool et al., 2018).

Although several changes in the metabolism are expected under water limitation, the maintenance of photosynthesis is of crucial importance, since it is one of the main events of the primary metabolism, and its capacity may directly influence crop yield (Lawlor and Tezara, 2009; Pinheiro e Chaves, 2011). Indeed, there are two biochemical processes that limit the photosynthesis, the maximum rate of carboxylation capacity of Rubisco (V_{cmax}) and the rate of regeneration of RuBP associated with the maximum linear electron flux via photosystem II (J_{max}) (Wong, 1979; Sage et al., 1989; Tissue et al., 1993; Vu et al., 1997; Sims et al., 1998). Decreases in V_{cmax} are positively correlated with g_s and chloroplastidic CO_2 concentration (C_c), suggesting that the deactivation of Rubisco sites could be induced by low C_c as a result of water stress (Flexas et al., 2004; Galmés et al., 2010). Therefore, decreased CO_2 diffusion from the atmosphere to the carboxylation site is considered the main cause of decreased photosynthesis under mild to moderate water limitation (Chaves et al., 2003, 2009; Grassi and Magnani, 2005). Thus, it seems that the biochemical component of the photosynthetic limitations is relatively less imposed by the stomata than the diffusive limitation (Galmés et al., 2007; Flexas et al., 2008). This fact apart, stomatal pores, which are structurally simple, are surrounded by guard cells, one of the most specialized cell types in land plants (Bergmann and Sack, 2007). It is equally important to mention that stomatal are morphologically different from other epidermal cells. Perhaps, most importantly, stomatal movements are regulated by an exquisite signal transduction network, containing both a tightly regulated membrane ion transport system, and specialized metabolic pathways that are able to finally modulate guard cell turgor, subsequently, promoting stomatal opening and closure (Santelia and Lawson, 2016).

Stomatal pores open in response to increases in guard cell volume generated by reductions in water potential (Ψ_w) of the guard cell as a result of the osmolytes accumulation and subsequently water influx. On the other hand, during stomatal closure, an efflux of osmolytes from guard cells is required with an associated increase in guard cell Ψ_w and in turn water efflux (Assmann and Wang, 2001). Stomatal movements occur in response to the activation and inactivation of membrane proteins present in the guard cells. These proteins are responsible for the transport of molecules and ions between the guard cell cytosol and the mesophyll. In the presence of light, activation of channels carrying ions to the cytosol occurs (Ueno et al., 2005; Van and Raschke, 1978; Schroeder et al., 2001; Kim et al., 2010; Vahisalu et al., 2010). Potassium (K^+) and chloride (Cl^-) act as the main inorganic ions, while malate and sucrose are considered as the main organic osmolytes associated with stomatal movements (Amodeo et al., 1996; Kelly et al., 2013; Santelia and Lawson, 2016; Daloso et al., 2016; Inoue and Kinoshita, 2017; Medeiros et al., 2018).

Layout and aims of the chapters

This thesis is largely focused on the role of proteins involved in the stomatal movements in response to changes in both [CO_2] and water availability. Among the proteins involved in the transport of molecules for stomatal movement, this work is focused on the use of mutants of two stomatal proteins in *Arabidopsis thaliana*, SLAC1 (*slac1-3* and *slac1-4*) and ABCB14 (*abcb14-1* and *abcb14-2*). The main goal of this study is to increase our understanding of the stomatal regulation in response to a realistic future climate change scenario using a metabolic, physiological, anatomical and molecular characterization of mutant plants with opposite stomatal responses. Increases in atmospheric [CO_2] and water restrictions are known to individually have effects on plant development and metabolism, but their interactive effects have not been largely investigated under restrictive conditions.

Here, a combination of physiological, metabolic, and biochemical approaches was undertaken to understand how and to which extent changes in stomatal conductance caused by the specific mutations affect plant responses to [CO_2] and water availability. To this end, two mutants were used to further investigate the duality of the efficiency between the CO_2 influx and the water efflux by the stomata under elevated [CO_2] and water limitation. SLAC1 is considered a key protein for stomatal closure in response to drought and [CO_2] (Negi et al., 2008; Vahisalu et al., 2008), while ABCB14 is the sole influx transporter of malate of the guard cell and is only responsive to increased CO_2 (Lee et al., 2008). It was hypothesized that *slac1* plants will present higher g_s and will be lower sensitive to [CO_2] and water restriction, whereas *abcb14* plants will present lower g_s under elevated [CO_2]. To clarify this, water restriction was imposed as much as capable of affecting stomatal conductance without being drastic enough to paralyze growth. This approach was taken to answer the following questions: (*i*) independent of the growth condition, will the greater g_s of *slac1* promote higher A_N and growth? (ii) Does the reduced g_s of *abcb14* mutant plants under high [CO_2] allow the maintenance of A_N and greater *WUE* under water restriction?

CHAPTER 1: Enhanced stomatal aperture due to the functional lack of SLAC1 modifies guard cell metabolism without impacting photosynthesis under elevated [CO_2] and moderated water restriction

A coupled regulation of photosynthesis and *WUE* is directly influenced by the aperture of the stomatal pore, which is actively regulated by the metabolism of the surrounding guard cells. In *Arabidopsis*, the ABA-sensitive channel is the SLAC1 that plays a central role in the control of stomatal closure and higher *WUE*. Mutant plants with loss of SLAC1 function showed a lower sensitivity to ABA, compromising stomatal closure in response to CO_2 and drought. Thus, our main goal was to investigate the independent and combined effects of elevated CO_2 and water limitation by comparing plants with a constitutive increase of the stomatal opening (*slac1* mutant plants) with *Arabidopsis thaliana* wild type (WT) plants. Our results demonstrated that *slac1* mutant plants are seemingly constantly under stress effect, regardless of the water restriction, since to sustain the increased g_s *slac-1* mutant plants display an elegant metabolic reprogramming that is apparently crucial for growth survival under moderate water limitation.

CHAPTER 2: The functional lack of ABCB14 impacts stomatal responses but does not compromise photosynthetic capacity and growth under elevated [CO_2] and water restriction

Water limitation is one of the most factors influencing plant productivity. Simultaneously, the future higher levels of atmospheric CO_2, will likely also affect plant growth and development. As well as both water limitation and high [CO_2] are known to show distinct effects when each factor is applied separately. Thus, here we hypothesized that ABCB14 may play an important role while allowing a modest stomatal opening that may be essential for continuity of gas exchanges under high [CO_2] conditions. Our results demonstrate that despite the reductions in the stomatal opening, the absence of a functional guard cell ABCB14 protein does not compromise overall photosynthetic activity and growth and that an exquisite metabolic and genetic regulation occurs in guard cells likely compensating, at least partially, the functional lack of *abcb14*.

During the increase of [CO_2], SLAC1 and ABCB14 are activated, but they work by transporting ions in opposite directions. While SLAC1 is activated for the transport of chloride (Cl^{-2}) and nitrate (NO^{-3}) from the cytosol to the apoplast, ABCB14 is activated for the transport of malate from apoplast to the cells of guards (Negi et al., 2008; Vahisalu et al., 2008, Lee et al., 2008). The transport performed by SLAC1 induces stomatal closure, while transport of malate by ABCB14 keeps the stomata partially open. Thus, SLAC1 operation is essential for reducing water loss, while ABCB14 allows the CO_2 entry. It is important to point out that previous works have contributed to our understanding of SLAC1 and ABCB14. However, the metabolic impact of changes in stomatal conductance caused mutations in the genes encoding SLAC1 and ABCB14 was not comprehensively evaluated. The reason for working with the two mutations is to investigate the duality of the efficiency between the CO_2 input amplitude and the water output by the stomata under high water restriction and [CO_2]. Thus, *slac1* plants present higher g_s and are lower sensitive to [CO_2] and water restriction, while *abcb14* plants will have lower g_s under high [CO_2]. As the imposed water restriction can affect g_s without being drastic enough to paralyze growth, we tried to answer the following questions: *(i)* independent of the condition, will the greater g_s of *slac1* promote higher A_N and growth? *(ii)* Does the reduced g_s of plants *abcb14* under high [CO_2] allow to maintain A_N and greater *WUE* under water restriction? Thus, the present study aimed to investigate the importance of stomatal conductance in a future climate change scenario using a metabolic, physiological, anatomical and molecular characterization of mutant plants with opposite functions in *WUE*.

REFERENCES

Ainsworth EA, Rogers A (2007) The response of photosynthesis and stomatal conductance to rising [CO_2]: Mechanisms and environmental interactions, Plant Cell Environ 30: 258-270

Ainsworth EA, Davey PA, Bernacchi CJ, Dermody OC, Heaton EA, Moore DJ, Morgan PB, Naidu SL, Yoo Ra HS, Zhu XG, Curtis PS, Long SP (2002) A meta analysis of elevated [CO_2] effects on soybean (Glycine max) physiology, growth, and yield. Glob Change Biol 8: 695-709

Ainsworth EA, Long SP (2005) What have we learned from 15 years of free air CO_2 enrichment (FACE)? A meta-analytic review of the responses of photosynthesis, canopy properties and plant production to rising CO_2. New Phytologist 165: 351-371

Aliniaeifard S, van Meeteren U (2013) Can prolonged exposure to low VPD disturb the ABA signaling in stomatal guard cells? Journal Experimental Botany. 64: 3551-66

Ameye M, Wertin TM, Bauweraerts I, Mcguire MA, Teskey RO, Steppe K (2012) The effect of induced heat waves on *Pinus taeda* and *Quercus rubra* seedlings in ambient and elevated CO_2 atmospheres. New Phytologist 196: 448-461

Amodeo G, Talbott LD, Zeiger E (1996) Use of potassium and sucrose by onion guard cells during a daily cycle of osmoregulation. Plant Cell Physiology 37: 575-579

Antonio C, Pinheiro C, Chaves MM, Ricardo CP, Ortuno MF, Thomas-Oates J (2008) Analysis of carbohydrates in *Lupinus albus* stems on imposition of water deficit, using porous graphitic carbon liquid chromatography–electrospray ionization mass spectrometry. Journal of Chromatography A 1187: 111-118

Araus JL, Slafer GA, Reynolds MP, Royo C (2002) Plant breeding and drought in C-3 cereals, what should we breed for? Annual Botany 89: 925-40

Assmann SM, Wang XQ (2001) From milliseconds to millions of years: guard cells and environmental responses. Curr Opin Plant Biol 4: 421–428

Aubert Y, Vile D, Pervent M, Aldon D, Ranty B, Simonneau T, Vavasseur A, Galaud JP (2010) RD20, a stress-inducible caleosin, participates in stomatal control, transpiration and drought tolerance in *Arabidopsis thaliana*. Plant and Cell Physiology 51: 1975-1987

Bagley J, Rosenthal DM, Ruiz-Vera UM, Siebers MH, Kumar P, Ort DR, Bernacchi CJ (2015) The influence of photosynthetic acclimation to rising CO_2 and warmer temperatures on leaf and canopy photosynthesis models. Global Biogeochemical Cycles 29: 194-206

Batool S, Uslu VV, Rajab H, Ahmad N, Waadt R, Geiger D, Malagoli M, Xiang CB, Hedrich R, Rennenberg H, Herschbach C, Hell R, Wirtz M (2018) Sulfate is incorporated into cysteine to trigger ABA production and stomata closure. The Plant Cell 30: 2973-2987

Bauweraerts I, Wertin TM, Ameye M, Mcguire MA, Teskey RO, Steppe K (2013) The effect of heat waves, elevated CO_2 and low soil water availability on northern red oak (*Quercus rubra* L.) seedlings. Global Change Biology 19: 517-528

Bechtold U, Penfold CA, Jenkins DJ, Legaie R, Moore JD, Lawson T, Matthews JS, Vialet-Chabrand SR, Baxter L, Subramaniam S, Hickman R, Florance H, Sambles C, Salmon DL, Feil R, Bowden L, Hill C, Baker NR, Lunn JE, Finkenstädt B, Mead A, Buchanan-Wollaston V, Beynon J, Rand DA, Wild DL, Denby KJ, Ott S, Smirnoff N, Mullineaux PM (2016) Time-series transcriptomics reveals that AGAMOUS-LIKE22 affects primary metabolism and developmental processes in drought-stressed *Arabidopsis*. Plant Cell 28: 345-366

Bergmann DC, Sack FD (2007) Stomatal development. Annual Review of Plant Biology 58: 163-181

Bernacchi CJ, Kimball BA, Quarles DR, Long SP, Ort DR (2007) Decreases in stomatal conductance of soybean under open air elevation of [CO_2] are closely coupled with decreases in ecosystem evapotranspiration. Plant Physiology. 143: 134-144

Bernacchi CJ, Morgan PB, Ort DR, Long SP (2005) The growth of soybean under free air CO_2 enrichment (FACE) stimulates photosynthesis while decreasing in vivo Rubisco capacity. Planta 220: 434-446

Chaves MM, Flexas J, Pinheiro C (2009) Photosynthesis under drought and salt stress: regulation mechanisms from whole plant to cell. Annals of Botany 103: 551-560

Chaves MM, Pereira JS, Maroco J (2003) Understanding plant response to drought from genes to the whole plant. Functional Plant Biology 30: 239-264

Cohen D, Bogeat-Triboulot MB, Tisserant E, Balzergue S, Martin-Magniette ML, Lelandais G, Ningre N, Renou JP, Tamby JP, Le Thiec D, Hummel I (2010) Comparative transcriptomic of drought responses in *Populus*: a meta-analysis of genome-wide expression profiling in mature leaves and root apices across two genotypes. BMC Genomics 11: 630

Creese C1, Oberbauer S, Rundel P, Sack L (2014) Are fern stomatal responses to different stimuli coordinated? Testing responses to light, vapor pressure deficit, and CO_2 for diverse species grown under contrasting irradiances. New Phytol 204: 92-104

Cuming AC, Cho SH, Kamisugi Y, Graham H, Quatrano RS (2007) Microarray analysis of transcriptional responses to abcisic acid and osmotic, salt, and drought stress in the moss, Physcomitrella patens. New Phytologist 176: 275-287

Curtis PS, Wang X (1998) A meta-analysis of elevated CO_2 effects on woody plant mass form and physiology. Oecologia 113: 299-313

Daloso DM, Williams TCR, Antunes WC, Pinheiro DP, Müller C, Loureiro ME, Fernie AR (2016) Guard cell-specific upregulation of sucrose synthase 3 reveals that the role of sucrose in stomatal function is primarily energetic. New Phytologist 209: 1470-1483

Flexas J, Bota J, Loreto F, Cornic G, Sharkey TD (2004) Diffusive and metabolic limitations to photosynthesis under drought and salinity in C3 plants. Plant Biology 6: 269-279

Flexas J, Diaz-Espejo A, Conesa MA, Coopman RE, Douthe C, Gago J, Galle A, Galmes J, Medrano H, Ribas-Carbo M, Tomas M, Niinemets U (2016) Mesophyll conductance to CO_2 and rubisco as targets for improving intrinsic water use efficiency in C3 plants. Plant, Cell and Environment 39: 965-982

Flexas J, Ribas-Carbo M, Diaz-Espejo A, Galmés J, Medrano H (2008) Mesophyll conductance to CO_2: current knowledge and future prospects. Plant, Cell and Environment 31: 602-612

Foito A, Byrne SL, Shepherd T, Stewart D, Barth S (2009) Transcriptional and metabolic profiles of Lolium perenne L. genotypes in response to a PEG-induced water stress. Plant Biotechnology Journal 7: 719-732

Fumagalli E, Baldoni E, Abbruscato P, Piffanelli P, Genga A, Lamanna R, Consonni R (2009) NMR techniques coupled with multivariate statistical analysis: tools to analyse *Oryza sativa* metabolic content under stress conditions. Journal of Agronomy and Crop Science 195: 77-88

Gago J, Daloso D de M, Figueroa CM, Flexas J, Fernie AR, Nikoloski Z (2016) Relationships of Leaf Net Photosynthesis, Stomatal Conductance, and Mesophyll Conductance to Primary Metabolism: A Multispecies Meta-Analysis Approach. Plant Physiology 171: 265-79

Galmé J, Ribas-Carbó M, Medrano H, Flexas J (2010) Rubisco activity in Mediterranean species is regulated by the chloroplastic CO_2 concentration under water stress. Journal of Experimental Botany 62: 653-665

Galmés J, Medrano H, Flexas J (2007) Photosynthetic limitations in response to water stress and recovery in Mediterranean plants with different growth forms. New Phytologist 175: 81-93

Grassi G, Magnani F (2005) Stomatal, mesophyll conductance and biochemical limitations to photosynthesis as affected by drought and leaf ontogeny in ash and oak trees. Plant, Cell and Environment 28: 834-849

Gutiérrez D, Morcuende R, Del Pozo A, Martínez-Carrasco R, Pérez P (2013) Involvement of nitrogen and cytokinins in photosynthetic acclimation to elevated CO_2 of spring wheat. Journal Plant Physiology 170: 1337-43

Inoue S, Kinoshita T (2017) Blue light regulation of stomatal opening and the plasma membrane H+-ATPase. Plant Physiol. 174: 531-538

IPCC. Climate change 2013: the physical science basis. In: Stocker TF, Qin D, Plattner G-K, Tignor M, Allen SK, Boschung J, Nauels A, Xia Y, Bex V, Midgley PM, eds. Contribution of working group I to the fifth assessment report of the Intergovernmental Panel on Climate Change. Cambridge, UK and New York, NY, USA: Cambridge University Press

IPCC. Climate change 2014: Mitigation of climate change. Contribution of Working Group III to the fifth assessment report of the Intergovernmental Panel on

Climate Change. Cambridge University Press, Cambridge, UK and New York, NY, USA

Jifon JL, Wolfe DW (2002) Photosynthetic acclimation to elevated CO_2 in Phaseolus vulgaris L. is altered by growth response to nitrogen supply. Global Change Biology 8: 1018-1027

Kelly G, Moshelion M, David-Schwartz R, Halperin O, Wallach R, Attia Z, Belausov E, Granot, D (2013) Hexokinase mediates stomatal closure. Plant Journal 75: 977-988

Kim TH, Böhmer M, Hu H, Nishimura N and Schroeder JI (2010) Guard Cell Signal Transduction Network: Advances in Understanding Abscisic Acid, CO_2, and Ca^{2+} Signaling. Annual Review of Plant Biology 61: 561-591

Lawlor DW, Tezara W (2009) Causes of decreased photosynthetic rate and metabolic capacity in water-deficient leaf cells: a critical evaluation of mechanisms and integration of processes. Annals of Botany 103: 561-579

Lawson T, Simkin AJ, Kelly G, Granot D (2014) Mesophyll photosynthesis and guard cell metabolism impacts on stomatal behaviour. New Phytologist 203: 1064-81

Leakey ADB, Bishop KA, Ainsworth EA (2012) A multi-biome gap in understanding of crop and ecosystem responses to elevated CO_2. Current Opinion in Plant Biology 15: 228-236

Leakey ADB, Uribelarrea M, Ainsworth EA, Naidu SL, Rogers A, Ort DR, Long SP (2006) Photosynthesis, productivity and yield of maize are not affected by open-air elevation of CO_2 concentration in the absence of drought. Plant Physiology 140: 779-790

Lee M, Choi Y, Burla B, Kim YY, Jeon B, Maeshima M, Yoo JY, Martinoia E, Lee Y (2008) The ABC transporter *At*ABCB14 is a malate importer and modulates stomatal response to CO_2. Nature Cell Biology 10: 1217-1223

Lobell, DB, Schlenker W and Costa-Roberts J (2011) Climate trends and global crop production since 1980. Science 333: 616-620

Long SP, Ainsworth EA, Rogers A, Ort DR (2004) Rising atmospheric carbon dioxide: plants face the future. Annual Review of Plant Biolology 55: 591-628

Lugan R, Niogret MF, Kervazo L, Larher FR, Kopka J, Bouchereau A (2009) Metabolome and water status phenotyping of *Arabidopsis* under abiotic stress cues reveals new insight into ESK1 function. Plant Cell and Environment 32: 95-108

Mane SP, Robinet CV, Ulanov A, Schafleitner R, Tincopa L, Gaudin A, Nomberto G, Alvarado C, Solis C, Bolivar LA, Blas R, Ortega O, Solis J, Panta A, Rivera C, Samolski I, Carbajulca DH, Bonierbale M, Pati A, Heath LS, Bohnert HJ, Gren, R (2008) Molecular and Physiological adaptation to prolonged drought stress in the leaves of two Andean patato Genotype. Functional Plant Biology 35: 669-688

Maurel C, Verdoucq L, Rodrigues O (2016) Aquaporins and plant transpiration. Plant Cell and Environment 39: 2580-2587

Medeiros DB, Perez Souza L, Antunes WC, Araújo WL, Daloso DM, Fernie AR (2018) Sucrose breakdown within guard cells provides substrates for glycolysis and glutamine biosynthesis during light-induced stomatal opening. Plant Journal 94: 583-594

Merilo E, Jalakas P, Kollist H, Brosché M (2015) The role of ABA recycling and transporter proteins in rapid stomatal responses to reduced air humidity, elevated CO_2, and exogenous ABA. Molecular Plant 8: 657-9

Merilo E, Laanemets K, Hu H, Xue S, Jakobson L, Tulva I, Gonzalez-Guzman M, Rodriguez PL, Schroeder JI, Broschè M, Kollist H (2013) PYR/RCAR Receptors Contribute to Ozone, Reduced Air Humidity, Darkness, and CO_2Induced Stomatal Regulation. Plant Physiology 162: 1652-1668

Naudts K, Van Den Berge J, Janssens IA, Nijs I, Ceulemans R (2013) Combined effects of warming and elevated CO_2 on the impact of drought in grassland species. Plant and Soil 369: 497-507

Naya L, Ladrera R, Ramos J, Gonzalez EM, Arrese-Igor MF, Becana M (2007) The response of carbon metabolism and antioxidant defenses of alfalfa nodules to drought stress and to the subsequent recovery of plants. Plant Physiology 144: 1104-1114

Negi J, Matsuda O, Nagasawa T, Oba Y, Takahashi H, Kawai-Yamada M, Uchimiya H, Hashimoto M, Iba K (2008) CO_2 regulator SLAC1, and its homologues are essential for anion homeostasis in plant cells. Nature 452: 483-486

Nowak RS, Ellsworth DS, Smith SD (2004) Functional responses of plants to elevated atmospheric CO_2 - Do photosynthetic and productivity data from FACE experiments support early predictions? New Phytologist. 162: 253-280

Osakabe Y, Yamaguchi-Shinozaki K, Shinozaki K, Tran, LSP (2014) ABA control of plant macroelement membrane transport systems in response to water deficit and high salinity. New Phytologist 202: 35-49

Peñuelas J, Sardans J, Estiarte M, Ogaya R, Carnicer J, Coll M, Barbeta A, Rivas-Ubach A, Llusià J, Garbulsky M, Filella I, Jump AS (2013) Evidence of current impact of climate change on life: a walk from genes to the biosphere. Global Change Biology 19: 2303-2338

Pinheiro C, Chaves M (2011) Photosynthesis and drought: can we make metabolic connections from available data? Journal of Experimental Botany 62: 869-882

Pinheiro C, Dickinson E, Marriott A, Ribeiro IC, Pintó-Marijuan M4,5, António C, Zarrouk O, Chaves MM, Dodd IC, Munné-Bosch S, Thomas-Oates J, Wilson J (2019) Distinctive phytohormonal and metabolic profiles of *Arabidopsis thaliana* and *Eutrema salsugineum* under similar soil drying.

Poorter H, Perez-Soba M (2001) The growth response of plants to elevated CO_2 under non-optimal environmental conditions. Oecologia 129: 1-20

Pustovoitova TN, Drozdova IS, Zhdanova NE Zholke-vich VN (2003) Leaf growth, photosynthetic rate and phytohormone contents in Cucumis sativus plants under progressive soil drought. Russian Journal of Plant Physiology 50: 441-443

Rivas-Ubach A, Sardans J, Perez-Trujillo M, Estiarte M, Peñuelas J (2012) Strong relationship between elemental stoichiometry and metabolome in plants. Proceedings of the National Academy of Sciences of the United States of America 109: 4181-4186

Rizhsky L, Liang HJ, Shuman J, Shulaev V, Davletova S, Mittler R (2004) When defense pathways collide. The response of *Arabidopsis* to a combination of drought and heat stress. Plant Physiology 134: 1683-1696

Rogers A, Allen DJ, Davey PA, Morgan PB, Ainsworth EA, Bernacchi CJ, Cornic G, Dermody O, Dohleman FG, Heaton EA, Mahoney J, Zhu XG, Delucia EH, Ort DR, Long SP (2004) Leaf photosynthesis and carbohydrate dynamics of soybeans grown throughout their life-cycle under free-air carbon dioxide enrichment. Plant Cell and Environment 27: 449-458

Rosenthal DM, Ruiz-Vera UM, Siebers MH, Gray SB, Bernacchi CJ, Ort DR (2014) Biochemical acclimation, stomatal limitation and precipitation patterns underlie decreases in photosynthetic stimulation of soybean (Glycine max) at elevated [CO_2] and temperatures underfully open air field conditions. Plant Sciense 226: 136-46

Ruiz-Vera UM, Siebers M, Gray SB, Drag DW, Rosenthal DM, Kimball BA, Ort DR, Bernacchi CJ (2013) Global warming can negate the expected CO_2 stimulation in photosynthesis and productivity for soybean grown in the Midwestern United States. Plant Physiology 162: 410-423

Sage RF, Sharkey TD, Seemann JR (1989) Acclimation of photosynthesis to elevated CO_2 in five C3 species. Plant Physiology 89: 590-596

Sanchez DH, Schwabe F, Erban A, Udvardi MK, Kopka J (2012) Comparative metabolomics of drought acclimation in model and forage legumes. Plant Cell and Environment 35: 136-149

Santelia D, Lawson T (2016) Rethinking guard cell metabolism. Plant Physiology 172: 1371-1392

Schroeder JI, Allen GJ, Hugouvieux V, Kwak JM, Waner D (2001) Guard cell signal transduction. Annual Review of Plant Physiology and Plant Molecular Biology 52: 627-658

Sims DA, Luo Y, Seemann JR (1998) Comparison of photosynthetic acclimation to elevated CO_2 and limited nitrogen supply in soybean. Plant Cell and Environment 21: 945-952

Stitt M, KrappA (1999) The interaction between elevated carbon dioxide and nitrogen nutrition: the physiological and molecular background. Plant Cell Environ 22: 583-621

Tissue DT, Thomas RB, Strain BR (1993) Long-term effects of elevated CO_2 and nutrients on photosynthesis and Rubisco in loblolly pine seedlings, Plant Cell Environ 16: 859-865

Ueno K, Kinoshita T, Inoue S, Emi T, Shimazaki K (2005) Biochemical Characterization of Plasma Membrane H^+-ATPase Activation in Guard Cell Protoplasts of *Arabidopsis thaliana* in Response to Blue Light. Plant and Cell Physiology 46: 955-963

Vahisalu T, Puzõrjova I, Brosché M, Valk E, Lepiku M, Moldau H, Pechter P, Wang YS, Lindgren O, Salojärvi J (2010) Ozone-triggered rapid stomatal response involves the production of reactive oxygen species and is controlled by SLAC1 and OST1. The Plant Journal 62: 442-453

Vahisalu T, Kollist H, Wang YF, Nishimura N, Chan WY, Valerio G, Lamminmäki A, Brosché M, Moldau H, Desikan R, Schroeder JI, Kangasjärvi J (2008) SLAC1 is required for plant guard cell S-type anion channel function in stomatal signalling. Nature 452: 487-491

Vu JCV, Allen LH, Boote KJ, Bowes G (1997) Effects of elevated CO_2 and temperature on photosynthesis and Rubisco in rice and soybean. Plant Cell and Environment 20: 68-76

Wang Y, Hills A, Vialet-Chabrand S, Papanatsiou M, Griffiths H, Rogers S, Lawson T, Lew VL, Blatt MR (2017) Unexpected Connections between Humidity and Ion Transport Discovered Using a Model to Bridge Guard Cell-to-Leaf Scales. Plant Cell 29: 2921-2939

Wong SC (1979) Elevated atmospheric partial pressure of CO_2 and plant growth: Interactions of nitrogen nutrition and photosynthetic capacity in C3 and C4 plants. Oecologia 44: 68-74

Zinta G, AbdElgawad H, Domagalska MA, Vergauwen L, Knapen D, Nijs I, Janssens IA, Beemster GT, Asard H (2014) Physiological, biochemical, and genome-wide transcriptional analysis reveals that elevated CO_2 mitigates the impact of combined heat wave and drought stress in *Arabidopsis thaliana* at multiple organizational levels. Global Chang Biology 2014 20: 3670-3685

Chapter 1

Enhanced stomatal aperture due to the functional lack of SLAC1 modifies guard cell metabolism without impacting photosynthesis under elevated [CO_2] and moderated water restriction

CHAPTER 1: Enhanced stomatal aperture due to the functional lack of SLAC1 modifies guard cell metabolism without impacting photosynthesis under elevated [CO_2] and moderated water restriction

ABSTRACT

Understanding changes in stomatal movement in response to fluctuations in atmospheric carbon dioxide concentration [CO_2] and water deficit is crucial to predicting the overall impacts of global changes on plants. In *Arabidopsis*, the main CO_2- and drought-sensitive channel is the slow-type anion channel (SLAC1) that plays a central role in the control of stomatal closure and higher water use efficiency (*WUE*). In order to examine the stomatal limitations to photosynthesis, we postulated that plants with higher stomatal conductance (g_s; *slac1* mutants) of moderate water restriction might sustain higher A_N and continuous growth. Together, the results demonstrated that under moderate water limitations and elevated [CO_2], plants with higher g_s are characterized by similar photosynthetic performance and growth to plants with unaltered stomatal control under enriched CO_2 and water deficit conditions. Furthermore, our results also suggest that the constitutive increased stomatal aperture observed in *slac-1* mutant plants is associated with an exquisite reorganization of primary metabolism in guard cells, increasing mainly sugars, amino acids, and organic acids. Thus, the results presented here indicate the higher stomatal conductance of mutant *slac1* plants, independent of CO_2 and water conditions, does not always result into better photosynthetic performance and that mutant plants *slac1* naturally produce key metabolites to overcome water deficiency stress.

Key-words: *Arabidopsis thaliana*, guard cell metabolism, stomatal conductance, water use efficiency.

INTRODUCTION

Stomata, pairs of specialized epidermal guard cells which are often surrounded by subsidiary cells, function as major gateways for both CO_2 influx from the atmosphere and transpirational water loss of plants (Brodribb and McAdam, 2011). The precise combination of adjustable stomata with an internal water transport system was a turning point in plant evolution that enabled vascular plants to invade most terrestrial environments (Raven, 2002). Thus, a coupled regulation of photosynthesis and *WUE* is directly influenced by the aperture of the stomatal pore, which is actively regulated by the metabolism of the surrounding guard cells. Accordingly, increased g_s may lead to increased photosynthesis in plants under well-irrigated growth conditions (Buckley and Mott, 2013). However, elevated CO_2 concentration and soil water restriction may induce partial stomatal closure and synergistically increase *WUE* (Pazzagli et al., 2016; Kumar et al., 2014). This is possible because g_s is more sensitive to elevated [CO_2] and water restriction than A_N. In such conditions, reductions of biomass production are generally lower than the reduced percentage of water supplied (Liu et al., 2005, 2006). In this case, CO_2 enrichment may prolong assimilation periods during episodes of moderate and temporary drought (Vu and Allen, 2009; Nackley et al., 2014). Despite the significant breakthrough obtained during the last decades, the knowledge concerning the guard cell metabolic changes following stress condition remains largely elusive. Therefore, understanding how changes in stomatal movement in response to fluctuations in the atmospheric concentration of CO_2 and water deficit is crucial for predicting the overall impacts of global climate changes on plants.

Stomatal movement is performed through the reprogramming of cellular processes triggered by a network of signaling events (Fujita et al., 2013; Vishwakarma et al., 2018). The increase in abscisic acid (ABA) concentration is one of the main routes of signal transduction under drought and high [CO_2] (Schroeder et al., 2001; Schachtman and Goodger, 2008). Thus, it is not surprising that the mechanisms by which ABA control stomatal closure have been widely investigated at the transcriptional level given its potential to identify and to produce drought tolerant genotypes (Gago et al., 2014; Flexas, 2016). In *Arabidopsis*, the ABA-sensitive channel is the SLAC1 that plays a central role in the control of stomatal closure channel controlling the stomatal closure is the SLAC1 (Negi et al., 2008; Vahisalu et al., 2008). SLAC1 functioning is relatively well characterized and it is activated by the ABA signaling cascade binds to the pyrabactin resistance/regulatory components of ABA receptor (PYR1/PYL) in guard cells, sequestering the protein type 2C phosphatases (PP2Cs). The formation of this heteromeric complex PYR-ABA-PP2C releases the negative regulation of ABA exerted by PP2C on the open stomata1/ sucrose nonfermenting 1-related protein kinase 2-6 (OST1/SnRK2.6) protein kinase (Yoshida et al, 2006; Yamamoto et al., 2016). Accordingly, SLAC1 is activated when phosphorylated by certain kinases (e.g OST1, calcium-dependent protein kinases - CDPKs) and thus a conformational change allows the channel pore closure (Chen et al., 2010; Maierhofer et al., 2014). Once SLAC1 is active, it transports chloride and nitrate to the apoplastic direction, resulting in the stomatal closure (Geiger et al., 2009, Lee et al., 2009; Pilot et al., 2001). In good agreement with this, mutant plants with loss of SLAC1 function showed lower sensitive to ABA compromising stomatal closure in response to CO_2 and drought (Negi et al., 2008). Other studies also revealed an ABA-independent pathway, where high [CO_2] and high activity of β-carbonic anhydrases (βCA) activates the resistant to high CO_2 (RHC1), a membrane protein that functions as a bicarbonate sensor (Tian et al., 2015; Yamamoto et al., 2016). Once activated, RHC1 repress high leaf temperature (HT1), a kinase that negatively regulates stomatal closure by inhibiting OST1 (Hashimoto et al., 2006). After HT1 repression, OST1 autophosphorylates and phosphorylates SLAC1 by activating stomatal closure (Tian et al, 2015; Yamamoto et al., 2016). It is worth to mention that, regardless of the signaling pathway, SLAC1 loss-of-function *Arabidopsis* plants showed a lower sensitivity to ABA and constitutively higher g_s in response to elevated CO_2 and drought as well as higher water loss from detached rosettes (Negi et al, 2008, Vahisalu et al., 2008). Recently, Mizokami et al. (2018) demonstrated that in *slac1* knockout plants the elevated [CO_2] decreased mesophyll conductance (g_m) whereas g_s remained unchanged, assuming independence of the responses between g_s and g_m. In addition, rice plants with mutation in SLAC1 cultivated under greenhouse showed higher g_s, net photosynthesis rate (A_N) and ratio between substomatal CO_2 concentration and the atmospheric concentration of CO_2 (C_i/C_a) as well as low leaf temperature (Kusumi et al., 2012), showing that the higher g_s increases the CO_2 fixation in rice plants.

While some of the role surrounding stomata movement mediated by SLAC1 has been dissipated by the considerable knowledge obtained about this important transport during recent years, a number of key questions still remain unanswered. In order to examine the stomatal limitations to photosynthesis, we postulated that plants with higher g_s (*slac1* mutant) under conditions of moderate water restriction might sustain higher A_N and continuous growth (higher photosynthetic performance). Due to the increasing occurrence of moderate drought episodes and the expected rise in [CO_2], we hypothesized that the manipulation of stomatal conductance will facilitate increases in photosynthesis, leading to higher water use efficiency. Thus, our main goal was to investigate the independent and combined effects of elevated CO_2 and water limitation by comparing plants with a constitutive increase of the stomatal opening (*slac-1* mutant plants) with *Arabidopsis thaliana* wild type (WT) plants. To this end, a range of parameters including gas exchange, growth, metabolism and gene expression were analyzed. Our results demonstrated that to sustain the increased g_s *slac-1* mutant plants display an elegant metabolic reprogramming that is crucial for growth survival under moderate water limitation. The data obtained are discussed in the context of the roles of SLAC1 on both generally with respect to photosynthetic metabolism and specifically with respect to its function in the regulation of stomatal aperture.

MATERIAL AND METHODS

Plant material

All *Arabidopsis thaliana* plants used here were ecotype Columbia (Col-0) background. The T-DNA lines *slac1-3* (SALK_099139) and *slac1-4* (SALK_137265) were identified and characterized as described by Vahisalu et al. (2008). Both knockout lines contain T-DNA insertion into exons of SLAC1 gene (for details, see Vahisalu et al., 2008). The expression of the mutant lines was identified by PCR using specific primers for *slac1-3* (forward - GTTTCTCAGTGCTCAACAGAG and reverse-CTTCTCCCTGGTAAGTTTCC) and *slac1-4* (forward - ATCTACGGGCAATGGCTTTCGG and reverse - ACCACGCCACTGAGAACTTAAATC).

The *Arabidopsis* Genome Initiative locus numbers for the major genes discussed in this study are as follows: *SLAC1,* At1g12480 (The *Arabidopsis* Genome Initiative; http://www.arabidopsis.org/).

Growth conditions

Seeds of *Arabidopsis* were sown on a commercial substrate (Carolina soil®) in plastic pots and two weeks after sowing, plants were transferred to individual 0.08 dm^3 pots containing also Carolina soil®. WT and *slac1* plants were grown under short-day conditions (8h light/16h dark) and light intensity of 150 μmol m^2 s^{-1}, at a temperature of 23 ºC/18 °C throughout the day/night cycle, and 65±10% relative humidity.

For examination of phenotype including both gas exchange and metabolism along the day, plants with 14 days were transferred to chambers with modified carbon dioxide concentration [CO_2]. CO_2 was injected only during daylight hours corresponding to the period when the plants are photosynthetically active. Plants were kept under optimum growth conditions with fully available water regime. In a second moment, we decided to associate [CO_2] with water restriction. To this end, plants were transferred to chambers with either 400±50 ppm (ambient - aCO_2) or 800±50 ppm of CO_2 (elevated - eCO_2). After two weeks, half of the plants at both aCO_2 and eCO_2 were submitted to water restriction (WR). For this assay, half of the plants cultivated at both ambient ($aCO_{2\_100\%}$) and elevated CO_2 ($eCO_{2\_100\%}$) were cultivated to 100% of the substrate water capacity, equivalent to the tension of 10 kPa (CET), corresponding to control group. The water replenishment was suspended for 7 days until the substrate reached 50% (CET) water availability for the remaining half of the plants. After the 7th day, the amount of water lost by evapotranspiration was daily replaced, maintaining 50% water availability. Both control and water limited-plants were cultivated up to 4-5 weeks at aCO_2 and eCO_2.

To summarize, at 14 days after transplanting seedlings growing in either environment [CO_2] or elevated [CO_2] was submitted to water limitation conditions. Thus, four different treatments were applied: Control (ambient [CO_2] and 100% of the water capacity- $aCO_{2\_100\%}$), elevated [CO_2] and 100% of the water capacity- $eCO_{2\_100\%}$), ambient [CO_2] and 50% of the water capacity- $aCO_{2\_50\%}$) and elevated [CO_2] and 50% of the water capacity- $eCO_{2\_50\%}$). Measurements were performed during vegetative growth and the interaction treatments were maintained for the minimum of 17 days. Additionally, the experiments were repeated at least two times, even in different growth facilities, with similar phenotypes observed each time.

Growth analyses

Whole rosettes from at least 4-week-old plants were harvested and rosette dry weight (RDW), rosette fresh weight (RFW), rosette area (RA), total leaf area (LA), specific leaf area (SLA) and number of rosette leaves were evaluated. To determine dry weight, rosettes were dried in an oven with forced air circulation at 60 °C until constant weight. LA was estimated by digital image method where the images were obtained using a scanner and later processed in ImageJ software (Schindelin et al., 2015). SLA was estimated as described by Hunt et al. (2002).

Water loss measurements

Rosettes of four-week-old plants grown at aCO_2 were detached and incubated with abaxial surface turned to up. For the estimation of water loss, the weight of detached rosettes was determined over 4 h at the indicated time points. Water loss was calculated as a percentage of fresh weight loss relative to the initial fresh weight (Araújo et al., 2011).

Relative water content (RWC)

The relative water content was determined at the middle of the light period. To this, one leaf of each plant was detached and then immediately weighed to obtain the fresh weight (FW). Thereafter, the leaves were hydrated for 2 h in Petri dish containing distilled water until saturation, when the turgid (TW) weight was recorded. Finally, the leaves were oven dried at 60 °C for 72 h; next, the leaves were weighted, obtaining thus dry weight (DW). The relative water content was calculated according to the equation: $RWC = (FW - DW) / (TW - DW)$.

Morpho-anatomical traits

The median region of the 9th leaf totally expanded of 4,5-week-old plants from WR experiment was collected. These samples were immediately fixed at formaldehyde-acetic acid-ethanol (FAA) 50% (Johansen, 1940) for 24 h and subsequently stored in 70% alcohol. This material was included in methacrylate (Historesin-Leica), according to manufacturer's recommendations and transversely sectioned (5µm thick) in an auto-feed rotary microtome (model RM2155, Leica Microsystems Inc., Heidelberg, Germany), and stained with toluidine blue (O'Brien et al., 1964). Each sample was represented by the average of five replicates, each replicate being composed of measurements in three distinct points. The material was photographed under a light microscope (AX-70 TRF, Olympus Optical, Tokyo, Japan) coupled to a digital photographic camera (Zeiss AxioCam HRc model, Göttinger, Germany) and computer with Axion Vision image capture program. Finally, in the internerval region, the palisade and lacunaceous parenchyma thickness, mesophyll thickness, leaf thickness, and mesophyll intercellular spaces were analyzed using Image-Pro® Plus software (version 4.1, Media Cybernetics, Inc., Silver Spring, USA).

Stomatal opening and closing kinetics measurements

The stomatal responses to ABA were evaluated in the 9th fully expanded leaf of each genotype grown at either 400 or 800 ppm. First, leaves were cut and maintained in opening buffer (10 mM KCl, 50 µM $CaCl_2$, and 5 mM MES-Tris, pH 6.15) for 15 min (150 µmol m^{-2} s^{-1}) to stimulate the stomatal opening (Azoulay-Shemer et al., 2015). Finally, 1 µM of ABA solution was added to the opening buffer. Stomatal conductance (g_s) values were recorded at intervals of 40 s for over 25 min using an open-flow infrared gas exchange analyzer system (LI-6400XT; LI-COR Inc., Lincoln, NE) equipped with an integrated fluorescence chamber (LI-6400-40; LI-COR Inc.).

Gas exchange parameters

Gas exchange parameters were determined simultaneously with chlorophyll *a* (Chl *a*) fluorescence measurements using the same gas exchange system described above. Instantaneous gas exchanges, including net assimilation rate of carbon (A), stomatal conductance (g_s) and the internal carbon dioxide concentration (C_i), were measured after 1 h illumination during the light period under 150 µmol m^{-2} s^{-1} (light of growth) or 1000 µmol m^{-2} s^{-1} (non-photoinhibitory light saturation) at the leaf level of photosynthetically active photon flux density (PPFD). The reference CO_2 concentration was set at 400 or 800 µmol CO_2 mol^{-1} air under ambient or elevated [CO_2] conditions, respectively. All measurements were performed using the 2 cm^2 leaf chamber at 25 °C, as well as a 0.5 stomatal ratio (amphistomatic leaves), and leaf-to-air vapor pressure deficit, was kept between 1.0-1.5 kPa, while the amount of blue light was set to 10% PPFD to optimize stomatal aperture. The WR experiment, the gas exchange was measured only in the flux intensity of 150 µmol m^{-2} s^{-1}. Dark respiration (R_d) was measured using the same gas exchange system as described above on leaves adapted to the dark for at least 2 hours after the end of the light period. In complement, the mitochondrial respiration in light (R_l) was estimated as half of R_d (Pinelli and Loreto, 2003; Centritto et al., 2009). The photorespiratory rate (R_p) of Rubisco was estimated according to Valentini et al. (1995), as R_p=1/12[ETR – 4(A+R_l)].

Photosynthetic light-response curves (A/PPFD) were determined in plants from at least 4-week-old varying the PPFD from 0 to 1400 µmol (photons) m^{-2} s^{-1} under growing ambient CO_2 concentration (C_a) of 400 or 800 µmol mol^{-1}. Likewise, the responses of A_N to C_i (A_N /C_i curves) were performed at saturated light of 1000 µmol m^{-2} s^{-1} at 25°C under ambient O_2. Briefly, the measurements started at ambient CO_2 concentration (C_a) of 400 µmol mol^{-1} and when the steady state was reached, C_a was decreased stepwise to 50 µmol mol^{-1}. Upon completion of the measurements at low C_a, C_a was returned to 400 µmol mol^{-1} to restore the original A_N. Next, C_a was increased stepwise to 1600 µmol mol^{-1} in a total of 13 different C_a values (Long and Bernacchi, 2003). Corrections for the leakage of CO_2 into and water vapor out of the leaf chamber of the LI-6400 have been applied to all gas-exchange data, according to Rodeghiero et al. (2007).

From the A/C_i curves, the maximum carboxylation rate ($V_{cmax\text{-}Ci}$) and maximum rate of electron transport ($J_{max\text{-}Ci}$) were calculated by fitting the mechanistic model of CO_2 assimilation proposed by Farquhar et al. (1980) using the temperature dependence of the kinetic parameters of Rubisco (Bernacchi, 2002). The Michaelis-Menten constants used for CO_2 and O_2 were K_c= 265 µbar and K_o= 201000 µbar, while the CO_2 compensation point (Γ^*) was 36.4 µbar, as previously demonstrated by Walker et al. (2013). Curve-fitting procedures are detailed elsewhere (Martins et al. 2013). Afterward, the photosynthetic parameters V_{cmax} and J_{max} were normalized to 25 °C using the temperature response equations from Sharkey et al. (2007). C_c and g_m were estimated according to Martins et al. (2013). Using C_c data, A/C_c curves were performed and the values of maximum carboxylation rate ($V_{cmax\text{-}Cc}$) and maximum rate of electron transport ($J_{max\text{-}Cc}$) were estimated. The observed photosynthetic limitations were estimated based on the method previously described (Grassi and Magnani, 2005). This method uses values of A, g_s, g_m, $V_{cmax\text{-}Cc}$, Γ*, C_c, Km = K_c (1+ O/K_o) and allows the partitioning of functional components that limit photosynthesis relative to stomatal (SL), mesophilic (ML) and biochemical (BL) limitations. The water use efficiency was estimated as the ratio between photosynthesis and g_s.

The initial fluorescence (F_0) was measured by illuminating previously dark-adapted leaves (1 h) with weak modulated measuring beams (0.03 µmol m^{-2} s^{-1}). Saturating white light pulses (8000 µmol photons m^{-2} s^{-1}) was applied for 0.8 s to obtain the maximum fluorescence (F_m), from which the variable-to-maximum Chl fluorescence ratio, was then calculated: F_v/F_m= [(F_m - F_0)/F_m)]. In light-adapted leaves, the steady-state fluorescence yield (F_s) was measured with the application of a saturating white light pulse (8000 µmol m^{-2} s^{-1}, 0.8 s) to achieve the light-adapted maximum fluorescence (F_m'). The actinic light was then turned off and a far-red illumination (2 µmol m^{-2} s^{-1}) was applied to measure the light-adapted initial fluorescence (F_0'). The capture efficiency of excitation energy by open photosystem (PSII) reaction centers (F_v'/F_m') was estimated following Logan et al. (2007) and the actual PSII photochemical efficiency (δPSII) was estimated as δPSII = (F_m'- F_s)/F_m' (Genty et al., 1989). In addition, the coefficients of photochemical quenching (*qP*), non-photochemical quenching (*NPQ*) and the electron transport rate (*ETR*) were determined as previously described (Martins et al., 2013).

Determination of metabolite levels

In order to evaluate metabolic changes during the light/dark cycle, whole rosettes were collected at the beginning, middle and end of the light period. For the WR experiment, plants were collected only in the middle of the day. In addition, harvesting were carried out in three distinct moments after the imposition of WR as follow: (*i*) end of the second week (when the restriction was started); (*ii*) end of the third week (when the plants reached 50% of water into the soil) and 17 days after WR, while plants were maintained at 50% of water into the soil. All samples were immediately flash frozen in liquid nitrogen and stored at -80 °C until analysis.

Samples were submitted to methanolic hot extraction, and the levels of photosynthetic pigments (Porra et al., 1989), glucose, fructose and sucrose (Fernie et al., 2001), malate and fumarate (Nunes-Nesi et al., 2007), total amino acids (Yemm et al., 1955), and nitrate (Mori, 2000) levels were quantified insoluble fraction, while starch (Fernie, et al., 2001) and total protein contents (Bradford, 1976) were determined in insoluble fraction.

Isolation of guard cell-enriched epidermal fragments

Isolation of guard cell enriched epidermal fragments was performed as previously described by Pandey et al. (2002) with minor modifications. Briefly, 4 to 5 whole rosettes per sample were rendered for approximately 1 min with a blender containing an internal filter that separates the epidermal fragments from mesophilic and fibrous cells. Subsequently, the epidermal fragments were collected on a nylon membrane (200 µm mesh) and washed with rinsing water and were immediately flash frozen in liquid nitrogen and stored at -80 °C until analysis. The fragments were used for both gene expression and metabolic profile.

Metabolic profile of guard cell-enriched epidermal fragments

Metabolites profile performed by gas chromatography coupled to mass spectrometry (GC-MS) and it was carried out in samples (leaves and epidermal fragments) harvested at the middle of the day. The extraction was performed using 1mL of methanol and shaking (800 rpm) at 70 ºC during 15 min, 60 µL of Ribitol (0.2mg mL^{-1}) was added as an internal standard, as previously described by Lisec et al. (2006). The chromatograms and mass spectra generated were manually annotated, and ion intensity was determined by the aid of TagFinder software (Luedemann et al., 2008), based on the FAME MDN35 reference library from the Golm Metabolome Database (http://gmd.mpimp-gol.mpg.de/download/) (Kopka et al., 2005) and following the reporting recommendations (Fernie et al., 2011). This analysis allowed the determination of approximately 20 different metabolites, representing the main classes of compounds (amino acids, organic acids, sugars, among others).

Gene expression analysis

Total RNA was extracted from the samples with TRIzol reagent (Ambion, Life Technology). After purification, the RNA was quantified by NanoDrop ND-2000 spectrophotometer (Thermo Scientific NanoDrop Technologies, Wilmington, Delaware, United States) and analyzed on a 1% (w/v) agarose gel. A total of 0.5 µg of RNA was treated with DNAse I (Invitrogen®, Carlsbad, California, United States) to remove potential contamination with genomic DNA. The cDNA synthesis was performed using 0.5 µg of total RNA using SuperscriptTM III reverse transcriptase (Invitrogen®, Carlsbad, California, United States). For analysis of gene expression, the Fast SYBR®

Green PCR Master Mix was used with the MicroAmp^{TM} Optical 96-well Reaction Plate (both from Applied Biosystems, Singapore, China) and MicroAmp^{TM} Optical Adhesive Film (Applied Biosystems, Foster City, CA, USA). The R^2 from the regression equation was calculated for each gene in order to verify the reaction efficiency. Standard curves were prepared for each pair of primers using serially diluted cDNA to calculate the relative amount values for each sample. A standard curve was used to calculate the relative quantification values of each sample for each gene (Larionov et al., 2005).

The relative expression levels were normalized using the constitutively expressed genes *ACTIN* (Czechowski et al., 2005). The primers used for qRT-PCR were designed using the QuantPrime software (Arvidsson et al., 2008) or taken from those described by Laanemets et al. (2013). Detailed primers information is described in the Supplemental Table S2. The following genes related to water deficiency, [CO_2], signaling and transport of ions through guard-cell membranes were analyzed: aluminum activated malate transporter 6 and -9, *ALMT6* and *ALMT9*; ATP-binding cassette B14, *ABCB14* (Lee et al., 2008); H^+-ATPase 1, -2 and -5, *AHA1*, *AHA2* and *AHA5* (Ueno et al., 2005); potassium channel 1, *KAT1* (Nakamura et al., 1995) and *KAT2* (Pilot et al., 2001); K^+ transporter 1, *AKT1* (Cao et al., 1995); K^+ rectifying channel 1, *KC1* (Reintanz et al., 2002); K^+ gated outwardly-rectifying K^+ channel, *GORK* (Ache et al., 2000); two-pore channel 1, *TPC1* (Peiter et al., 2005); high leaf temperature 1, *HT1* (Hashimoto et al., 2006); resistant to high CO_2, *RHC1* (Tian et al., 2015); β-carbonic anhydrases 1, *βCA4* (Hu et al., 2010); response to dehydration A and B, *RD29A/RD29B* (Narusaka et al., 2003; Dong et al., 2004); 9-cis-epoxycarotenoid dioxygenase 5, *NCED5* (Qin et al, 1999; Barrero et al., 2006); open stomata 1, *OST1* (Belin et al., 2006). The independent genotypes were represented by at least three plants and the mean value of the expression was calculated. The results were analyzed using Student's *t*-test.

Experimental design and statistical analysis

All experiments were performed in a completely randomized experimental design. All data are expressed as the mean ± standard error (SE) of 3-6 independent replicates per genotype, and when was the case, over time. All data was submitted to an unpaired two-tailed Student *t*-test used for the comparative analysis between the two treatments or genotypes, and an ANOVA was used for three or more treatments or genotypes. The comparison of the means was performed through the Tukey HSD (honestly significant difference) test for balanced data and Tukey-Kramer for unbalanced data. *P*-values lower than 0.05 ($P<0.05$) were considered statistically significant. All the statistical analyses were performed using the statistical software R version 3.3.2 (R Foundation for Statistical Computing, Vienna, Austria).

RESULTS

slac1 mutants are poorly sensitive to ABA and display higher water loss

To investigate the impact of CO_2 on the ABA sensitivity, WT and *slac1* were grown at aCO_2 and eCO_2 and then 1 µM ABA was applied. While both *slac1-3* and *slac1-4* mutant lines showed only relatively small reductions in g_s (~ 25% and 35 % at aCO_2 and eCO_2, respectively), in WT plants a much strong reduction was observed (~ 60% and 70% at aCO_2 and eCO_2, respectively) in response to exogenous ABA application (Supplemental Fig. S1, A and B). This incapacity to closing stomata in response to ABA was further confirmed by the greater fresh mass loss in detached rosettes in both mutant lines (74 and 79% for *slac1-3* and *slac1-4*, respectively) growing at aCO_2 when compared to WT (only 55%; Supplemental Fig. S1C).

Increasing g_s results in higher C_i and decreased photosynthesis in *slac1* mutants

Regardless of [CO_2] and light, A_N and C_i/C_a ratio were similar between WT and *slac1*. In addition, g_s remained higher in *slac1*, which led to a lower *WUE* as compared to WT. F_v'/F_m' and ETR did not vary between genotypes (Supplemental Fig. S2, A-F). In order to better understand the mechanisms underlying changes of g_s in response to the variation of [CO_2], we performed A_N/C_i and A_N/C_c curves under saturating light conditions (Supplemental Fig. S3 A-D). Mutant plants did not present higher photosynthetic activity as compared to WT, while both stomatal limitation and C_i were significantly altered. Irrespective of [CO_2], V_{cmax} and J_{max} in both C_i and C_c basis tended to be smaller in *slac1* than in WT (Table 1). All the other parameters were virtually invariable between genotypes. We evaluated also the photosynthesis as a function of PPFD. Mutant plants exhibited A_N similar to WT, independently of PPFD and [CO_2] (Supplemental Fig. S3, E and F).

Irrespective of changes found in g_s, when we analyzed *A*/PPFD responses A_{max} (only higher for *slac1-4* at aCO_2) and the light use efficiency (1/*Φ*) were similar among the studied genotypes (Supplemental Table S1), as well as were the compensation irradiance (I_c) and the saturation irradiance (I_s); they averaged respectively on 10.3, 20.0, 15.0 and 560 $\mu mol\ m^{-2}s^{-1}$ at aCO_2 and 17.0, 14.3, 9.0 and 625 $\mu mol\ m^{-2}s^{-1}$ at eCO_2 (Fig. 3).

Higher g_s did not lead to changes in growth in *slac1*

All genotypes studied showed similar values of leaf RWC (approximately ~93%) even under moderate water limitation (Fig. 1), without the appearance of early symptoms of leaf wilting. Plant growth phenotype between *slac1* and WT plants showed little difference under similar CO_2 and water conditions (Fig. 1). Rosette area (Fig. 2A) and leaf area (Fig. 2B) significantly reduced in *slac1-4* plants as compared to WT under $aCO_{2\_100\%}$. Similarly, RFW reduced in two mutant lines under $aCO_{2\_50\%}$, as well as the number of leaves (only in *slac1-4*) when compared to WT (Fig. 2, C and F). SLA and RDW did not change significantly between genotypes (Fig. 2, D and E).

Water restriction decreases leaf blade thickness in *slac1-3*, without impacting intercellular spaces.

To enhance our understanding of the significance of *slac1* on *Arabidopsis* plants, anatomical parameters were analyzed in plants cultivated under fluctuating conditions of [CO_2] and water availability (Fig. 3). Briefly, leaf lamina thickness (LLT), mesophyll thickness (MT), palisade mesophyll thickness (PMT), spongy mesophyll thickness (SMT), adaxial epidermis thickness (AdET) and abaxial epidermis thickness (AbET) significantly reduced in *slac1-3* plants under $aCO_{2\_50\%}$ as compared to *slac1-3* plants at $aCO_{2\_100\%}$ (Fig. 3, A, B, D E and F). SMT tended to be higher in *slac1-3* mutant plants under $eCO_{2\_100\%}$ in comparison to WT plants (Fig. 3D). Overall, WT plants did not show any major changes in the analyzed anatomical parameters, yet AdET and intercellular space (IS) were significantly reduced under $eCO_{2\_50\%}$ when compared to $aCO_{2\_100\%}$ (Fig. 3E and G). By comparing the genotypes used here, it was observed that only AdET was significantly higher in *slac1-3* plants than in WT under $eCO_{2\_100\%}$ (Fig. 3E). Notably, IS was almost invariant regardless of [CO_2] and WR (Fig. 3G).

Table 1. Response of the photosynthesis parameters to CO_2 curve. aCO_2 and eCO_2 represent plants grown at ambient and elevated [CO_2], respectively. Values are presented as means ± SE (n = 4). Lowercase letters compare a genotype under different conditions of [CO_2] and uppercase letters compare the three genotypes under the same treatment condition. Means followed by the same letter not differentiated by a one-way ANOVA followed by Tukey test ($P < 0.05$) between genotypes or treatments.

Parameters*	WT		*slac1-3*		*slac1-4*	
	aCO_2	eCO_2	aCO_2	eCO_2	aCO_2	eCO_2
C_i (µmol CO_2 mol^{-1})	320.17 ± 7.37 Aa	630.74 ± 12.54 Ab	335.16 ± 8.71 Aa	667.29 ± 4.98 ABb	338.21 ± 4.81 Aa	686.40 ± 12.91 Bb
C_c (µmol CO_2 mol^{-1})	168.22 ± 5.80 Aa	504.92 ± 16.89 Ab	187.48 ± 7.96Aa	538.25 ± 64.81Ab	184.42 ± 11.51 Aa	529.54 ± 33.83 Ab
C_c:C_i	0.52 ± 0.01 Aa	0.80 ± 0.01 Ab	0.56 ± 0.02 Aa	0.80 ± 0.09 Ab	0.54 ± 0.03 Aa	0.77 ± 0.03 Ab
g_{m_Harley} (mol CO_2 m^{-2} s^{-1} bar^{-1})	0.095 ± 0.010 Aa	0.101 ± 0.025 Aa	0.090 ± 0.003 Aa	0.065 ± 0.002 Ab	0.078 ± 0.006 Aa	0.091 ± 0.005 Ab
g_{m_Ethier} (mol CO_2 m^{-2} s^{-1} bar^{-1})	0.063 ± 0.003 Aa	0.072 ± 0.007 Aa	0.051 ± 0.005 Aa	0.066 ± 0.015 Aa	0.056 ± 0.005 Aa	0.067± 0.011 Aa
V_{cmax_Ci} (µmol m^{-2} s^{-1})	44.28 ± 3.08 Aa	46.66 ± 3.09 Aa	40.37 ± 3.03 Aa	45.32 ± 2.89 Aa	35.45 ± 1.48 Aa	42.31 ± 1.48 Ab
V_{cmax_Cc} (µmol m^{-2} s^{-1})	67.44 ± 5.33 Aa	69.65 ± 2.20 Aa	65.19 ± 5.23 Aa	66.46 ± 2.55 Aa	61.58 ± 4.26 Aa	72.90 ± 7.50 Aa
J_{max_Ci} (µmol m^{-2} s^{-1})	94.41 ± 8.28 Aa	104.33 ± 2.89 Aa	86.95 ± 7.26 Aa	98.07 ± 2.22 Aa	81.58 ± 3.66 Aa	94.41 ± 2.85 Ab
J_{max_Cc} (µmol m^{-2} s^{-1})	118.74 ± 13.78 Aa	107.76 ± 3.61 Aa	95.06 ± 7.86 Aa	101.86 ± 2.59 Aa	90.26 ± 4.93 Aa	105.15 ± 5.64 Aa
J_{max_Ci} : V_{cmax_Ci}	2.12 ± 0.064 Aa	2.25 ± 0.105 Aa	2.16 ± 0.085 Aa	2.18 ± 0.096 Aa	2.30 ± 0.047 Aa	2.23 ± 0.052 Aa
J_{max_Cc} : V_{cmax_Cc}	1.77 ± 0.193 Aa	1.55 ± 0.04 Aa	1.47 ± 0.084 Aa	1.54 ± 0.039 Aa	1.47 ± 0.043 Aa	1.47 ± 0.078 Aa
Stomatal limitation	0.25 ± 0.024 Aa	0.18 ± 0.0177 Ab	0.21 ± 0.022 ABa	0.078 ± 0.006 Bb	0.149 ± 0.004 Ba	0.10 ± 0.01 Bb
Mesophyll limitation	0.35 ± 0.023 Aa	0.23 ± 0.042 Ab	0.38 ± 0.016 Aa	0.32 ± 0.033 Aa	0.41 ± 0.033 Aa	0.25 ± 0.017 Ab
Biochemical limitation	0.37 ± 0.026 Aa	0.69 ± 0.031 Ab	0.44 ± 0.018 Aa	0.69 ± 0.053 Ab	0.44 ± 0.032 Aa	0.64 ± 0.017 Ab

*C_i, Substomatal CO_2 concentration; C_c, chloroplastic CO_2 concentration; C_c/C_i, ratio between chloroplastic CO_2 concentration and substomatal CO_2 concentration; g_m, mesophyll conductance to CO_2 estimated according to the Harley or Ethier method; V_{cmax_Ci} or C_c, maximum carboxylation capacity based on C_i or C_c; $J_{max\_Ci\ or\ Cc}$, maximum capacity for electron transport rate based on C_i or C_c.

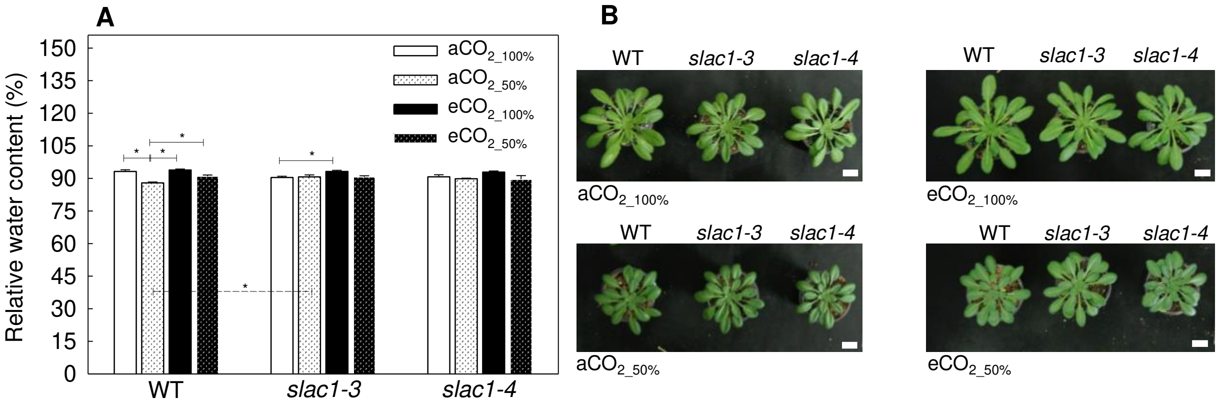

Figure 1. Water status and growth phenotype of *slac1* mutant plants in response to isolated or combination of water restriction and elevated [CO$_2$]. Relative water content (RWC) (A) and phenotype (B) of 4,5-week-old, short-day-grown Arabidopsis mutants and wild-type (WT). Plants growing under either ambient (aCO$_2$) (A) or elevated [CO$_2$] (eCO$_2$) after water limitation. Water suspension was imposed on 2-week-old plants after transplanting. The parameters were analyzed 10 days after the plants reached 50% of water in the soil. The water was replenished daily in order to maintain 50 and 100% of water in the soil. aCO$_{2\_100\%}$, plants were grown at ambient [CO$_2$] and with 100% water content replenished daily; aCO$_{2\_50\%}$, plants were grown at ambient [CO$_2$] and with 50% water content replenished daily; eCO$_{2\_100\%}$, plants were grown at elevated [CO$_2$] and with 100% water content replenished daily; eCO$_{2\_50\%}$, plants were grown at ambient [CO$_2$] and with 50% water content replenished daily. Values are presented as means ± SE (n = 5). Means followed by the same letter are not different by a one-way ANOVA followed by the Tukey test between genotypes or treatments. Dashed line compares the three genotypes under the same condition. Continuous line compares a genotype under different conditions. An asterisk (*) indicates a significant difference (P<0.05). White scale bar = 2 cm.

Changes in g_s did not affect photosynthesis impacting water use efficiency

The functional lack of the protein SLAC1 had little, if any, the effect on photosynthetic parameters; this fact apart, eCO$_2$ increased significantly *A* whereas middle and slow water limitation did not promote reductions in A_N in all genotypes (Fig. 4A). Interestingly, under aCO$_{2\_50\%}$ it was possible to observe that A was similar to the values found at aCO$_{2\_100\%}$ in the mutants suggesting a mitigatory role of CO$_2$ under water limitations (Fig. 4, A and C). In WT plants it was observed a significant reduction in A_N aCO$_{2\_50\%}$ when compared to aCO$_{2\_100\%}$ (Fig. 4A). On the other hand, no differences in *slac1* lines were observed when the same conditions are compared. *slac1* lines cultivated under aCO$_{2\_100\%}$ display relatively minor increased C_i when compared to WT (Fig. 4B). While g_s is reduced under all conditions in WT plants, only under eCO$_{2\_50\%}$ it was observed significant reductions in g_s of *slac1* mutant lines. Lower reductions in g_s observed in WT plants led to higher *WUE* (Fig. 4, C and D). R_d was virtually unaffected in *slac1* plants under either aCO$_2$ or eCO$_2$, whereas major changes were observed in WT plants (Fig. 4E). Accordingly, R_p was affected mainly under WR conditions in all genotypes, being significantly smaller in *slac1-4* under eCO$_{2\_50\%}$ when compared to WT (Fig. 4F). *ETR* and F_v/F_m were not modified when comparing either treatments or genotypes (Fig. 4, G and H).

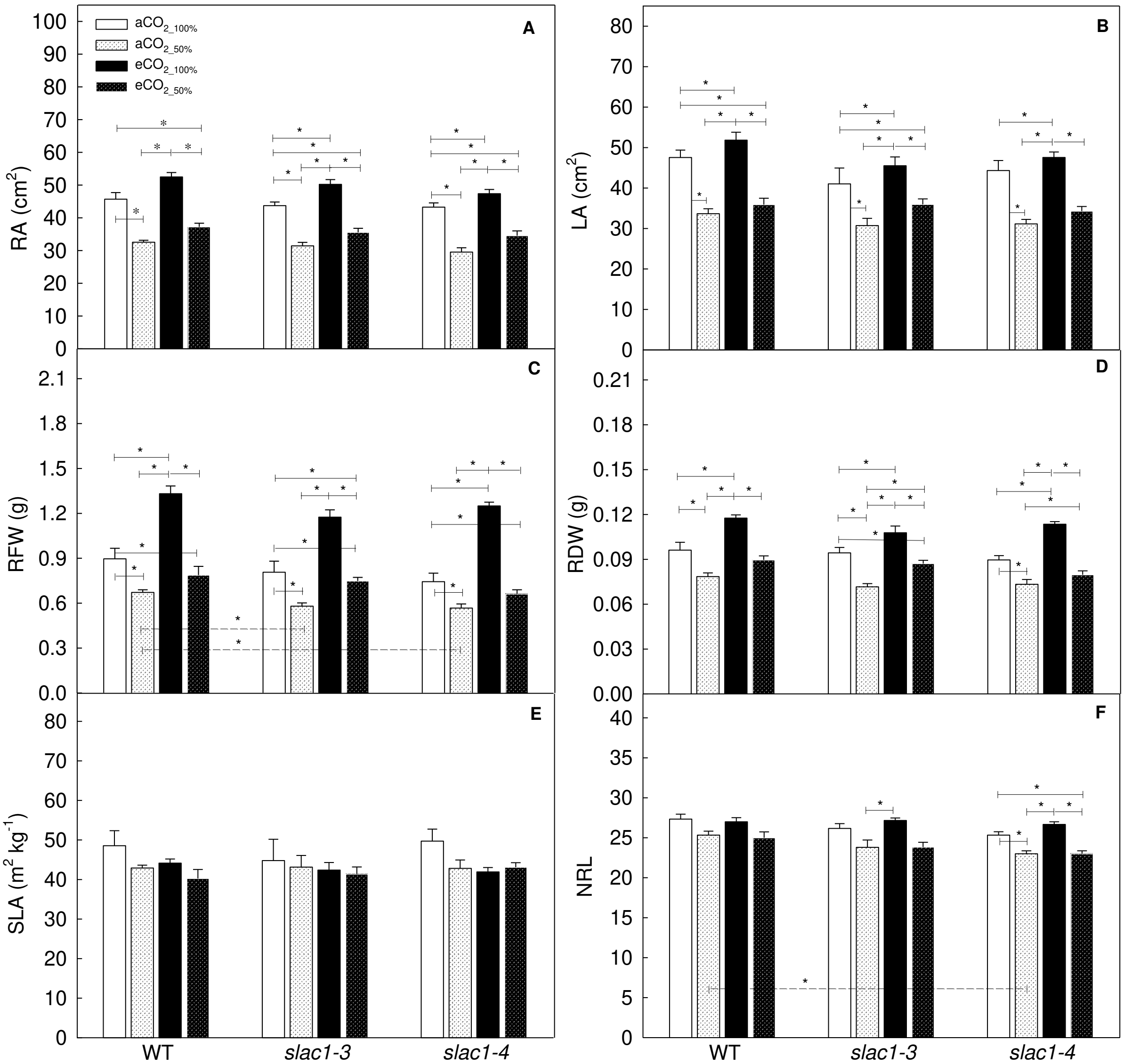

Figure 2. Differential responses of biomass accumulation and growth of *slac1* mutant plants in response to isolated or combination of water restriction and elevated [CO$_2$]. (A) RA, Rosette area; (B) LA, Leaf area; (C) RFW, Rosette fresh weight; (D) RDW, Rosette dry weight; (E) SLA, Specific leaf area; (F) NRL, Number of rosette leaves. Detail as in Figure 1. Values are presented as means ± SE (n = 5-6). Dashed line compares the three genotypes under the same condition. Continuous line compares a genotype under different conditions.

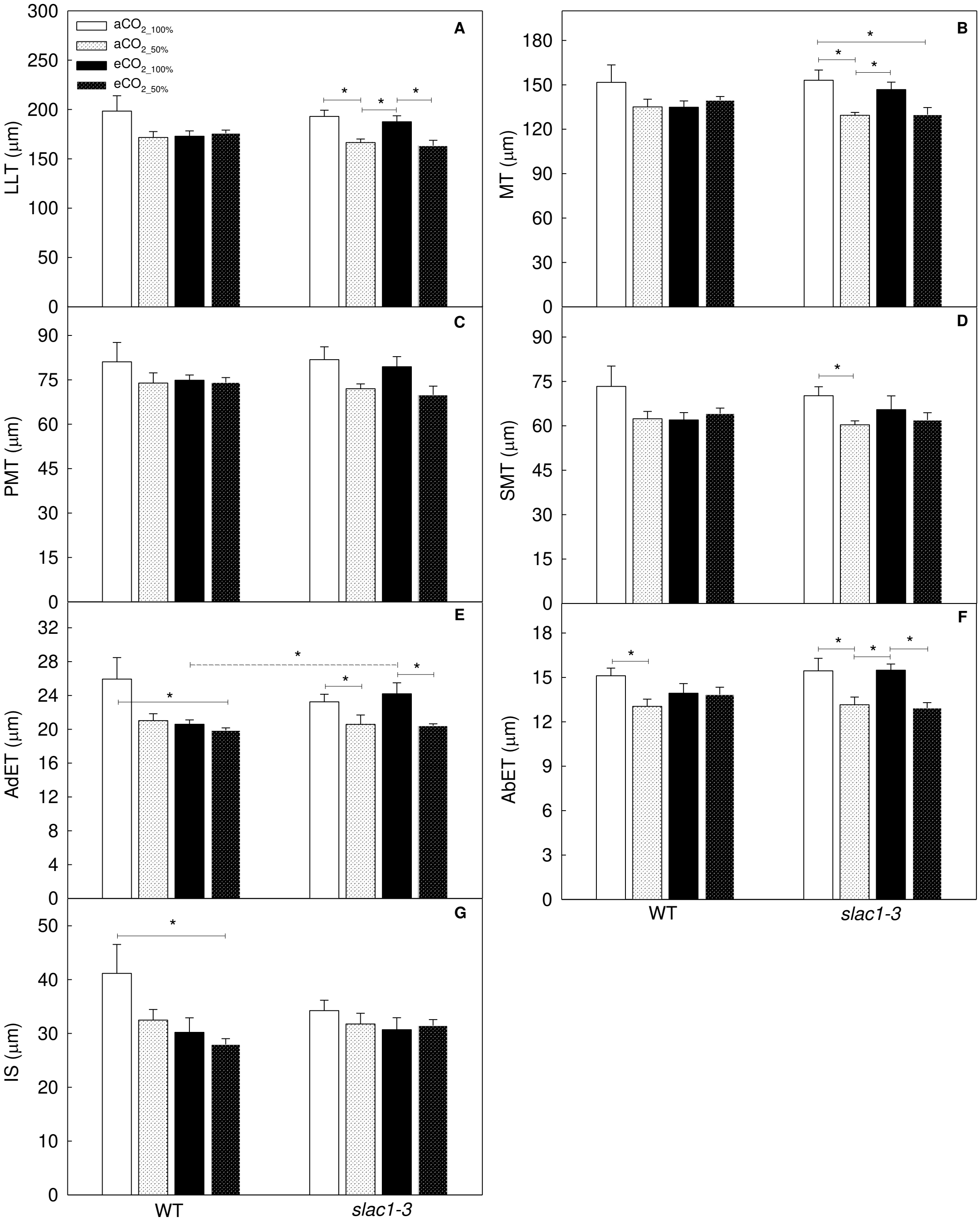

Figure 3. Data of leaf anatomical traits in light micrographs. Differential responses of the leaf anatomy to the combination of water restriction under ambient and elevated CO_2 concentrations in both WT and *slac1-3* plants. (A) LLT, Leaf lamina thickness; (B) MT, Mesophyll thickness; (C) PMT, Palisade mesophyll thickness; (D) SMT, Spongy mesophyll thickness; (E) AdET, Adaxial epidermis thickness; (F) AbET, Abaxial epidermis thickness; (G) IS, Intercellular space. Detail as in Figure 1. Values are presented as means ± SE (n = 5-6). Dashed line compares the three genotypes under the same treatment condition. Continuous line compares a genotype under different conditions.

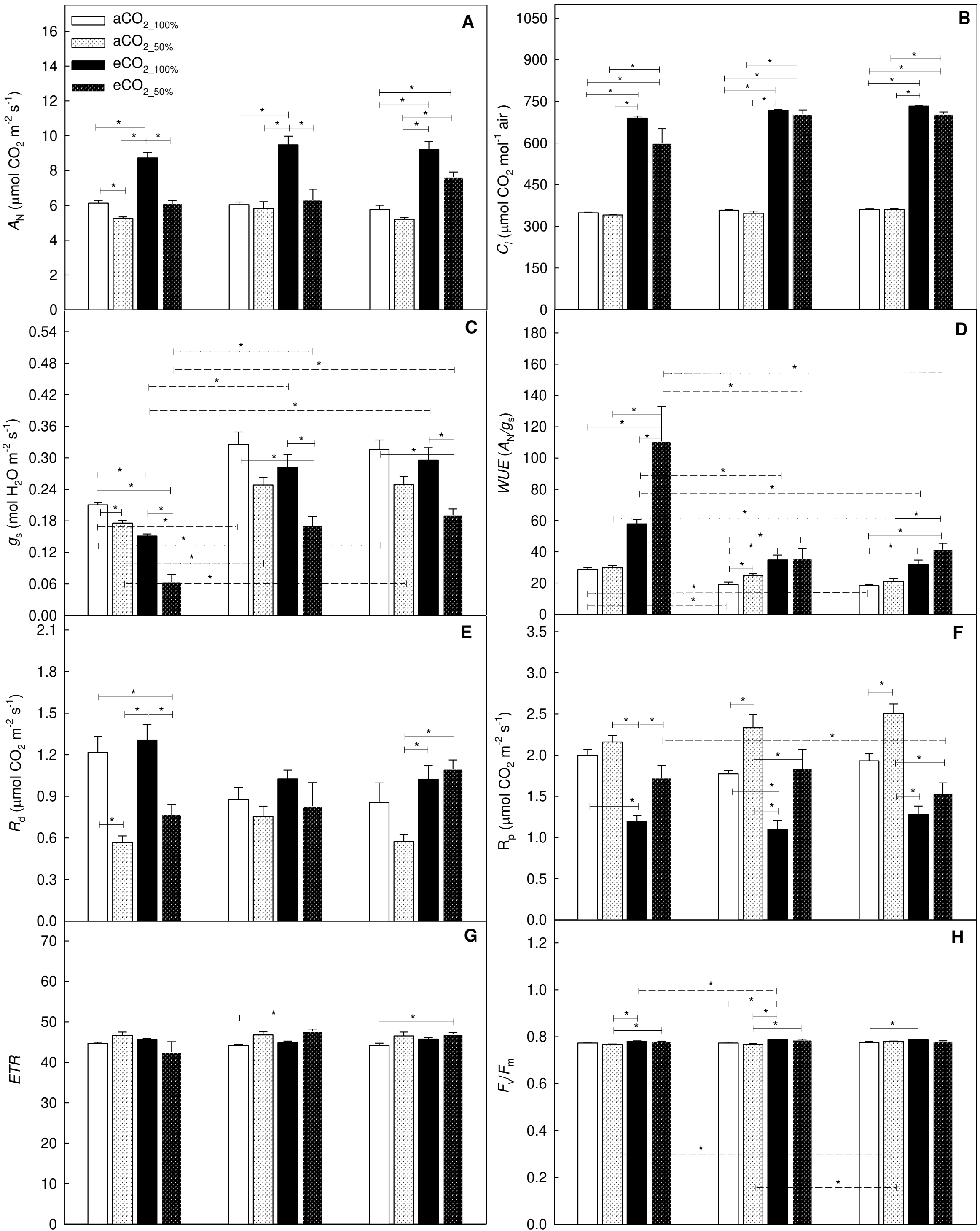

Figure 4. Photosynthetic characterization of *slac1* mutant plants in response to isolated or combination of water restriction and elevated [CO$_2$]. (A) A_N, Net photosynthesis rate; (B) C_i/C_a, ratio between concentration internal carbon and atmospheric carbon; (C) g_s, stomatal conductance; (D) WUE_i, intrinsic water use efficiency; (E) R_d, dark respiration; (F) R_p, photorespiration; (G) ETR, electron transport rate estimated by chlorophyll fluorescence parameters(H) F_v/F_m, maximum PSII photochemical efficiency. Gas exchange parameters were obtained in 4week-old-plants cultivated under either ambient (aCO$_2$) (A) or elevated [CO$_2$] (eCO$_2$) after water limitation. Detail as in Figure 1. Values are presented as means ± SE (n = 5-6).

Mutation in SLAC1 little affects the metabolism of leaves in both elevated [CO_2] and water restriction

Chlorophyll content was not greatly altered between treatments and genotypes (Supplemental fig. S5 A and B). Significant changes were observed in glucose, fructose and sucrose in all genotypes, mainly under both $aCO_{2\_50\%}$ and $eCO_{2\_50\%}$ (Fig. 5, A, B and C), which means that water availability is rather important in the regulation of the sugar levels. For example, glucose levels were generally to be higher in the *slac1* mutant lines as compared to WT plants after 17WR, irrespective of [CO_2] (Fig. 5C). The starch level also tended to be higher in *slac1-4* when compared to WT under $aCO_{2\_50\%}$, with no changes under the other conditions (Supplemental Fig. S5 E). No changes in the levels of malate and fumarate were observed (Fig. 5, A and B). On the other hand, nitrate levels reduced under both $aCO_{2\_100\%}$ and $eCO_{2\_100\%}$ in at least one of the mutant lines (Fig. 5C). The content of amino acids, as well as proteins, increased under both $eCO_{2\_100\%}$ and $eCO_{2\_50\%}$, and it was observed that *slac1-3* showed a significant increase in amino acids levels as compared to WT under $aCO_{2\_50\%}$ (Fig. 5, D and E).

The metabolic profile of guard cells was affected by the mutation of SLAC1

Further metabolic characterization of the stomatal phenotype in the mutants was performed by a detailed analysis of the primary metabolism in guard cell-enriched epidermal fragments by using the established GC-MS approach (Lisec et al., 2006). Our metabolite analysis revealed that, among the 20 successfully annotated compounds, considerable changes in amino acids, as well as in both tricarboxylic acid cycle and photorespiratory intermediates, were observed. Thus, the functional lack of SLAC1 greatly affected the metabolic profile in guard cells (GC) of mutant lines (Fig. 6 and Supplemental Table S3). Briefly, all metabolites identified were significantly increased in guard cells of *slac1-3* under $aCO_{2\_100\%}$. Similarly, almost all metabolites were increased in *slac1-3* plants under $eCO_{2\_50\%}$, an exception was methionine and sucrose levels which reduced, and glycerol, that was invariant. Sucrose was the only metabolite that decreased in all genotypes under eCO_2. Highest levels of fructose, glucose, and rhamnose were observed at eCO_2, regardless of water conditions. Interestingly, proline remained higher in *slac1-3*, irrespective of [CO_2] or WR (Fig. 6).

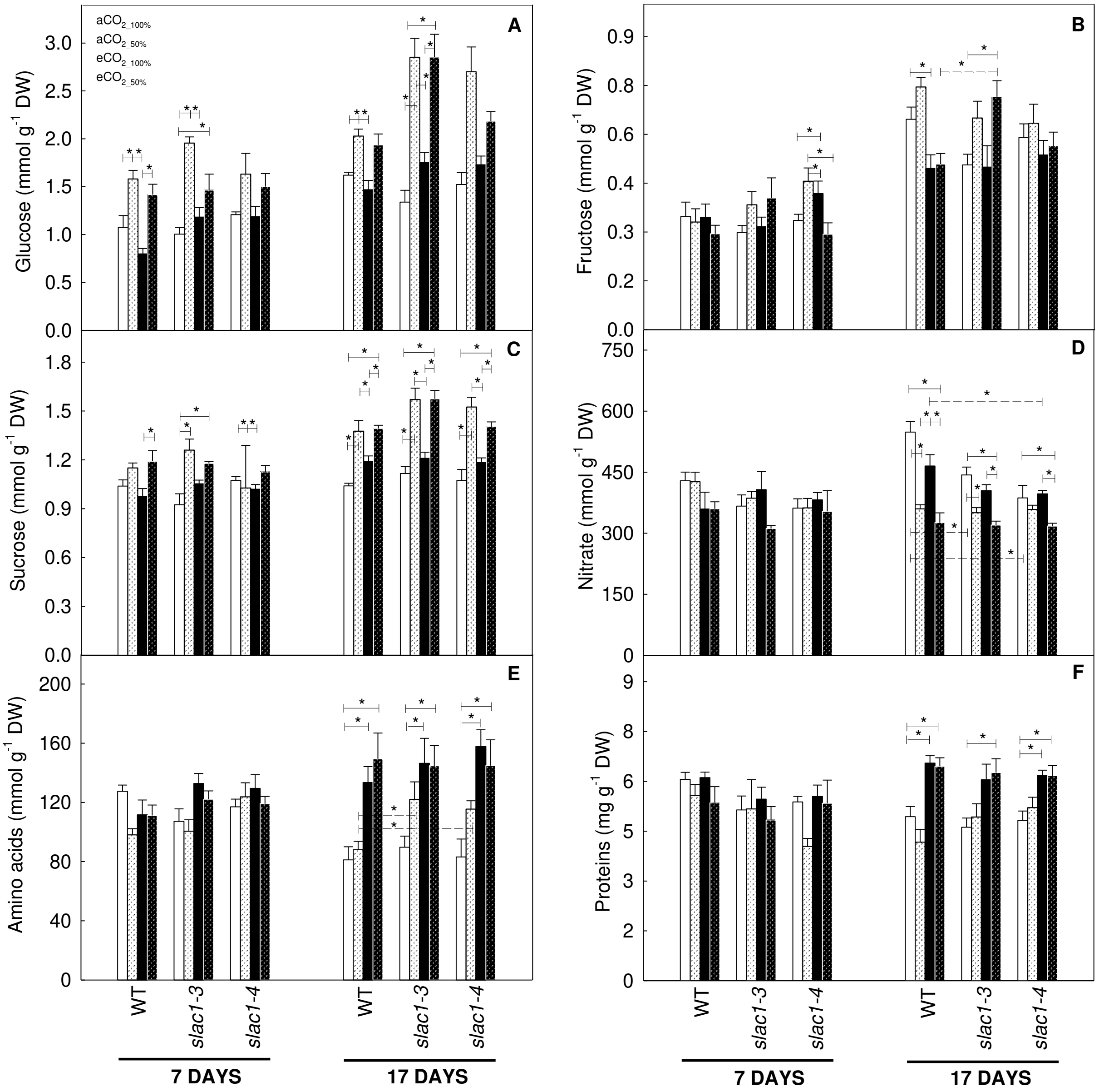

Figure 5. Metabolic responses of leaves *slac1* mutant plants in response to isolated or combination of water restriction and elevated [CO$_2$]. (A) Glucose; (B) Fructose; (C) Sucrose; (D) Nitrate; (E) Amino acids; (F) Proteins. 7 days: plants analyzed 7 days after reaching 50% of water in the soil; 10 days: plants analyzed 10 days after reaching 50% of water in the soil. Detail as in Figure 1. Values are presented as means ± SE (n = 5). Dashed line compares the three genotypes under the same condition. Continuous line compares a genotype under different conditions.

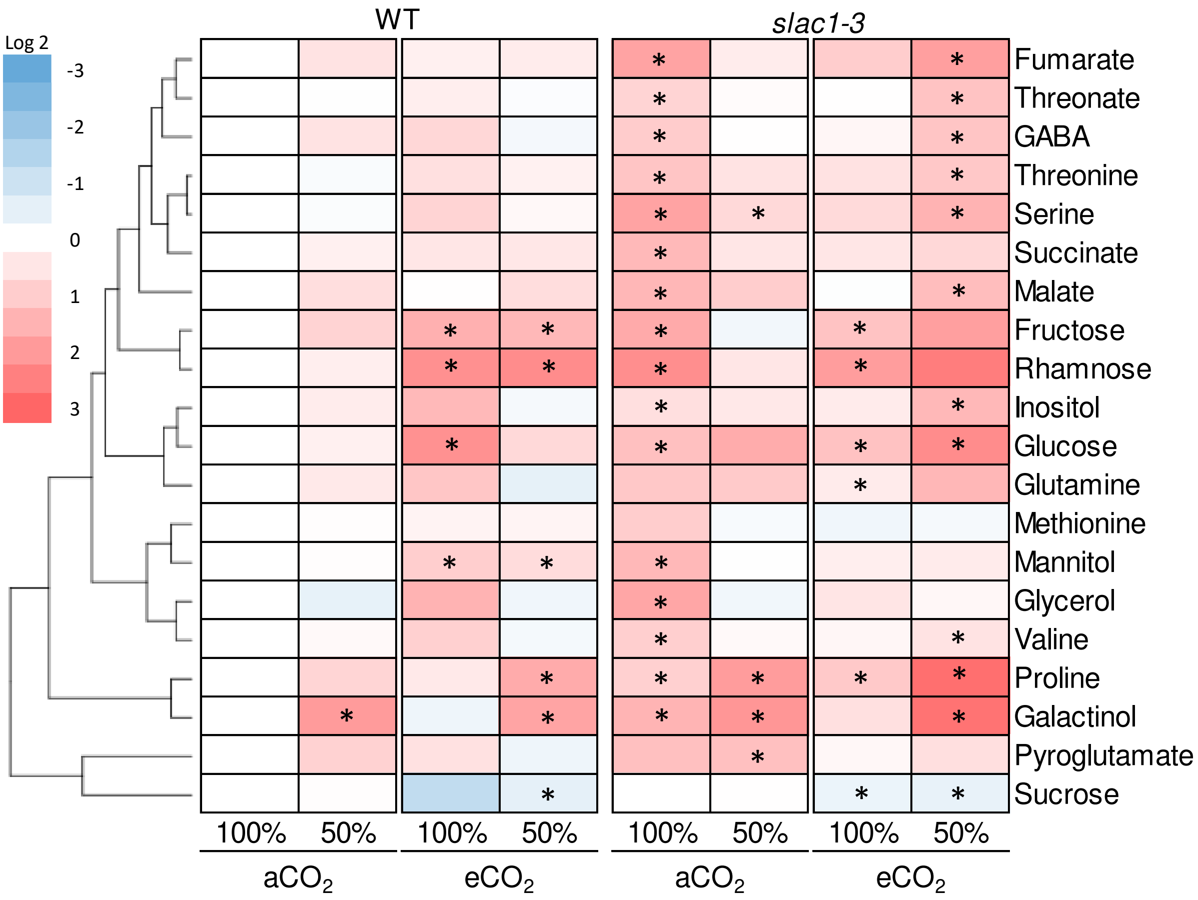

Figure 6. Changes in the relative metabolite content in guard cell-enriched epidermal fragments from *slac1* mutant plants in response to isolated or combination of water restriction and elevated [CO_2]. The full data sets from these metabolic profiling studies are additionally available in Supplemental Table S3. Data are normalized with respect to the mean response calculated for the wild-type (WT) growing under ambient and fully available water ($aCO_{2\_100\%}$). To allow statistical assessment, individual plants from this set were normalized in the same way. Detail as in Figure 1. Values are presented as means ± SE (n = 4-5). The results from plants *slac1-3* and WT were compared with WT $aCO_{2\_100\%}$ by Student's *t*-test. An asterisk (*) indicate significantly different by the Student's *t* test (*P*<0.05).

NCED5 gene expression increased in *slac1-3* independently of either [CO_2] or water restriction.

We next evaluated whether the metabolic perturbations observed were accompanied by changes in the expression of important stomata related genes in guard cell-enriched epidermal fragments, which are several genes encoding ion channels, transporters and signaling proteins in guard cells as well as stress markers (Supplemental Table S3). To our surprise, gene expression pattern was highly similar in both *slac1-3* and WT plants. Accordingly, the expression of genes involved in either stomatal closure or opening did not present a clear response to the variation of either

[CO2] or water restriction. Thus, CA4, OST1, KAT2, and ALMT6 expression decreased regardless of growth conditions; by contrast, AHA2 was increased. It was also observed that the expression of ABCB14 and NCED5 displayed a negative correlation with eCO2 only in WT under $eCO_{2\_100\%}$. Interestingly, NCED5 expression increased in *slac1-3* when compared to WT under $aCO_{2\_100\%}$, irrespectively of the growth conditions (Fig. 7).

.

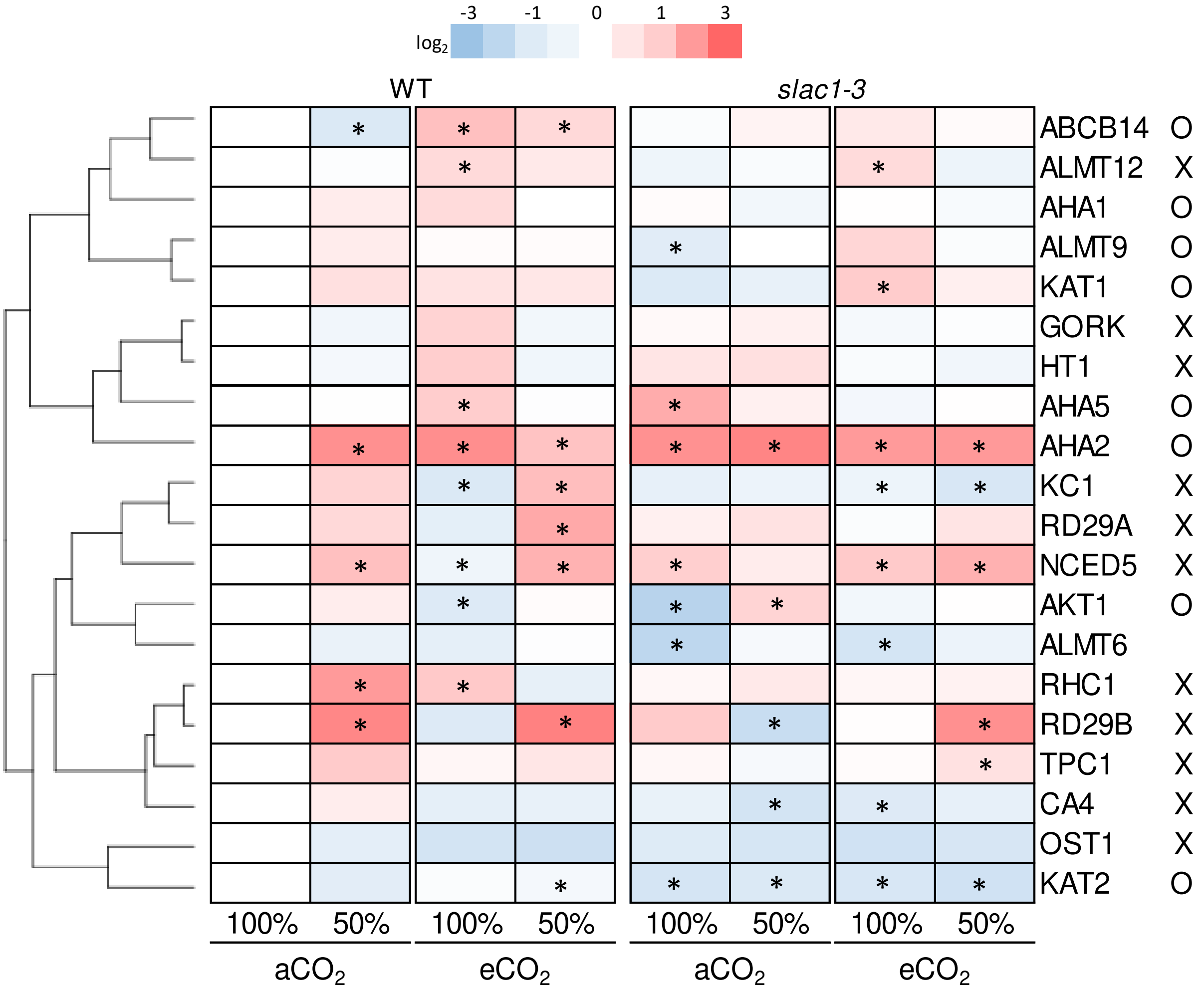

Figure 7. Changes in relative transcript levels of genes involved in stomatal responses in *slac1* mutant plants. Selected genes are associated with the opening (O) or closing (X) stomatal responses. RNA was isolated from guard cell-enriched epidermal fragments isolated from 4-week-old plants from WT and *slac1-3* mutant. Data are normalized with respect to the mean response calculated for the corresponding constitutively expressed *ACTIN* gene. In addition, data are normalized with respect to the mean response calculated for the corresponding WT of each growth condition. The full data sets from these gene studies are additionally available in Supplemental Table S4. Detail as in Figure 1. Values are presented as means ± SE (n = 4-5). The results from plants *slac1-3 and* WT were compared with WT $aCO_{2\_100\%}$ by Student's *t*-test. An asterisk (*) indicate significantly different by the Student's *t* test ($P<0.05$).

DISCUSSION

Stomata pores, formed by two surrounding guard cells in the epidermis of plant leaves, act as the pressure regulator of the xylem, preventing vessels cavitation under limited water availability (David et al., 2007). Simultaneously, this highly specialized cell type allows the influx of atmospheric CO_2 in exchange for transpirational water loss. Notably, under optimal growth conditions, plants with increased g_s have been characterized by increased photosynthetic rates and growth as well as a reduction in leaf temperature (Araújo et al., 2011; Medeiros et al., 2016; Chaves et al., 2016). On the other hand, both stomatal and mesophyll limitations (Flexas et al., 2008) may decrease the CO_2 diffusion from the atmosphere to the carboxylation site being the major cause of decreasing in photosynthesis under mild to moderate water limitation (Chaves et al., 2009; Flexas et al., 2004; Grassi and Magnani, 2005). Accordingly, the aperture of stomatal pores is effectively regulated by the transport of osmotically active ions and metabolites across guard cell membranes. S-type anion channels are directly modulated by the signaling cascade mediated by ABA and contribute to chloride and nitrate release from guard cells, which in turn initiates stomatal closure (Negi at al., 2008; Yamamoto et al., 2016). SLAC1 was the first component of the guard cell S-type anion channel identified and showed be essential in response to elevated [CO_2] (Negi et al., 2008), low air humidity and high vapor pressure difference (VPD; Wang et al., 2012), ozone (Vahisalu et al, 2010), drought-stress (Geiger et al., 2009) and microorganism infection (Deger et al., 2015). Despite the vital role of guard cells in controlling plant water loss, and established knowledge that rate of photosynthesis is directly modulated by distinct diffusive conductances that govern the CO_2 transfer from the atmosphere to the carboxylation sites, it still remains unclear how changes in stomatal function respond to environmental fluctuations. To further enhance our understanding of the stomatal regulation we compared plants that (*i*) have normal control of the stomatal movement (wild type; WT) and (*ii*) plants that have constitutively high g_s and low sensitivity to ABA (*slac1* mutants). Collectively, the results presented here demonstrate the combined or isolated impact of decreased water availability on the soil and increased [CO_2] on both leaf morphology and leaf metabolism.

Enhanced g_s does not lead to changes in g_m and A_N in *slac1*

The functional lack of the SLAC1 protein lead to plants with low sensitivity to ABA in either aCO_2 or eCO_2 (Supplemental Fig. S1 A end B), in good agreement with previous results obtained by independent studies (Negi at al., 2008; Vahisalu et al., 2008; Tian et al., 2015; Yamamoto et al., 2016; Wang et al., 2016). This response favors a higher water loss of detached rosette leaves in two *slac1* lines (Supplemental Fig. S1 C), indicating that the absence of SLAC1 is likelily unfavorable in an environment with the occurrence of water restriction, an inevitable problem worldwide. This fact apart, our results demonstrate that, under a mild/moderate water restriction, *slac1* plants may be rather favorable due to the fact that higher g_s sustain photosynthetic rates. In the agreement, we observed that increased g_s (~60%) did not influence the photosynthesis in *slac1* plants compared to WT under a$CO_{2_100\%}$ and e$CO_{2_100\%}$ (Fig. 4A and C). Perhaps more importantly, this indifference in A_N among genotypes are not due to limiting light issues (Supplemental Fig. S2 A). Interestingly, it has been previously demonstrated that *quac1* mutant plants displaying ~ 31% higher g_s were characterized by increases in both A_N and growth compared to WT under ambient conditions of water and [CO_2] (Medeiros et al., 2016). Despite the smaller increase in g_s of *quac1* plants in comparison to *slac1* mutant plants, an increased g_m, V_{cmax}, and J_{max} were observed in *quac1*, whereas these parameters did not significantly vary between WT and *slac1* mutant plants (Table 1). In addition, neither leaf anatomical constraints nor mesophyll limitations were observed in *slac1* plants that would explain, at least partially, the absence of changes in g_m in plants with higher g_s (Fig. 3; Table 1; Ouyang et al., 2017). Our study also shows that *slac1* plants were characterized by higher g_s without impacts in both g_m and A_N, in good agreement with previous results (Mizokami et al., 2018). These authors did not observe significant changes between WT and mutant plants with higher g_s (*ost1* and *slac1-2*) and provided compelling evidence that reductions in g_m are not conditional on reductions of g_s under high [CO_2]. Furthermore, the highest g_s maintained by *slac1* plants under all growth conditions were coupled with relatively minor increases in the C_i/C_a ratio and a subtle increase in A_N under a$CO_{2_50\%}$, e$CO_{2_100\%}$, and e$CO_{2_50\%}$ compared to WT plants under the same conditions. Together, the results obtained here demonstrated that under moderate water limitations, plants with higher g_s are characterized by similar photosynthetic performance and growth to plants with unaltered stomatal control, despite lower *WUE* (Fig 2, Fig 4A, C, D).

Collectively, our results indicate that drought-tolerant plants can be developed by genetically modulating change in stomatal response. Although several independent studies have reported transgenic plants with improved drought tolerance under either laboratory conditions (Van Houtte et al., 2013; Matsuda et al., 2016; Kuromori et al., 2017; Li et al., 2017; Kaundal et al., 2017) or field trials (Selvaraj et al., 2017; Parent et al., 2015), further research is clearly required to uncover the regulatory mechanism of drought response and tolerance under field conditions, particularly, in the context of future global climate change. Efforts to develop cultivars having high water usage flexibility should aid in the generation of high-yield performance crops under at least moderate drought conditions.

slac1 guard cells accumulate higher levels of proline and galactinol

Biochemical analyses were performed with both 7 and 17 days of water restriction, while analyses of the epidermal fragments occurred with 17 days. It should be borne in mind that the water replenishment was performed daily to maintain 50% and 100% of the water into the soil whereas the [CO_2] was imposed from the beginning of the transplant. It is equally important to highlight that most of the differences in metabolite levels were observed in more advanced stress (17 days, Fig. 5). Thus, after 17 days, *slac1* tended to display higher content of glucose, sucrose and amino acids under $aCO_{2\_50\%}$ likely allowing a greater osmoprotective function (Granda and Camarero, 2017; Galili et al., 2016), which might be associated with the maintenance of stomatal opening in those plants. In guard cells, the metabolic modifications were mostly marked between WT and *slac1-3* under $aCO_{2\_100\%}$ and $eCO_{2\_50\%}$. Under these conditions, there was an overall increase in metabolites content in *slac1-3*. Noteworthy, one of the metabolites characterized by a highly significant accumulation was proline in *slac1-3* under all experimental conditions. It seems reasonable to suppose that the increased proline (up to 7 times fold) is likely due to the constitutive stomatal opening of *slac1* independent of the soil water supply. Furthermore, proline formation can function as an electron dissipation mechanism (Liang et al., 2013) by reducing the amount of singlet oxygen, which causes lipid peroxidation of thylakoid membranes (Alia et al., 1997), providing evidence that proline is an important contributor to cellular redox balance (Szabados and Savoure, 2010). Another stress-relieving substance found in almost all conditions except eCO$_{2\_100\%}$ was galactinol, that reached concentration up to 7x higher than the levels found under control (aCO$_{2\_100\%}$; Fig. 6). Galactinol was detected only in seeds and flowers under stressful conditions but showed significant accumulation of galactinol in transgenic plants of *AtGolS2* overexpression under normal conditions (Taji et al., 2002). The increased levels of galactinol in *slac1* probably performed a similar function as in the *AtGolS2* mutants, since the overexpression of *AtGolS2*, a key enzyme for galactinol production, was associated with reduction in leaf transpiration improving drought tolerance in *Arabidopsis* (Taji et al., 2002) and rice (Selvaraj et al., 2017). Other common stress-related amino acids, such as gamma-aminobutyric acid (GABA), serine, valine, and threonine, in addition to sugars and organic acids, increased significantly in *slac1* plants under aCO$_{2\_100\%}$ eCO$_{2\_50\%}$. It seems therefore that the constitutive increase of the stomatal opening observed in *slac-1* mutant plants is associated with an exquisite reorganization of primary metabolism, increasing mainly sugars, amino acids, and organic acids, and represent another likely adaptive mechanism for maintaining the rate of respiration in guard cells of these mutant genotypes. Strong connections of the plant metabolic network have been previously observed (Lawson et al., 2014; Daloso et al., 2017), and it does, however, clearly mean that considerable work is still required to achieve a mechanistic understanding of the significance of stomatal movements in governing plant growth from a metabolic perspective.

The lower sensibility of *slac1* to ABA is not related with changes in the expression of ABA-related genes

Changes in gene expression were similar between *slac1* and WT. Interestingly, the *KC1* gene, the negative regulator of *KAT*s and *AKT1* (Zhang et al., 2016), was downregulated in *slac1-3* plants in all treatments. It is known that SLAC1 regulates the activity of K$^+$ channels along with *KC1* (Zhang et al., 2016), thus, we expected that *SLAC1* have some regulatory action on KC1 and therefore it would be upregulated in an attempt to inhibit the transport of K$^+$ ions into the guard cells of *slac1-3* mutants. This premise would work as a compensatory measure for the stomatal closure since this gene is upregulated under water restriction in WT. In addition, increased expression of genes indicative of water stress *RD29A* and *NCED5* (Xiong et al., 1999;

Sussmilch et al., 2017), in *slac1-3* plants under normal water and CO_2 conditions is likely in agreement with this assumption. In addition, *NCED5* was upregulated in *slac1-3* under all conditions, assuming that these plants already have intrinsic ABA production. Likewise, study with mutants *slac1-2* and ost1 showed ABA increment of 5-6x greater than in WT (Mizokami et al., 2018). It evidences again, that plants *slac1* are under stress effect constantly, regardless of the water restriction. Although the greater g_s in *slac1* did not provide a significant increase in A_N in any of the experimental conditions tested here, it seems to have greatly altered the metabolism of guard cell, as well as the expression of key genes of the stomatal closure in order to compensate for the probable constitutive stress caused by the maximum of the stomatal opening.

In summary, the results presented here indicate the greater stomatal conductance of mutant *slac1* plants, independent of CO_2 and water conditions, does not always result in greater photosynthetic capacity and higher growth. We have also observed that *slac1* mutant plants naturally produce metabolites designed to cope with water deficiency. This response may be related to a high and constitutive stomatal opening which instead of benefiting the plant with greater absorption of CO_2 promotes metabolic responses in guard cells that are highly similar to the ones observed following stress conditions. It appears that in *slac1* the leaf loses water faster than its replenishing capacity from the water uptake by the roots. This allows us to speculate there is a limit on the increase in conductance that is able to increase photosynthesis and growth. When this limit is extrapolated, the effect seems to be opposite and changes in the guard cell metabolism to tolerate the water restriction are observed, as the great increase in proline and galactinol in addition to the high expression of NCED - directly related to ABA biosynthesis. The metabolic reprogramming observed in *slac1* plants appears to be important in inducing water retention and maintaining water content in leaves similar to wild type, especially when elevated CO_2 and water deficiency are associated.

REFERENCES

Alia, Saradhi PP, Mohanty P (1997) Involvement of proline in protecting thylakoid membranes against free radical-induced photodamage. Journal of Photochemistry and Photobiology B: Biology 38: 253-257

Araújo WL, Nunes-Nesi A, Osorio S, Usadel B, Fuentes D, Nagy R, Balbo I, Lehmann M, Studart-Witkowski C, Tohge T, Martinoia E, Jordana X, DaMatta FM, Fernie AR (2011) Antisense Inhibition of the Iron-Sulphur Subunit of Succinate Dehydrogenase Enhances Photosynthesis and Growth in Tomato via an Organic Acid–Mediated Effect on Stomatal Aperture. The Plant Cell 23: 600-627

Arvidsson S, Kwasniewski M, Riaño-Pachón DM, Mueller-Roeber B (2008) QuantPrime - a flexible tool for reliable high-throughput primer design for quantitative PCR. Bmc Bioinformatics 9

Azoulay-Shemer T, Palomares A, Bagheri A, Israelsson-Nordstrom M, Engineer CB, Bargmann BOR, Stephan AB, Schroeder JI (2015) Guard cell photosynthesis is critical for stomatal turgor production yet does not directly mediate CO_2- and ABA-induced stomatal closing. The Plant Journal 83: 567-581

Bernacchi CJ, Portis AR, Nakano H, von Caemmerer S, Long SP (2002) Temperature response of mesophyll conductance. Implications for the determination of Rubisco enzyme kinetics and for limitations to photosynthesis in vivo. Plant Physiol 130: 1992-1998

Bradford MM (1976) Rapid and Sensitive Method for the Quantitation of Microgram Quantities of Protein Utilizing the Principle of Protein-Dye Binding. Analytical Biochemistry 72: 248-254

Brodribb TJ, McAdam SAM (2011) Passive origins of stomatal control in vascular plants. Science 331*:* 582-585

Buckley TN, Mott KA (2013) Modelling stomatal conductance in response to environmental factors. Plant, Cell and Environment 36: 1691-1699

Centritto M, Lauteri M, Monteverdi MC, Serraj R (2009) Leaf gas exchange, carbon isotope discrimination, and grain yield in contrasting rice genotypes subjected to water deficits during the reproductive stage. Journal Of Experimental Botany 60: 2325-2339

Chaves MM, Flexas J, Pinheiro C (2009) Photosynthesis under drought and salt stress: regulation mechanisms from whole plant to cell. Annals of Botany 103: 551-560

Chaves MMM, Costa JMM, Zarrouk O, Pinheiro C, Lopes CMM, Pereira JSS (2016) Controlling stomatal aperture in semi-arid regions-the dilemma of saving water or being cool? Plant Sciense 251: 54-64

Chen YH, Hu L, Punta M, Bruni R, Hillerich B, Kloss B, Rost B, Love J, Siegelbaum SA, Hendrickson WA (2010) Homologue structure of the SLAC1 anion channel for closing stomata in leaves. Nature 467: 1074-1080

Czechowski T, Stitt M, Altmann T, Udvardi MK, Scheible W-R (2005) Genome-wide identification and testing of superior reference genes for transcript normalization in *Arabidopsis*. Plant Physiology 139: 5-17

Daloso DM, Medeiros DB, Dos Anjos L, Yoshida T, Araújo WL, Fernie AR (2017) Metabolism within the specialized guard cells of plants. New Phytologist 16: 1018-1033

David TS, Henriques MO, Kurz-Besson C, Nunes J, Valente F, Vaz M, Pereira JS, Siegwolf R, Chaves MM, Gazarini LC, David JS (2007) Water use strategies in two co-occurring Mediterranean evergreen oaks: surviving the summer drought. Tree Physiology 27: 793-803

Deger, AG, Scherzer S, Nuhkat M, Kedzierska J, Kollist H, Brosché M, Unyayar S, Boudsocq M, Hedrich R, Roelfsema M R G (2015) Guard cell SLAC1-type anion channels mediate flagellin-induced stomatal closure. New Phytologist 208: 62-173

Farquhar GD, von Caemmerer S, Berry JA (1980) A biochemical model of photosynthetic CO_2 assimilation in leaves of C3 species. Planta 149: 78-90

Fernie AR, Aharoni A, Willmitzer L, Stitt M, Tohge T, Kopka J, Carroll AJ, Saito K, Fraser PD, DeLuca V (2011) Recommendations for Reporting Metabolite Data. The Plant Cell 23: 2477-2482

Fernie AR, Roscher A, Ratcliffe RG, Kruger NJ (2001) Fructose 2,6-bisphosphate activates pyrophosphate: fructose-6-phosphate 1-phosphotransferase and increases triose phosphate to hexose phosphate cycling in heterotrophic cells. Planta 212: 250-263

Flexas J, Bota J, Loreto F, Cornic G, Sharkey TD (2004) Diffusive and metabolic limitations to photosynthesis under drought and salinity in C3 plants. Plant Biology 6: 269-279

Flexas J, Ribas-Carbo M, Diaz-Espejo A, Galmes J, Medrano H (2008) Mesophyll conductance to CO_2: Current knowledge and future prospects. Plant, Cell and Environment 31: 602-621

Fujita T, Noguchi K, Terashima I (2013) Apoplastic mesophyll signals induce rapid stomatal responses to CO_2 in *Commelina communis*. New Phytologist 199: 395-406

Galili G, Amir R, Fernie AR (2016) The Regulation of Essential Amino Acid Synthesis and Accumulation in Plants. Annual Review of Plant Biology 67:153-78

Geiger D, Scherzer S, Mumm P, Stange A, Marten I, Bauer H, Ache P, Matschi S, Liese A, Al-Rasheid KA, Romeis T, Hedrich R (2009) Activity of guard cell anion channel SLAC1 is controlled by drought-stress signaling kinase-phosphatase pair. Proceedings of the National Academy of Sciences 106: 21425-21430

Genty B, Briantais JM, Baker NR (1989) The relationship between the quantum yield of photosynthetic electron transport and quenching of chlorophyll fluorescence. Biochimica Et Biophysica Acta (BBA) - General Subjects 990: 87-92

Granda E1, Camarero JJ (2017) Drought reduces growth and stimulates sugar accumulation: new evidence of environmentally driven non-structural carbohydrate use. Tree Physiology 37:997-1000

Grassi G, Magnani F (2005) Stomatal, mesophyll conductance and biochemical limitations to photosynthesis as affected by drought and leaf ontogeny in ash and oak trees. Plant, Cell and Environment 28: 834-849

Hashimoto M, Negi J, Young J, Israelsson M, Schroeder JI, Iba K (2006) *Arabidopsis* HT1 kinase controls stomatal movements in response to CO_2. Nature Cell Biology 8: 391-397

Hunt R, Causton DR, Shipley B, Askew AP (2002) A modern tool for classical plant growth analysis. Ann Bot (Lond) 90: 485-488

Johansen DA (1940) Plant microtechnique. New York: Mcgraw-Hill Book 523 p

Kaundal A, Ramu VS, Oh S, Lee S, Pant B, Lee HK, Rojas CM, Senthil-Kumar M, Mysore KS (2017) General control nonrepressible4 Degrades 14-3-3 and the RIN4 Complex to Regulate Stomatal Aperture with Implications on Nonhost Disease Resistance and Drought Tolerance. Plant Cell 29: 2233-2248

Kopka J, Schauer N, Krueger S, Birkemeyer C, Usadel B, Bergmuller E, Dormann P, Gibon Y, Stitt M, Willmitzer, L, Fernie AR, Steinhauser D (2005) GMD@CSBDB: The Golm Metabolome Database. Bioinformatics 21: 1635-1638

Kumar R, Arya GC, Bisht NC (2014) Differential expression and interaction specificity of heterotrimeric G-protein family in *Brassica nigra* reveal their developmental and condition-specific roles. Plant and Cell Physiology 55: 1954-1968

Kuromori T, Sugimoto E, Ohiraki H, Yamaguchi-Shinozaki K, Shinozaki K (2017) Functional relationship of AtABCG21 and AtABCG22 in stomatal regulation. Scientific Reports 7: 12501

Kusumi K, Hirotsuka S, Kumamaru T, Iba K (2012) Increased leaf photosynthesis caused by elevated stomatal conductance in a rice mutant deficient in SLAC1, a guard cell anion channel protein. Journal of Experimental Botany 63: 5635-5644

Laanemets K, Wang YF, Lindgren O, Wu J, Nishimura N, Lee S, Caddell D, Merilo E, Brosche M, Kilk K, Soomets U, Kangasjärvi J, Schroeder JI, Kollist H (2012) Mutations in the SLAC1 anion channel slow stomatal opening and severely reduce K^+ uptake channel activity via enhanced cytosolic [Ca^{2+}] and increased Ca^{2+} sensitivity of K^+ uptake channels. New Phytologist 197: 88-98

Larionov A Krause A, Miller W (2005) A standard curve as ed method for relative real time PCR data processing. BMC Bioinformatics 6: 62

Lawson T, Simkin AJ, Kelly G, Granot D (2014) Mesophyll photosynthesis and guard cell metabolism impacts on stomatal behaviour. New Phytologist 203: 1064-81

Lee SC, Lan WZ, Buchanan BB, Luan S (2009) A protein kinase-phosphatase pair interacts with an ion channel to regulate ABA signaling in plant guard cells. Proceedings of the National Academy of Sciences, USA 106: 21419-21424

Li J, Li Y, Yin Z, Jiang J, Zhang M, Guo X, Ye Z, Zhao Y, Xiong H, Zhang Z, Shao Y, Jiang C, Zhang H, An G, Paek NC, Ali J, Li Z (2017) OsASR5 enhances drought tolerance through a stomatal closure pathway associated with ABA and H_2O_2 signalling in rice. Plant Biotechnology Journal 215: 183-196

Liang Liang X, Zhang L, Natarajan SK, Donald F (2013) Proline Mechanisms of Stress Survival Antioxid Redox Signal 19: 998-1011

Lisec J, Schauer N, Kopka J, Willmitzer L, Fernie AR (2006) Gas chromatography mass spectrometry–based metabolite profiling in plants. Nature Protocols 1: 387-396

Liu F, Jensen CR, Shahanzari A, Andersen MN, Jacobsen SE (2005) ABA regulated stomatal control and photosynthetic water use efficiency of potato (*Solanum tuberosum* L.) during progressive soil drying. The Plant Science 168: 831-836

Liu F, Shahnazari A, Andersen MN, Jacobsen SE, Jensen CR (2006) Effects of deficit irrigation (DI) and partial root drying (PRD) on gas exchange biomass partitioning, and water use efficiency in potato. Scientia Horticulturae 109: 113-117

Logan BA, Adams WIII, Demmig-Adams B (2007) Avoiding common pitfalls of chlorophyll fluorescence analysis under field conditions 34: 853-859

Long SP, Bernacchi CJ (2003) Gas exchange measurements, what can they tell us about the underlying limitations to photosynthesis? Procedures and sources of error. Journal Experimental Botany 54: 2393-2401

Luedemann A, Strassburg K, Erban A, Kopka J (2008) TagFinder for the quantitative analysis of gas chromatography-mass spectrometry (GC-MS)-based metabolite profiling experiments. Bioinformatics 24: 732-737

Maierhofer T, Diekmann M, Offenborn JN, Lind C, Bauer H, Hashimoto K, KA SAR, Luan S, Kudla J, Geiger D, Hedrich R (2014) Site- and kinase-specific phosphorylation-mediated activation of SLAC1, a guard cell anion channel stimulated by abscisic acid. Science Signaling 7: ra86

Martins SCV, Galmés J, Molins A, DaMatta FM (2013) Improving the estimation of mesophyll conductance to CO_2: on the role of electron transport rate correction and respiration. Journal Experimental Botany 64: 1-14

Matsuda S, Takano S, Sato M, Furukawa K, Nagasawa H, Yoshikawa S, Kasuga J, Tokuji Y, Yazaki K, Nakazono M, Takamure I, Kato K (2016) Rice Stomatal Closure Requires Guard Cell Plasma Membrane ATP-Binding Cassette Transporter RCN1/OsABCG5. Molecular Plant 9: 417-427

Medeiros DB, Martins SCV, Cavalcanti JHF, Daloso DM, Martinoia E, Nunes-Nesi A, DaMatta FM, Fernie AR, Araújo WL (2016) Enhanced Photosynthesis and Growth in *atquac1* Knockout Mutants Are Due to Altered Organic Acid Accumulation and an Increase in Both Stomatal and Mesophyll Conductance. Plant Physiology 170: 86-101

Mizokami Y, Noguchi K, Kojima M, Sakakibara H, Terashima I Effects of instantaneous and growth CO_2 levels and abscisic acid on stomatal and mesophyll conductances (2018) Plant Cell and Environment 1-13

Mori H (2000) Direct determination of nitrate using nitrate reductase in a flow system. Journal of Health Sciences 46: 385-388

Nackley LL, Vogt KA, Kim S (2014) Arundo donax water use and photosynthetic responses to drought and elevated CO_2. Agricultural Water Management 136: 13-22

Negi J, Matsuda O, Nagasawa T, Oba Y, Takahashi H, Kawai-Yamada M, Uchimiya H, Hashimoto M, Iba K (2008) CO_2 regulator SLAC1 and its homologues are essential for anion homeostasis in plant cells. Nature 452: 483-486

Nunes-Nesi A, Carrari F, Gibon Y, Sulpice R, Lytovchenko A, Fisahn J, Graham J, Ratcliffe RG, Sweetlove LJ, Fernie AR (2007) Deficiency of mitochondrial fumarase activity in tomato plants impairs photosynthesis via an effect on stomatal function. The Plant Journal 50: 1093-1106

O'Brien TP, Feder N, Mccully ME (1964) Polychromatic staining of plant cell walls by toluidine blue O. Protoplasma 59: 368-373

Ouyang W, Struik PC, Yin X, Yang J (2017) Stomatal conductance, mesophyll conductance, and transpiration efficiency in relation to leaf anatomy in rice and wheat genotypes under drought. Journal of Experimental Botany 68:5191-5205

Pandey S, Wang X-Q, Coursol SA, Assmann SM (2002) Preparation and applications of *Arabidopsis thaliana* guard cell protoplasts. New Phytologist 153: 517-526

Parent B, Shahinnia F, Maphosa L, Berger B, Rabie H, Chalmers K, Kovalchuk A, Langridge P, Fleury D (2015) Combining field performance with controlled environment plant imaging to identify the genetic control of growth and transpiration underlying yield response to water-deficit stress in wheat. Journal Experimental Botany 66: 5481-92

Pazzagli PT, Weiner J, Liu F (2016) Effects of CO_2 elevation and irrigation regimes on leaf gas exchange, plant water relations, and water use efficiency of two tomato cultivars. Agricultural Water Management 169: 26-33

Pilot G, Lacombe B, Gaymard F, Chérel I, Boucherez J, Thibaud JB, Sentenac H. (2001) Guard cell inward K^+ channel activity in *Arabidopsis* involves expression of the twin channel subunits KAT1 and KAT2. Journal of Biological Chemistry 276: 3215-3221

Pinelli P, Loreto F (2003) $^{12}CO_2$ emission from different metabolic pathways measured in illuminated and darkened C3 and C4 leaves at low, atmospheric and elevated CO_2 concentration. Journal of Experimental Botany v. 54: 1761-1769

Porra R, Thompson W, Kriedemann P (1989) Determination of accurate extinction coefficients and simultaneous equations for assaying chlorophylls a and b extracted with four different solvents: verification of the concentration of chlorophyll standards by atomic absorption spectroscopy. Biochimica Et Biophysica Acta (BBA) - Bioenergetics 975: 384-394

Raven JA (2002) Selection pressures on stomatal evolution. New Phytologist 153: 371-386.

Rodeghiero M, Niinemets U, Cescatti A (2007) Major diffusion leaks of clamp-on leaf cuvettes still unaccounted: how erroneous are the estimates of Farquhar et al. model parameters? Plant, Cell and Environment 30: 1006-1022

Schachtman DP, Goodger JQ (2008) Chemical root to shoot signaling under drought. Trends Plant Science 13:281-7

Schindelin J, Rueden CT, Hiner MC, Eliceiri KW (2015) The ImageJ ecosystem: an open platform for biomedical image analysis. Mol Reprod Dev 82: 518-529

Schroeder JI1, Kwak JM, Allen GJ (2001) Guard cell abscisic acid signalling and engineering drought hardiness in plants. Nature 410: 327-30

Selvaraj MG, Ishizaki T, Valencia M, Ogawa S, Dedicova B, Ogata T, Yoshiwara K, Maruyama K, Kusano M, Saito K, Takahashi F, Shinozaki K, Nakashima K, Ishitani M (2017) Overexpression of an *Arabidopsis* thaliana galactinol synthase gene improves drought tolerance in transgenic rice and increased grain yield in the field. Plant Biotechnology Journal 15: 1465-1477

Sharkey TD, Bernacchi CJ, Farquhar GD, Singsaas EL (2007) Fitting photosynthetic carbon dioxide response curves for C3 leaves. Plant, Cell and Environment 30: 1035-1040

Sussmilch FC, Brodribb TJ, McAdam SAM (2017) Up-regulation of NCED3 and ABA biosynthesis occur within minutes of a decrease in leaf turgor but AHK1. Journal of Experimental Botany 68: 2913-2918

Szabados L, Savoure, A (2010) Proline: a multifunctional amino acid. Trends Plant Sciense. 15: 89-97

Taji T, Ohsumi C, Iuchi S, Seki M, Kasuga M, Kobayashi M (2002) Important roles of drought and cold-inducible genes for galactinol synthase in stress tolerance in *Arabidopsis thaliana*. The Plant Journal 29: 417-426

Tian W, Hou C, Ren Z, Pan Y, Jia J, Zhang H, Bai F, Zhang P, Zhu H, He Y, Luo S, Li L, Luan S (2015) A molecular pathway for CO_2 response in *Arabidopsis* guard cells. Nature Communications 6: 6057

Vahisalu T, Puzõrjova I, Brosché M, Valk E, Lepiku M, Moldau H, Pechter P, Wang YS, Lindgren O, Salojärvi J (2010) Ozone-triggered rapid stomatal response involves the production of reactive oxygen species and is controlled by SLAC1 and OST1. The Plant Journal 62: 442-453

Vahisalu T, Kollist H, Wang YF, Nishimura N, Chan WY, Valerio G, Lamminmäki A, Brosché M, Moldau H, Desikan R, Schroeder JI, Kangasjärvi J (2008) SLAC1 is required for plant guard cell S-type anion channel function in stomatal signalling. Nature 452: 487-491

Valentini R, Epron D, De Angelis P, Matteucci G, Dreyer E (1995) In situ estimation of net CO_2 assimilation, photosynthetic electron flow and photorespiration in

Turkey oak (*Quercus cerris* L.) leaves: diurnal cycles under different levels of water supply. Plant, Cell and Environment 18: 631-640

Van Houtte H, Vandesteene L, López-Galvis L, Lemmens L, Kissel E, Carpentier S, Feil R, Avonce N, Beeckman T, Lunn JE, Van Dijck P (2013) Overexpression of the trehalase gene AtTRE1 leads to increased drought stress tolerance in *Arabidopsis* and is involved in abscisic acid-induced stomatal closure. Plant Physiol. 161: 1158-71

Vishwakarma K, Upadhyay N, Kumar N, Yadav G, Singh J, Mishra RK, Kumar V, Verma R, Upadhyay RG, Pandey M, Sharma S (2018) Abscisic Acid Signaling and Abiotic Stress Tolerance in Plants: Review on Current Knowledgeand Future Prospects. Frontiers in Plant Science 20: 161

Vu JCV, Allen LH (2009) Growth at elevated CO_2 delays the adverse effects of drought stress on leaf photosynthesis of the C4 sugarcane. Journal of Plant Physiology 166:107-116

Walker B, Ariza LS, Kaines S, Badger MR, Cousins AB (2013) Temperature response of in vivo Rubisco kinetics and mesophyll conductance in *Arabidopsis thaliana*: comparisons to Nicotiana tabacum. Plant Cell Environ 36: 2108-2119

Wang C, Hu H, Qin X, Zeise B, Xu D, Rappel WJ, Boron WF, Schroeder JI (2016) Reconstitution of CO_2 Regulation of SLAC1 Anion Channel and Function of CO_2 -Permeable PIP2;1 Aquaporin as carbonic anhydrase4 Interactor. The Plant Cell 28: 568-582

Wang Y, Papanatsiou M, Eisenach CR, Williams M, Hills A, Lew VL, Blatt MR (2012) Systems Dynamic Modeling of a Guard Cell Cl^- Channel Mutant Uncovers an Emergent Homeostatic Network Regulating Stomatal Transpiration. Plant Physiology 160: 1956-1967

Xiong L, Ishitani M, Zhu JK (1999) Interaction of osmotic stress, temperature, and abscisic acid in the regulation of gene expression in *Arabidopsis*. Plant Physiology 119: 205-212

Yamamoto Y, Negi J, Wang C, Isogai Y, Schroeder JI, Iba K (2016) The Transmembrane Region of Guard Cell SLAC1 Channels Perceives CO_2 Signals via an ABA-Independent Pathway in *Arabidopsis*. The Plant Cell 28: 557-567

Yemm EW, Cocking E, Ricketts RE (1955) The Determination of Amino-Acids with Ninhydrin. The Analyst 80: 209

Yoshida R, Umezawa T, Mizoguchi T, Takahashi S, Takahashi F, Shinozaki K (2006) The regulatory domain of SRK2E/OST1/SnRK2.6 interacts with ABI1 and integrates abscisic acid (ABA) and osmotic stress signals controlling stomatal closure in *Arabidopsis*. The Journal of Biological Chemistry 281: 5310-8

Zhang A, Ren HM, Tan YQ, Qi GN, Yao FY, Wu GL, Yang LW, Hussain J, Sun SJ, Wang YF (2016) S-type Anion Channels SLAC1 and SLAH3 Function as Essential Negative Regulators of Inward K^+ Channels and Stomatal Opening in *Arabidopsis*. Plant Cell 28: 949-955

SUPPLEMENTAL DATA

Supplemental Table S1. Photosynthetic parameters from light-response curves in WT and *slac1* plants. Values are presented as means ± SE (n = 4-5). Lowercase letters compare a genotype under different conditions of [CO2] and uppercase letters compare the three genotypes under the same treatment condition. Means followed by the same letter not differentiated by a one-way ANOVA followed by Tukey test (P< 0.05) between genotypes or treatments.

Parameters*	WT		*slac1-3*		*slac1-4*	
	aCO_2	eCO_2	aCO_2	eCO_2	aCO_2	eCO_2
A_{max} (μmol CO_2 m^{-2} s^{-1})	9.81 ± 0.21 Aa	16.27 ± 0.62 Ab	9.94 ± 0.07 Aa	18.519 ± 0.71 Ab	11.2 ± 0.46 Ba	16.305 ± 1.09 Ab
I_c (μmol m^{-2} s^{-1})	11.59 ± 0.09 Aa	4.48 ± 1.74 Ab	14.17 ± 0.74 Aa	9.875 ± 2.61 Ab	19.24 ± 1.58 Aa	13.119 ± 0.32 Ab
I_s (μmol m^{-2} s^{-1})	358.3 ± 20.3 Aa	568.9 ± 66.06 Ab	459.0 ± 9.42 ABa	659.7 ± 41.17 Ab	860.21 ± 60.65 Ba	643.4 ± 73.11 Ab
$1/\phi$ (μmol photons mol^{-1} CO_2)	21.5 ± 0.84 Aa	15.36 ± 2.07 Ab	19.07 ± 0.62 Aa	13.353 ± 1.48 Ab	19.53 ± 1.11 Aa	14.292 ± 0.56 Ab

*A_{max}: net CO_2 assimilation rate saturated by light; I_c: light compensation point; I_s: light saturation point; $1/\phi$: light use efficiency.

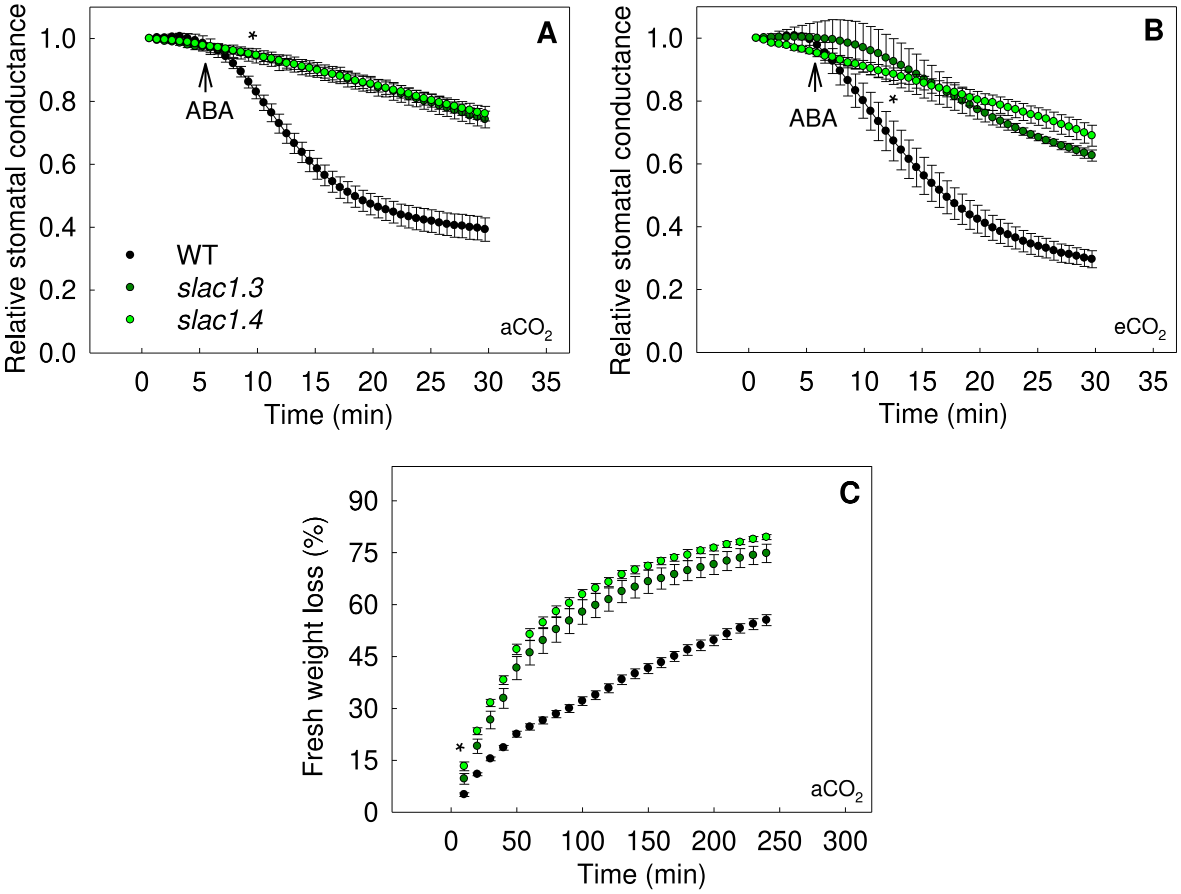

Supplemental Figure S1. Water loss from whole rosettes and analyses of ABA-induced stomatal conductance kinetics is altered in *slac1* mutant plants. Stomatal closing kinetics in response to exogenous ABA application in plants growing under either ambient [aCO_2] (A) or elevated [CO_2] (eCO_2) (B), and fresh weight loss from detached whole rosettes in WT (wild-type) and *slac1* mutant plants growing under ambient [CO_2] (C). In A and B the arrow indicates the application of exogenous ABA 1 μm on petri dishes where the leaf petiole was immersed. During the first initial minutes, the petiole was immersed only in the opening buffer (see Material and Methods for details). Ambient and elevated CO_2 represents plants grown at 400 and 800 ppm, respectively. IRGA analyzes were performed with the respective CO_2 concentration in which the plants were cultivated. The means of each genotype was relativized by their respective initial conductance. The data were submitted an unpaired two-tailed Student *t*-test used for the comparison between WT and *slac1*. An asterisk (*) indicates a significant difference ($P<0.05$).

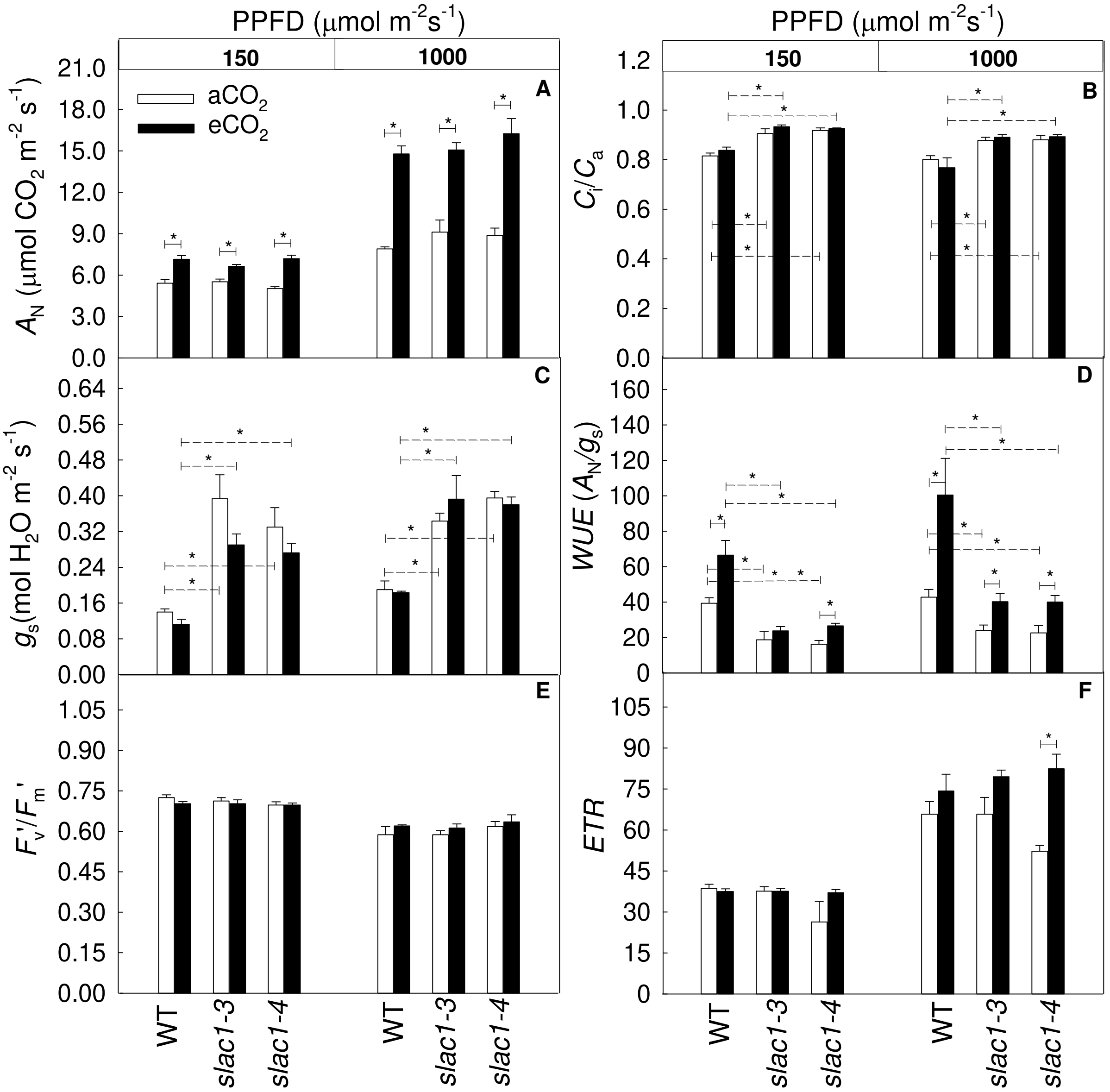

Supplemental Figure S2. Photosynthetic characterization of *slac1* mutant plants. Gas exchange and chlorophyll fluorescence parameters were determined in plants under growth irradiance (150 µmol photons m^{-2} s^{-1}) and saturation, but not photoinhibitory, irradiance (1000 µmol photons m^{-2} s^{-1}). (A) A_N, Net photosynthesis rate; (B) g_s, stomatal conductance; (C) C_i/C_a, ratio between concentration internal carbon and atmospheric carbon; (D) WUE_i, intrinsic water use efficiency; (E) F_v'/F_m', actual PSII photochemical efficiency; (F) ETR, electron transport rate estimated by chlorophyll fluorescence parameters. Values are presented as means ± SE (n = 5). Means followed by the same letter are not different by a one-way ANOVA followed by Tukey test between genotypes or treatments. Dashed lines compare the three genotypes under the same condition. Continuous line compares a genotype under different conditions. An asterisk (*) indicates a significant difference ($P<0.05$).

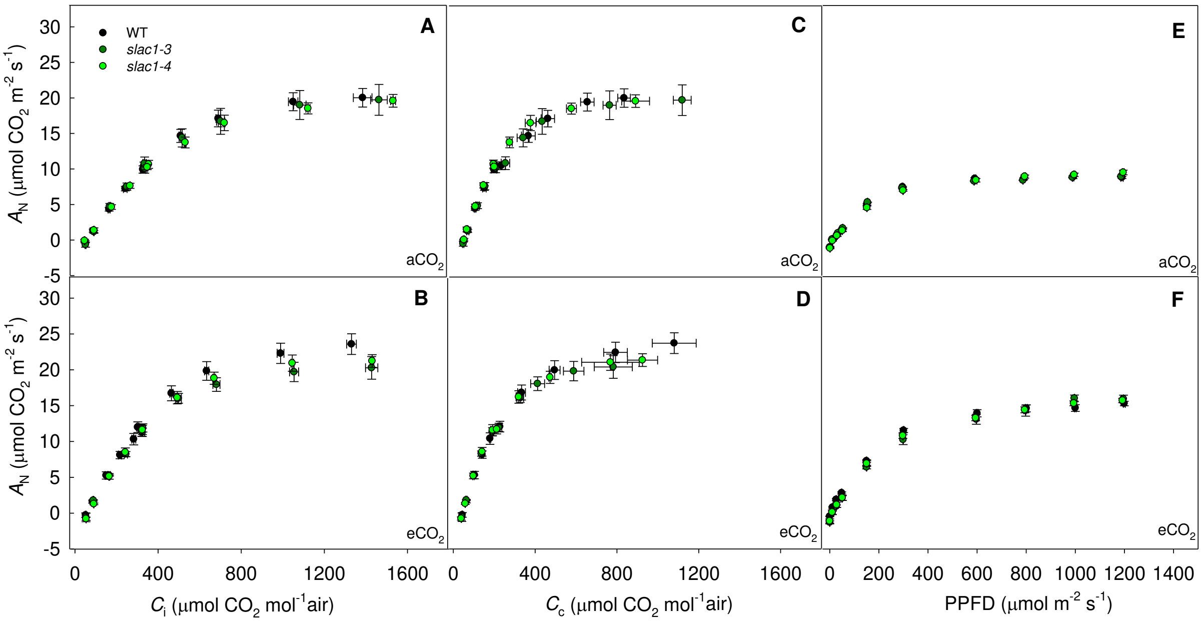

Supplemental Figure S3. Net photosynthesis (A_N) curves in response to changes in substomatal (C_i) or chloroplastic (C_c) CO$_2$ concentrations and photosynthetically active photon flux density (PPFD) of rosettes from at least 4-week-old. Ambient (aCO$_2$) or elevated (eCO$_2$) represents plants which were cultivated at either 400 and 800 ppm, respectively. Photosynthetic light-response curves *(A*/PPFD) were performed under growing ambient CO$_2$ concentration (C_a) of 400 or 800 µmol mol^{-1}. A_N /C_i curves were performed at saturated light of 1000 µmol m^{-2} s^{-1} at 25°C under ambient O$_2$ and started at ambient CO$_2$ concentration (C_a) of 400 µmol mol^{-1} independent of the growing conditions. Values were compared between WT (wild-type) and *slac1* mutant plants by Student's *t*-test (P<0.05). Values are presented as means ± SE (n = 4) obtained using the ninth leaf totally expanded from different plants per genotype in two independent assays.

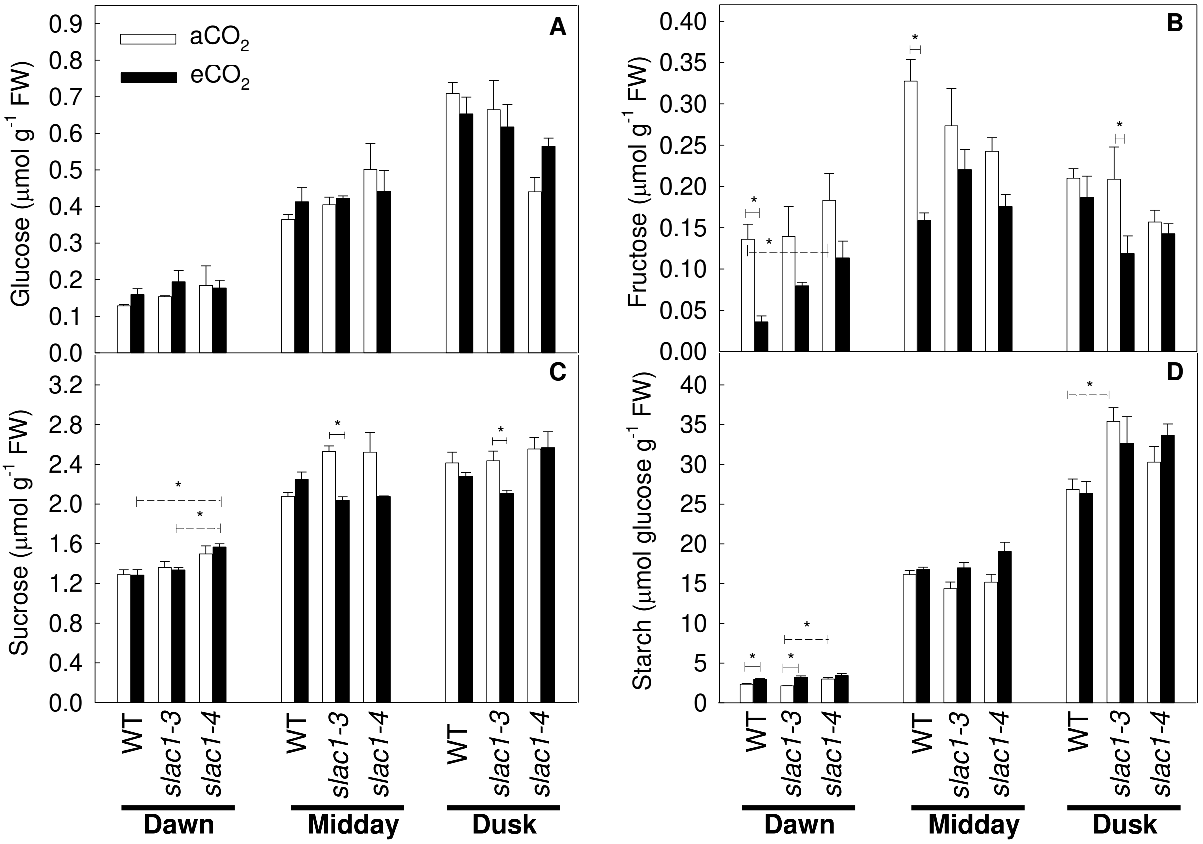

Supplemental Figure S4. Influence of [CO$_2$] on the metabolism along the day in mutant plants 4,5-week-old. Dawn, midday, and dusk represent plants collected before, in the middle and end of the photoperiod. Values are presented as means ± SE (n = 5). The means comparison was performed through a one-way ANOVA followed by Tukey test. Dashed line compares the three genotypes under the same treatment condition. Continuous line compares a genotype under different conditions. * indicates a significant difference (*P*<0.05).

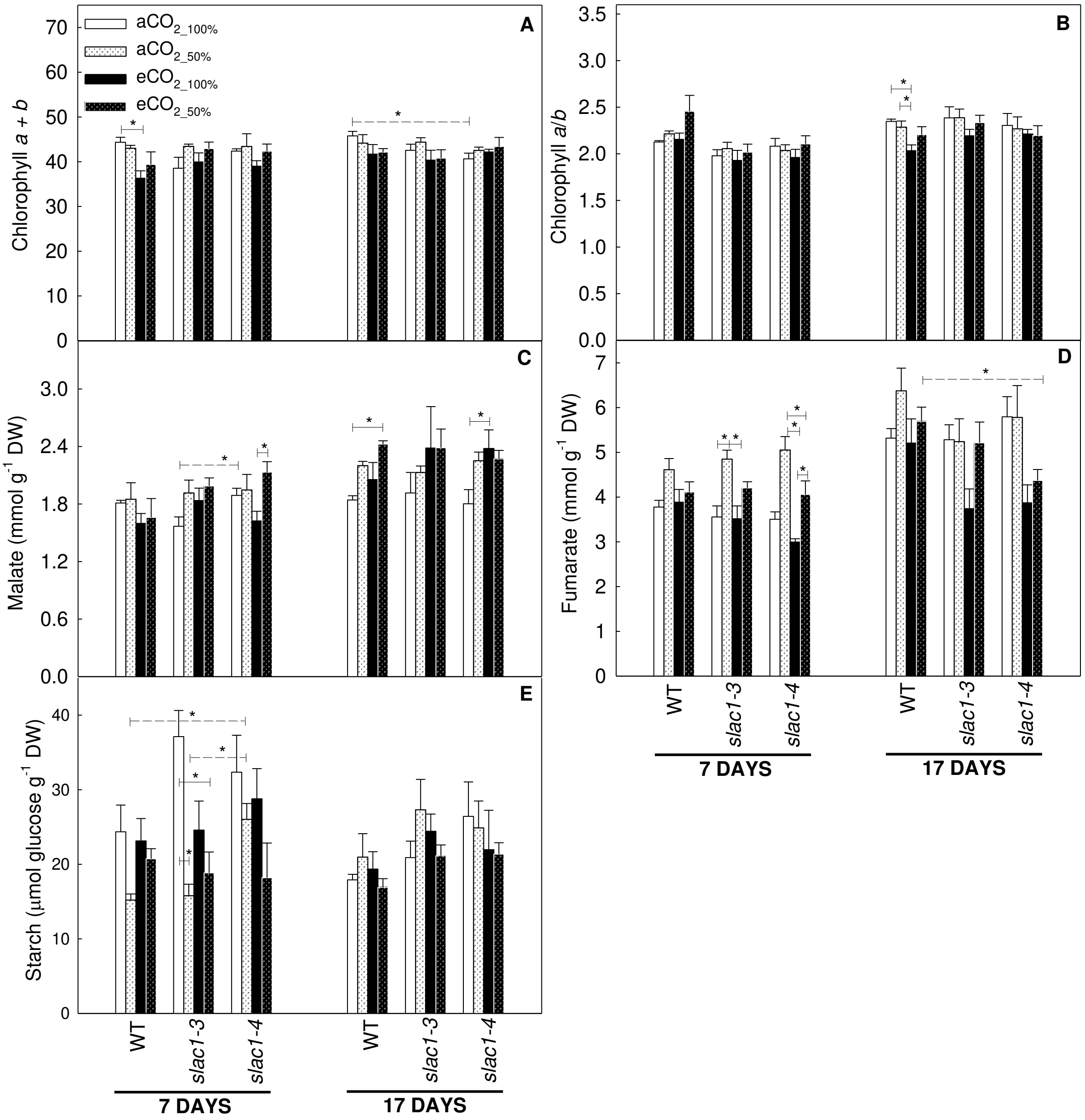

Supplemental Figure S5. Metabolic responses to a combination of water restriction under concentrations ambient and elevated of CO_2.Detail as in Figure 2. Values are presented as means ± SE (n = 5). Means followed by the same letter not differentiated by a one-way ANOVA followed by Tukey test between genotypes or treatments. Dashed line compares the three genotypes under the same treatment condition. Continuous line compares a genotype under different conditions. * indicates a significant difference (*P*<0.05).

Supplemental Table S2. Primers utilized to qRT-PCR.

Gene	Locus	Efficiency	Sequence
Actina (control)	At2g37620	**108.4**	Forward 5' - CTTGCACCAAGCAGCATGAA - 3' Reverse 5' - CCGATCCAGACACTGTACTTCCTT - 3'
ABC14	At1g28010	**113.35**	Forward 5' - AGCTTTTCTACAGACCCGAATGCC - 3' Reverse 5' - TGCATCCAACAAGCAACTCCAATC - 3'
AHA1	At2g18960	**103.89**	Forward 5' - CTGGGAGGCTACCAAGCCA - 3' Reverse 5' - CTCACACCGAACTTGTCCGA - 3'
AHA2	At4g30190	**107.49**	Forward 5' - CCGGAGTCTTCCCAGGTT- 3' Reverse 5' - TTTAGAGCAGGGGCATCATT- 3'
AHA5	At2g24520	**97.39**	Forward 5' - GGCTGTTGCAAGACAGGAA - 3' Reverse 5' - CGGAGGATCAAAAAGAGGTAAA - 3'
AKT1	At2g26650	**90.49**	Forward 5' - ACATCCTTGTGAACGGAACC - 3' Reverse 5' - CCTCTCTCACAATGCTTTCTGTT - 3'
ALMT12	At4g17970	**98.66**	Forward 5' - CGGCAAAGTCCTTCGAGCTATC - 3' Reverse 5' - ATATAAGTAGCAGCCGCTCCAATG - 3'
ALMT6	At2g17470	**140.83**	Forward 5' - AGCCTCCACATGGACCTTACAG - 3' Reverse 5' - CGTTTCTCTGGAGCTGCCTGTATC - 3'
ALMT9	At3g18440	**117.08**	Forward 5' - TCTCTCAGAAATCCAGGCACCAG - 3' Reverse 5' - ACGCCCACTCTCTGAAGTTCTTG - 3'
BCA4	At1g70410	**90.22**	Forward 5' - TGGGTGAAGATAGGCGCATCAG - 3' Reverse 5' - AGCGATACGTTCACAGCTTCCTTC - 3'
GORK	At5g37500	**102.21**	Forward 5' - GCATCAATCCGCGCCAAGATT - 3' Reverse 5' - GTGGAGCAGCCTTTGAAGAGA - 3'
HT1	At1g62400	**102.16**	Forward 5' - AGTTTAAGTCCGAGGTTGCTCTGC - 3' Reverse 5' - CATTCGGAGGTTTCCTTGTGACA - 3'
KAT1	At5g46240	**95.07**	Forward 5' - AGCATGGGATGGGAAGAGTGGAG - 3' Reverse 5' - AGAGCAGTGTCGGAAGTCGGAT - 3'
KAT2	At4g18290	**103.24**	Forward 5' - TAGCTCGCTGTTTGCAAGG - 3' Reverse 5' - CAAACAGTGTCACCGAAATGA - 3'
KC1	At4g32650	**115.09**	Forward 5' - CTCAAGACATGAAAATGGACAGAT- 3' Reverse 5' - GAATCACCATTGTTTTTGTTATCTTG - 3'
NCED5	At1g30100	**83.84**	Forward 5' - ACGCCGTTACGTTGGAACTAGAAG - 3' Reverse 5' - AACATATCCGCCGAATTCACGAAA - 3'
OST1	At4g33950	**157.15**	Forward 5' - GACCCTGCAAAGAGGATATCAAT - 3' Reverse 5' - TTTGGCCCGGTTGATCCGATTC - 3'
RD29A	At5g52310	**105.7**	Forward 5' - TGGACAAAGCAATGAGCATGAGC - 3' Reverse 5' - AGGTTTACCTGTTACGCCTGGTG - 3'
RD29B	At5g52300	**160.03**	Forward 5' - ACTGATCCCACGCATAAAGGTG - 3' Reverse 5' - CTCGTCGGAAAGTCTTCTTCGC - 3'
RHC1	At4g22790	**92.99**	Forward 5' - TGCCTTGAATGGTGGTGCTACG - 3' Reverse 5' - AGCTTGCACCGGGTTTGGTAAC - 3'
SLAC1	At1g12480	**118.71**	Forward 5' - ATGGCCAATTCGACGGATGTTC - 3' Reverse 5' - ACCACGCCACTGAGAACTTAAATC - 3'
TPC1	At4g03560	**86.45**	Forward 5' - CGCTTGATATCGAAGAAAGCTC - 3' Reverse 5' - TCTCCAACACATATATCCAACCA - 3'

Supplemental Table S3. Relative abundance of primary metabolite levels in guard cell-enriched epidermal fragments from *slac1-3* mutant plants in response to isolated or combination of water restriction and elevated [CO$_2$]. Data are normalized with respect to the mean response calculated for the wild-type (WT) growing under ambient and fully available water (aCO$_{2\_100\%}$). To allow statistical assessment, individual plants from this set were normalized in the same way. Detail as in Figure 1. Values are presented as means ± SE (n = 4-5).

METABOLITE	WT				*slac1-3*			
	aCO$_{2\_100\%}$	aCO$_{2\_50\%}$	eCO$_{2\_100\%}$	eCO$_{2\_50\%}$	aCO$_{2\_100\%}$	aCO$_{2\_50\%}$	eCO$_{2\_100\%}$	eCO$_{2\_50\%}$
Fumarate	1.00	1.48	1.24	1.31	**3.50**	1.31	1.98	**3.73**
Threonate	1.00	0.99	1.26	0.95	**1.82**	1.07	1.03	**2.29**
GABA	1.00	1.47	1.73	0.86	**2.01**	1.03	1.14	**2.21**
Threonine	1.00	0.93	1.54	1.21	**2.20**	1.48	1.49	**2.13**
Serine	1.00	0.94	1.81	1.11	**3.49**	**1.69**	1.66	**2.81**
Succinate	1.00	1.23	1.42	1.40	**2.61**	1.41	1.41	1.71
Malate	1.00	1.58	1.03	1.60	**2.68**	1.98	0.98	**2.48**
Fructose	1.00	1.84	**2.95**	**2.65**	**3.21**	0.84	**2.29**	3.70
Rhamnose	1.00	1.27	**4.54**	**4.78**	**4.69**	1.42	**3.82**	5.87
Inositol	1.00	1.30	2.62	0.87	**1.56**	1.38	1.32	**2.63**
Glucose	1.00	1.23	**4.51**	1.68	**2.37**	3.12	**2.29**	**4.82**
Glutamine	1.00	1.35	2.19	0.72	2.11	2.07	**1.32**	2.69
Methionine	1.00	1.03	1.19	1.17	1.99	0.91	0.82	0.88
Mannitol	1.00	1.04	**1.95**	**1.62**	**2.63**	1.00	1.27	1.32
Glycerol	1.00	0.73	2.84	0.82	**3.35**	0.83	1.43	1.12
Valine	1.00	1.09	1.91	0.87	**1.94**	1.10	1.14	**1.47**
Proline	1.00	1.78	1.36	**3.15**	**1.92**	**3.87**	**2.09**	**7.14**
Galactinol	1.00	**3.93**	0.80	**3.48**	**2.81**	**4.19**	1.54	**6.79**
Pyroglutamic acid	1.00	1.85	1.52	0.80	2.37	**2.38**	1.12	1.55
Sucrose	1.00	1.03	0.44	**0.71**	1.01	1.02	**0.77**	**0.74**

Supplemental Table S4. Changes in relative transcript levels of genes involved in stomatal responses in *slac1* mutant plants. Selected genes are associated with the opening (O) or closing (X) stomatal responses. RNA was isolated from guard cell-enriched epidermal fragments isolated from 4-week-old plants from WT and *slac1-3* mutant. Data are normalized with respect to the mean response calculated for the corresponding constitutively expressed *ACTIN* gene. In addition, data are normalized with respect to the mean response calculated for the corresponding WT of each growth condition. Detail as in Figure 1. Values are presented as means ± SE (n = 4-5).

GENE	WT				*slac1-3*			
	aCO$_{2\_100\%}$	aCO$_{2\_50\%}$	eCO$_{2\_100\%}$	eCO$_{2\_50\%}$	aCO$_{2\_100\%}$	aCO$_{2\_50\%}$	eCO$_{2\_100\%}$	eCO$_{2\_50\%}$
ABCB14	1.00	**0.47**	**2.37**	**1.68**	0.90	1.18	1.36	1.07
ALMT12	1.00	0.96	**1.67**	1.36	0.71	0.89	**1.65**	0.68
AHA1	1.00	1.30	1.64	1.00	1.06	0.77	1.02	0.85
ALMT9	1.00	1.30	1.07	1.07	**0.54**	1.00	1.77	0.91
KAT1	1.00	1.53	1.46	1.40	0.49	0.62	**2.01**	1.26
GORK	1.00	0.76	1.84	0.77	1.09	1.23	0.81	0.95
HT1	1.00	0.81	1.96	0.74	1.44	1.54	0.89	0.75
AHA5	1.00	1.00	1.98	0.97	**3.13**	1.24	0.78	1.02
AHA2	1.00	**4.53**	**4.68**	**2.26**	**4.51**	**5.26**	**4.00**	**4.02**
KC1	1.00	1.80	**0.47**	**2.43**	0.61	0.67	**0.69**	**0.44**
RD29A	1.00	1.69	0.58	**3.26**	1.23	1.49	0.91	1.45
NCED5	1.00	**2.36**	**0.72**	**2.85**	**1.94**	**1.30**	**2.07**	**2.90**
AKT1	1.00	1.28	**0.49**	1.07	**0.22**	**1.82**	**0.77**	1.02
ALMT6	1.00	0.65	0.58	0.96	**0.26**	0.83	**0.41**	**0.67**
RHC1	1.00	**3.97**	**2.10**	0.61	1.12	1.36	1.14	1.20
RD29B	1.00	**5.13**	0.49	**5.56**	2.04	**0.32**	1.03	**4.56**
TPC1	1.00	2.03	1.14	1.41	1.11	0.83	1.07	**1.51**
CA4	1.00	1.28	0.58	0.63	0.64	**0.40**	**0.50**	0.61
OST1	1.00	0.57	0.40	0.35	0.50	0.42	0.38	0.43
KAT2	1.00	0.55	0.91	0.81	**0.41**	**0.47**	**0.44**	**0.37**

Chapter 2

The functional lack of ABCB14 impacts stomatal responses but does not compromise photosynthetic capacity and growth under elevated [CO_2] and water restriction

CHAPTER 2: The functional lack of ABCB14 impacts stomatal responses but does not compromise photosynthetic capacity and growth under elevated [CO_2] and water restriction

ABSTRACT

The majority of the effects caused by the increased carbon dioxide concentration [CO_2] are derived from two classical responses: increased photosynthesis and reduced stomatal conductance, while drought reduces both parameters. The molecular identification and characterization of the ATP-binding cassette B14 (ABCB14) transporter demonstrated that its function under high [CO_2] is associated with the stomatal opening by modulating the transport of malate into the guard cell. Thus our efforts were devoted to the investigation at the physiological, metabolic and molecular responses of two mutant lines (*abcb14-1* and *abcb14-2*) and WT in a future a scenario of low water availability and elevated [CO_2]. Our results demonstrate that despite the reductions in the stomatal opening, the absence of a functional guard cell ABCB14 protein does not compromise overall photosynthetic activity and growth and that an exquisite metabolic and genetic regulations occur in guard cells likely compensating, at least partially, the functional lack of *abcb14*. Thus, the stomata may be benefiting partially of a metabolic and genetic regulation differentiated in guard cells, probably to keep higher stomatal conductance (g_s), that compensates part of the functional of *abcb14*. When considered together, this most likely indicates a relatively minor influence of ABCB14 on the growth of *Arabidopsis* plants and supports the notion that redundancy among guard cell transporter is likely in the species.

Key-words: *Arabidopsis thaliana*, apoplastic malate, low stomatal conductance, metabolism of guard cell.

INTRODUCTION

Water limitation is one of the most stressful factors often reduces plant growth and productivity. Stronger effects of drought are expected due to the occurrence of longer, more frequent and more intense drought episodes associated with climate changes (IPCC, 2014; Fang and Xiong, 2015; Peñuelas et al., 2013; De Souza et al., 2015). Simultaneously, the future atmosphere is also expected to contain considerably higher levels of CO_2, affecting plant growth and development. Both water limitation and high CO_2 are known to show distinct effects when each factor is applied separately (Roy et al., 2016; Robredo et al., 2011; Bauweraerts et al., 2013; Feng et al., 2014; Zinta et al., 2014, 2018). CO_2 and drought are usually investigated as isolated factors (Ainsworth and Long, 2005; Claeys, 2013; Terashima et al., 2014; Han et al., 2018). The common effects of drought include biomass reduction, inhibition of photosynthesis and induction of oxidative stress (Smirnoff, 1993; Liu and Huang, 2000; Wang et al., 2003; Salvucci and Craft-Brandner, 2004). Notably, a growing body of evidence demonstrated that elevated CO_2 mitigates these negatives effects by ameliorating soil water stress through increased plant water use efficiency (*WUE*) (Geissler et al., 2009; Van den Berge et al., 2011; Farfan-Vignolo and Asard, 2012; Salazar-Parra et al., 2012; Ameye et al., 2012, Bauweraerts et al., 2013, Naudts et al., 2013 and 2014), although both the strength and predictability of this mitigations is apparently widely variable both within and between experiments.

The majority of the effects caused by the increased [CO_2] are derived from two classical responses: increased photosynthesis and reduced stomatal conductance (Long et al., 2004). This fact apart, it is the combination of g_s and g_m that predominantly determines not only A_N but also *WUE*. Primarily, the response to CO_2 is detected by the stomata, microscopic pores surrounded by two specialized guard cells, based on intracellular [CO_2] (C_i) (Mott 1988). Distinct factors influence stomatal opening in land plants, including cytosolic calcium concentration, apoplast pH, membrane potential, phosphorylation/dephosphorylation of proteins and ion channels (Hetherington and Woodward, 2003; Daloso et al., 2017). Guard cells integrate all of these signals and convert them into appropriate turgor pressure changes by regulating the correct movement of ions and organic solutes into guard cells (Assmann, 1999). Remarkably, guard cells continuously respond to signals from the leaf environment, including abiotic and biotic stimuli, as well as long-distance signals from roots (Kim et al., 2010). It is expected that long term increases in atmospheric [CO_2] would lead to reductions of both stomatal apertures and stomatal density (Hetherington and Woodward, 2003). In turn, substantial reductions on gas exchange coupled with increases on intrinsic *WUE* and plant leaf temperatures are also expected, affecting ultimately crop yields. Due to the positive effects of elevated [CO_2], it is also expected that increased plant biomass may occur. This fact apart, climate changes are also associated with increased occurrence of abiotic stress, including drought, and as such elevated [CO_2] might not necessarily increase crop yield (Ruiz-Vera et al., 2015).

Stomatal responses are mediated by the transport of ions and water through transport proteins across the plasma and vacuolar membranes which in turn changes turgor and guard cell volume, thereby regulating stomatal aperture (Pandey et al., 2007). The main inorganic ions are potassium (K^+) and chloride (Cl^-) whereas malate and sucrose are considered as the main organic osmolytes associated with stomatal movements (Kollist et al., 2014). Compelling evidence has recently demonstrated that malate and, to a lower extent, fumarate act as important players during stomatal movements (Araújo et al., 2011; Medeiros et al., 2016). As such, channels and transporters were recently identified and functionally characterized to be involved with organic acid transport at both plasma membrane and tonoplast of guard cells (Martinoia, 2018). The efflux of malate to the apoplast stimulates the activity of the anion channel quick-activating anion channel 1 (QUAC1) maximizing stomatal closure (Hedrich and Marten, 1993; Hedrich et al., 1994; Meyer et al., 2010). In addition, elevated [CO_2] also induces the release of malate by mesophyll cells into the apoplast (Hedrich and Marten, 1993; Hedrich et al., 1994; Hedrich et al., 2001) by activating the inflow channel of malate in the opposite direction to QUAC1. This transport partially increases the osmotic pressure of the guard cells and leads to the partial stomatal opening. In *Arabidopsis*, the influx of apoplastic malate is mediated by the ABCB14. The activation of ABCB14 appears to occur from the increased concentration of malate in the apoplast caused by high intracellular [CO_2] (Hedrich et al., 1994; Lohaus et al., 2001; Lee et al., 2008). The molecular identification and characterization of the ABCB14 transporter demonstrated that its function under high [CO_2] is associated with stomatal closure by modulating the transport of malate into the guard cell (Lee et al., 2008). Interestingly, under normal conditions, *abcb14* mutant plants exhibit stomatal behavior similar to wild type (WT), revealing unnoticed importance of this carrier under ambient [CO_2] (Lee et al., 2008). This fact aside, the mechanisms by which CO_2 regulates stomatal movements and how exactly ABCB14 respond to changes in [CO_2] remains unknown.

Thus, here we hypothesized that ABCB14 may play an important role while allowing a modest stomatal opening that may be essential for continuity of gas exchanges under high [CO_2] conditions. Yet, the impacts of the reduced stomatal aperture provided by *abcb14* on photosynthetic rates, *WUE* and growth under high [CO_2] and water limitation were not investigated to update from a metabolic and molecular perspective. Insights from such studies can further enhance our understanding of how plants are currently processing the rising CO_2 levels and might allow further engineering of crop plants to adapt to climate change. Thus, here our efforts were devoted to the investigation of the physiological, metabolic and molecular responses of two mutant lines (*abcb14-1* and *abcb14-2*) and WT in a future a scenario of low water availability and elevated [CO_2].

MATERIAL AND METHODS

Plant material

All *Arabidopsis thaliana* plants used here were ecotype Columbia (Col-0) background. The T-DNA lines *abcb14-1* (SALK_099139) and *abcb14-2* (SALK_137265) were identified and characterized as described by Lee et al. (2008). Both knockout lines contain T-DNA insertion into exons of ABCB14 gene (for details, see Vahisalu et al., 2008). The expression of the mutant lines was identified by PCR using specific primers for *abcb14-1* (forward - TGGTCAAGTTAGGGAAACCGGA and reverse - GCAAGAACGGCACCAATTGAG) and *abcb14-2* (forward-GCAGACACAATCGTTGTATTGC and reverse-CCCAACACAATCGTATAACAAGTC).

Growth conditions

Seeds of *Arabidopsis* were directly sown on a commercial substrate (Carolina soil®) in plastic pots and two weeks after sowing, plants were transferred to individual 0.08 dm^3 pots containing also Carolina soil®. Wild-type (WT) and *abcb14* plants were grown under short-day conditions (8h light/16h dark) and light intensity of 150 $\mu mol\ m^{-2}\ s^{-1}$, at a temperature of 23 ºC/18 °C throughout the day/night cycle, and 65±10%

relative humidity. For examination of phenotype including both gas exchange and metabolism along the day, plants with 14 days were transferred to chambers with modified carbon dioxide concentration [CO_2]. CO_2 was injected only during daylight hours corresponding to the period when the plants are photosynthetically active. Plants were kept under optimum growth conditions with fully available water regime. In a second moment, we decided to associate [CO_2] with water restriction. To this end, plants were transferred to chambers with either 400±50 ppm (ambient - aCO_2) or 800±50 ppm of CO_2 (elevated - eCO_2). After two weeks, half of the plants at both aCO_2 and eCO_2 were submitted to water restriction (WR). For this assay, half of the plants cultivated at both ambient ($aCO_{2\_100\%}$) and elevated CO_2 ($eCO_{2\_100\%}$) were cultivated to 100% of the substrate water capacity, equivalent to the tension of 10 kPa (CET), corresponding to control group. The water replenishment was suspended for 7 days until the substrate reached 50% (CET) water availability for the remaining half of the plants. After the 7th day, the amount of water lost by evapotranspiration was daily replaced, maintaining 50% water availability. Both control and water limited-plants were cultivated up to 4-5 weeks at aCO_2 and eCO_2.

To summarize, at 14 days after transplanting seedlings growing in either aCO_2] or eCO_2 were submitted to water limitation conditions. Thus, four different treatments were applied: Control (ambient [CO_2] and 100% of the water capacity- $aCO_{2\_100\%}$), elevated [CO_2] and 100% of the water capacity- $eCO_{2\_100\%}$), ambient [CO_2] and 50% of the water capacity- $aCO_{2\_50\%}$) and elevated [CO_2] and 50% of the water capacity- $eCO_{2\_50\%}$). Measurements were performed during vegetative growth and the interaction treatments were maintained for the minimum of 17 days. Additionally, the experiments were repeated at least two times, even in different growth facilities, with similar phenotypes observed each time.

Growth analyses

Whole rosettes from at least 4-week-old plants were harvested and rosette dry weight (RDW), rosette fresh weight (RFW), rosette area (RA), total leaf area (LA), specific leaf area (SLA) and the number of rosette leaves were evaluated. To determine dry weight, rosettes were dried in an oven with forced air circulation at 60 °C until constant weight. LA was estimated by digital image method where the images were obtained using a scanner and later processed in ImageJ software (Schindelin et al., 2015). SLA was estimated as described by Hunt et al. (2002).

Water loss measurements

Whole rosettes from at least 4-week-old plants were detached and incubated with abaxial surface turned to up. For the estimation of water loss, the weight of detached rosettes was determined over 4 h at the indicated time points. Water loss was calculated as a percentage of fresh weight loss relative to the initial fresh weight (Araújo et al., 2011).

Relative water content (RWC)

The relative water content was determined in the middle of the light period. To this, one leaf of each plant was detached and then immediately weighed to obtain the fresh weight (FW). Thereafter, the leaves were hydrated for 2 h in Petri dish containing distilled water until saturation, when the turgid (TW) weight was recorded. Finally, the leaves were oven dried at 60 °C for 72 h; next, the leaves were weighted, obtaining thus dry weight (DW). The relative water content was calculated according to the equation: RWC = (FW - DW) / (TW - DW).

Morpho-anatomical traits

The median region of the 9th leaf totally expanded of rosettes from at least 4-week-old plants from WR and [CO_2] experiment was collected. These samples were immediately fixed at formaldehyde-acetic acid-ethanol (FAA) 50% (Johansen, 1940) for 24 h and subsequently stored in 70% alcohol. This material was included in methacrylate (Historesin-Leica), according to manufacturer's recommendations and transversely sectioned (5 µm thick) in auto-feed rotary microtome (model RM2155, Leica Microsystems Inc., Heidelberg, Germany), and stained with toluidine blue (O'Brien et al., 1964). Each sample was represented by the average of five replicates, each replicate being composed of measurements in three distinct points. The material was photographed under a light microscope (AX-70 TRF, Olympus Optical, Tokyo, Japan) coupled to a digital photographic camera (Zeiss AxioCam HRc model, Göttinger, Germany) and computer with Axion Vision image capture program. Finally, in the internerval region, the palisade and lacunaceous parenchyma thickness, mesophyll thickness, leaf thickness, and mesophyll intercellular spaces were analyzed using Image-Pro® Plus software (version 4.1, Media Cybernetics, Inc., Silver Spring, USA).

Stomatal opening and closing kinetics measurements

To assess the stomatal behavior in response to light/dark transition, stomatal conductance variations were recorded every 20 seconds using the same gas analyzer described above. Plants dark-adapted (at least 1h) were exposed to dark/light/dark transitions by 5/20/30 min, respectively, under CO_2 concentration of 400 µmol mol^{-1} (Meyer et al., 2010). To evaluate stomatal response to CO_2 concentration, leaves were exposed to transitions of 400/800/400 µmol CO_2 mol^{-1} by 5/40/40 min, respectively, under a light intensity of 150 µmol m^{-2} s^{-1} (Meyer et al., 2010). The stomatal responses to abscisic acid (ABA) were evaluated in the 9th fully expanded leaf of each genotype grown at either 400 or 800 ppm. First, leaves were cut and maintained in opening buffer (10 mM KCl, 50 µM $CaCl_2$, and 5 mM MES-Tris, pH 6.15) for 15 min (150 µmol m^{-2} s^{-1}) to stimulate the stomatal opening (Azoulay-Shemer et al., 2015). Finally, 1 µM of ABA solution was added to the opening buffer. Stomatal conductance values were recorded at intervals of 40 for over 25 min using an open-flow infrared gas exchange analyzer system (LI-6400XT; LI-COR Inc., Lincoln, NE) equipped with an integrated fluorescence chamber (LI-6400-40; LI-COR Inc.).

Gas exchange parameters

Gas exchange parameters were determined simultaneously with chlorophyll *a* (Chl *a*) fluorescence measurements using the same gas exchange system described above. Instantaneous gas exchanges, including net assimilation rate of carbon (A_N), stomatal conductance (g_s) and the internal carbon dioxide concentration (C_i), were measured after 1 h illumination during the light period under 150 µmol m^{-2} s^{-1} (light of growth) or 1000 µmol m^{-2} s^{-1} (non-photoinhibitory light saturation) at the leaf level of photosynthetically active photon flux density (PPFD). The reference CO_2 concentration was set at 400 or 800 µmol CO_2 mol^{-1} air under ambient or elevated [CO_2] conditions, respectively. All measurements were performed using the 2 cm^2 leaf chamber at 25 °C, as well as a 0.5 stomatal ratio (amphistomatic leaves), and leaf-to-air vapor pressure deficit, was kept between 1.0-1.5 kPa, while the amount of blue light was set to 10% PPFD to optimize stomatal aperture. The WR experiment, the gas exchange was measured only in the flux intensity of 150 µmol m^{-2} s^{-1}. Dark respiration (R_d) was measured using the same gas exchange system as described above on leaves adapted to the dark for at least 2 hours after the end of the light period. In complement, the mitochondrial respiration in light (R_l) was estimated as half of R_d (Pinelli and Loreto, 2003; Centritto et al., 2009). The photorespiratory rate of Rubisco (R_p) was estimated according to Valentini et al. (1995), as R_p=1/12[ETR – 4(A+R_l)].

Photosynthetic light-response curves *(A*/PPFD) were determined in plants from at least 4-week-old varying the PPFD from 0 to 1400 µmol (photons) m^{-2} s^{-1} under growing ambient CO_2 concentration (C_a) of 400 or 800 µmol mol^{-1}. Likewise, the responses of A_N to C_i (A_N /C_i curves) were performed at saturated light of 1000 µmol m^{-2} s^{-1} at 25°C under ambient O_2. Briefly, the measurements started at ambient CO_2 concentration (C_a) of 400 µmol mol^{-1} and when the steady state was reached, C_a was decreased stepwise to 50 µmol mol^{-1}. Upon completion of the measurements at low C_a, C_a was returned to 400 µmol mol^{-1} to restore the original A_N. Next, C_a was increased stepwise to 1600 µmol mol^{-1} in a total of 13 different C_a values (Long and Bernacchi, 2003). Corrections for the leakage of CO_2 into and water vapor out of the leaf chamber of the LI-6400 have been applied to all gas-exchange data, according to Rodeghiero et al. (2007).

From the A/C_i curves, the maximum carboxylation rate ($V_{cmax\text{-}Ci}$) and maximum rate of electron transport ($J_{max\text{-}Ci}$) were calculated by fitting the mechanistic model of CO_2 assimilation proposed by Farquhar et al. (1980) using the temperature dependence of the kinetic parameters of Rubisco (Bernacchi, 2002). The Michaelis-Menten constants used for CO_2 and O_2 were K_c= 265 µbar and K_o= 201000 µbar, while the CO_2 compensation point (Γ^*) was 36.4 µbar, as previously demonstrated by Walker et al. (2013). Curve-fitting procedures are detailed elsewhere (Martins et al. 2013). Afterward, the photosynthetic parameters V_{cmax} and J_{max} were normalized to 25 °C using the temperature response equations from Sharkey et al. (2007). C_c and g_m were estimated according to Martins et al. (2013). Using C_c data, A/C_c curves were performed and the values of maximum carboxylation rate ($V_{cmax\text{-}Cc}$) and maximum rate of electron transport ($J_{max\text{-}Cc}$) were estimated. The observed photosynthetic limitations were estimated based on the method previously described (Grassi and Magnani, 2005). This method uses values of A, g_s, g_m, $V_{cmax\text{-}Cc}$, Γ^*, C_c, Km = K_c (1+ O/K_o) and allows the partitioning of functional components that limit photosynthesis relative to stomatal (SL), mesophilic (ML) and biochemical (BL) limitations. The water use efficiency was estimated as the ratio between photosynthesis and g_s.

The initial fluorescence (F_0) was measured by illuminating previously dark-adapted leaves (1h) with weak modulated measuring beams (0.03 µmol m^{-2} s^{-1}). Saturating white light pulses (8000 µmol photons m^{-2} s^{-1}) was applied for 0.8 s to obtain the maximum fluorescence (F_m), from which the variable-to-maximum Chl fluorescence ratio, was then calculated: $F_v/F_m = [(F_m - F_0)/F_m)]$. In light-adapted leaves, the steady-state fluorescence yield (F_s) was measured with the application of a saturating white light pulse (8000 µmol m^{-2} s^{-1}, 0.8 s) to achieve the light-adapted maximum fluorescence (F_m'). The actinic light was then turned off and a far-red illumination (2 µmol m^{-2} s^{-1}) was applied to measure the light-adapted initial fluorescence (F_0'). The capture efficiency of excitation energy by open photosystem (PSII) reaction centers (F_v'/F_m') was estimated following Logan et al. (2007) and the actual PSII photochemical efficiency (δPSII) was estimated as $\delta PSII = (F_m' - F_s)/F_m'$ (Genty et al., 1989). In addition, the coefficients of photochemical quenching (*qP*), non-photochemical quenching (*NPQ*) and the electron transport rate (*ETR*) were determined as previously described (Martins et al., 2013).

Determination of metabolite levels

In order to evaluate metabolic changes during the light/dark cycle, whole rosettes were collected at the beginning, middle and end of the light period. For the WR experiment, plants were collected only in the middle of the day. In addition, harvesting were carried out in three distinct moments after the imposition of WR as follow: (*i*) end of the second week (when the restriction was started); (*ii*) end of the third week (when the plants reached 50% of water into the soil) and 17 days after WR, while plants were maintained at 50% of water into the soil. All samples were immediately flash frozen in liquid nitrogen and stored at -80 °C until analysis.

Samples were submitted to methanolic hot extraction, and the levels of photosynthetic pigments (Porra et al., 1989), glucose, fructose and sucrose (Fernie et al., 2001), malate and fumarate (Nunes-Nesi et al., 2007), total amino acids (Yemm et al., 1955), and nitrate (Mori, 2000) levels were quantified in soluble fraction, while starch (Fernie, et al., 2001) and total protein contents (Bradford, 1976) were determined in insoluble fraction.

Isolation of guard cell- enriched epidermal fragments

Isolation of guard cell enriched epidermal fragments was performed as previously described by Pandey et al. (2002) with minor modifications. Briefly, 4 whole rosettes from at least 4-week-old per sample were ground for approximately 1 min with a blender containing an internal filter that separates the epidermal fragments from mesophilic and fibrous cells. Subsequently, the epidermal fragments were collected on a nylon membrane (200 µm mesh) and washed with rinsing water, dried in paper and were immediately flash frozen in liquid nitrogen and stored at -80 °C until analysis. The fragments were used for both gene expression and metabolic profile.

Metabolic profile of guard cell-enriched epidermal fragments

Metabolites profile performed by gas chromatography coupled to mass spectrometry (GC-MS) and it was carried out in samples (leaves and epidermal fragments) harvested at the middle of the day. The extraction was performed using 1mL of methanol and shaking (800 rpm) at 70 ºC during 15 min, 60 µL of Ribitol (0.2mg mL^{-1}) was added as an internal standard, as previously described by Lisec et al. (2006). The chromatograms and mass spectra generated were manually annotated, and ion intensity was determined by the aid of TagFinder software (Luedemann et al., 2008), based on the FAME MDN35 reference library from the Golm Metabolome Database (http://gmd.mpimp-gol.mpg.de/download/) (Kopka et al., 2005) and following the reporting recommendations (Fernie et al., 2011). This analysis allowed the determination of approximately 20 different metabolites, representing the main classes of compounds (amino acids, organic acids, sugars, among others).

Gene expression analysis

Total RNA was extracted from the samples with TRIzol reagent (Ambion, Life Technology). After purification, the RNA was quantified by NanoDrop ND-2000 spectrophotometer (Thermo Scientific NanoDrop Technologies, Wilmington, Delaware, United States) and analyzed on a 1% (w/v) agarose gel. A total of 0.5 µg of RNA was treated with DNAse I (Invitrogen®, Carlsbad, California, United States) to remove potential contamination with genomic DNA. The cDNA synthesis was performed using 0.5 µg of total RNA using SuperscriptTM III reverse transcriptase (Invitrogen®, Carlsbad, California, United States). For analysis of gene expression, the Fast SYBR® Green PCR Master Mix was used with the MicroAmp™ Optical 96-well Reaction Plate (both from Applied Biosystems, Singapore, China) and MicroAmp™ Optical Adhesive Film (Applied Biosystems, Foster City, CA, USA). The R^2 from the regression equation was calculated for each gene in order to verify the reaction efficiency. Standard curves were prepared for each pair of primers using serially diluted cDNA to calculate the relative amount values for each sample. A standard curve was used to calculate the relative quantification values of each sample for each gene (Larionov et al., 2005).

The relative expression levels were normalized using the constitutively expressed genes *ACTIN* (Czechowski et al., 2005). The primers used for qRT-PCR were designed using the QuantPrime software (Arvidsson et al., 2008) or taken from those described by Laanemets et al. (2013). Detailed primers information is described in the Supplemental (Supplemental Table S2). The following genes related to water deficiency, [CO_2], signaling and transport of ions through guard-cell membranes were analyzed: aluminum activated malate transporter 6 and -9, *ALMT6* and *ALMT9*; slow-type anion channel, *SLAC1* (Negi et al., 2008); H^+-ATPase 1, -2 and -5, *AHA1*, *AHA2* and *AHA5* (Ueno et al., 2005); potassium channel 1, *KAT1* (Nakamura et al., 1995) and *KAT2* (Pilot et al., 2001); K^+ transporter 1, *AKT1* (Cao et al., 1995); K^+ rectifying channel 1, *KC1* (Reintanz et al., 2002); K^+ gated outwardly-rectifying K^+ channel, *GORK* (Ache et al., 2000); two-pore channel 1, *TPC1* (Peiter et al., 2005); high leaf temperature 1, *HT1* (Hashimoto et al., 2006); resistant to high CO_2, *RHC1* (Tian et al., 2015); β-carbonic anhydrases 1, *βCA4* (Hu et al., 2010); response to dehydration A and B, *RD29A/RD29B* (Narusaka et al., 2003; Dong et al., 2004); 9-cis-epoxycarotenoid dioxygenase 5, *NCED5* (Qin et al, 1999; Barrero et al., 2006); open stomata 1, *OST1* (Belin et al., 2006). The independent genotypes were represented by at least three plants and the mean value of the expression was calculated. The results were analyzed using Student's *t*-test.

Experimental design and statistical analysis

All experiments were performed in a completely randomized experimental design. All data are expressed as the mean ± standard error (SE) of 3-6 independent replicates per genotype, and when was the case, over time. All data were submitted to an unpaired two-tailed Student *t*-test used for the comparative analysis between the two treatments or genotypes, and an ANOVA was used for three or more treatments or genotypes. The comparison of the means was performed through the Tukey HSD (honestly significant difference) test for balanced data and Tukey-Kramer for unbalanced data. *P*-values lower than 0.05 ($P<0.05$) were considered statistically significant. All the statistical analyses were performed using the statistical software R version 3.3.2 (R Foundation for Statistical Computing, Vienna, Austria).

RESULTS

The functional absence of ABCB14 does not impair sensitivity to ABA and dark, but affect CO_2 sensitivity

Due to the previously recognized function of ABCB14 on stomatal responses, here we further investigated the effects of CO_2, dark, light and ABA on g_s in *abcb14-1* and *abcb14-2* plants by using the same gas exchange system described above. Firstly, we evaluated the stomatal kinetics following changes from normal-to-high and high-to-normal CO_2 concentrations. After reaching a steady state of g_s at normal CO_2 concentrations (400 ppm CO_2), the rising to high CO_2 concentrations (800 ppm of CO_2) decreased g_s similarly in both WT and mutant lines. Afterward, g_s increased in all genotypes following the return to normal CO_2 concentration (Supplemental Fig. S1 A). Second, the stomatal kinetics during dark-to-light and light-to-dark transitions were evaluated showing that the functional absence of ABCB14 did not compromise the stomatal responses to dark-light transitions, as compared to WT (Supplemental Fig. S1 B). Given to the fact that the stomatal responses are also associated with changes in leaf concentrations of ABA, we next investigated the response of excised leaves from plants cultivated in either aCO_2 or eCO_2 following incubation with ABA in an opening buffer solution. Notably, no effect on the stomatal aperture as measured by g_s following the incubation with ABA was observed in all conditions used here (Supplemental Fig. S1 C and D). Finally, to further assess the impact of the lack of a functional ABCB14 on water loss in *Arabidopsis* plants, a time scale water loss experiment from excised rosettes was performed by analyzing fresh weight loss. Consistent with the aforementioned results, we did not observe any apparent effect of the mutation on the water loss in detached rosettes at aCO_2 (Supplemental Fig. S1 E).

The degree of stomatal opening does not affect photosynthesis, but promotes different effects on water use efficiency

To further investigate the significance of the lack of a functional ABCB14 on gas exchange parameters were analyzed at growth light (150 µmol m^{-2} s^{-1}) and light saturating light, but not photoinhibitory conditions (1000 µmol m^{-2} s^{-1}) in plants cultivated at either aCO_2 or eCO_2 conditions (Supplemental Fig. S3). The A_N did not differ among genotypes (Supplemental Fig. S3 A), however, it was observed the combined effect of eCO_2 and high luminosity caused a greater increase in A_N than isolated effects. Although it was observed that C_i/C_a was slightly reduced in *abcb14* lines at eCO_2/saturating light, C_i/C_a was virtually unchanged (Figure 4B). The effect of the eCO_2 on g_s was observed in both mutant lines at both light conditions (Supplemental Fig. S3 B and C). Despite the increased A_N at eCO_2, decreased g_s was observed in both light conditions leading to higher *WUE* (Supplemental Fig. S3 C and D). Under both light conditions, *abcb14* mutant lines tended to display higher *WUE* when compared to WT plants. This fact aside, ETR was similar between genotypes and increased in response to high light conditions similarly between genotypes (Supplemental Fig. S3 D and E). The observed differences in A_N cannot be related to photochemical constraints given that capture efficiency of excitation energy (F_v'/F_m') remained stable (Supplemental Fig. S3 F).

Photosynthetic parameters responsive to CO_2 and light curves

In order to better understand the mechanisms underlying photosynthesis and the involvement of g_s in response to changes in CO_2 concentration, response of A_N to the internal CO_2 concentration (A_N/C_i curves, Supplemental Fig. S2, A and B) was obtained and then converted into responses of A_N to chloroplast CO_2 concentration (A_N/C_c curves; Supplemental Fig. S2, C and D). Interestingly, C_i and C_c estimations, as well as g_m and g_s, were found to be similar between WT and *abcb14* mutants, regardless growth conditions (Table1). In addition, V_{cmax}, J_{max}, and J_{max}/V_{cmax} under either C_i or C_c basis did not show significant differences between genotypes. Moreover, the similarities in these parameters suggest that an adequate functional balance between carboxylation and electron transport rates probably occurred despite changes in g_s (table 1).

By further analyzing gas exchange under photosynthetically active photon flux density that ranged from 0 to 1200 µmol m^{-2} s^{-1}, we observed that overall mutant plants exhibited no changes in the parameter obtained regardless of the CO_2 concentration (Supplemental Fig. S2 A and B). Indeed, the parameters derived from this analysis shown that both CO_2 assimilation rate saturated by light (A_{max}) was higher and light compensation point (I_c) lower at aCO_2 when compared to eCO_2 in all genotypes. It is important to mention that both light saturation points (I_s) increased whereas light use efficiency ($1/\phi$) reduced only for WT at eCO_2 being virtually invariant for the *abcb14* mutant lines (Supplemental Table S1).

Phenotype of *abcb14* plants under conditions of water deficit and high [CO_2]

Given the ABCB14 is a guard cell protein that responds to eCO_2, we next investigated whether the functional absence of ABCB14 in plants at eCO_2 in association with WR may affect plant growth. After 17 days in water restriction (50%) and without the appearance of leaf wilt symptoms, 4-5-week-old plants were evaluated for relative water content (RWC) and growth parameters (Fig. 1). Only in WT plants a minor reduction of 6% and 4% in RWC was observed at $aCO_{2\_50\%}$ and at $eCO_{2\_50\%}$, respectively, in comparison to their respective control plants at $aCO_{2\_100\%}$ and at $eCO_{2\_100\%}$ (Fig. 1A). There was no significant difference in RWC between mutant plants in all growth conditions (Fig.3 B). Differences in growth were observed between treatments for all genotypes, mainly in LA and RA (Fig. 2 A and B). The reduction in both FW and DW of the rosette under WR was similar for all genotypes, although the DW in *abcb14* lines was higher in plants under $eCO_{2\_100\%}$ than in $aCO_{2\_100\%}$.

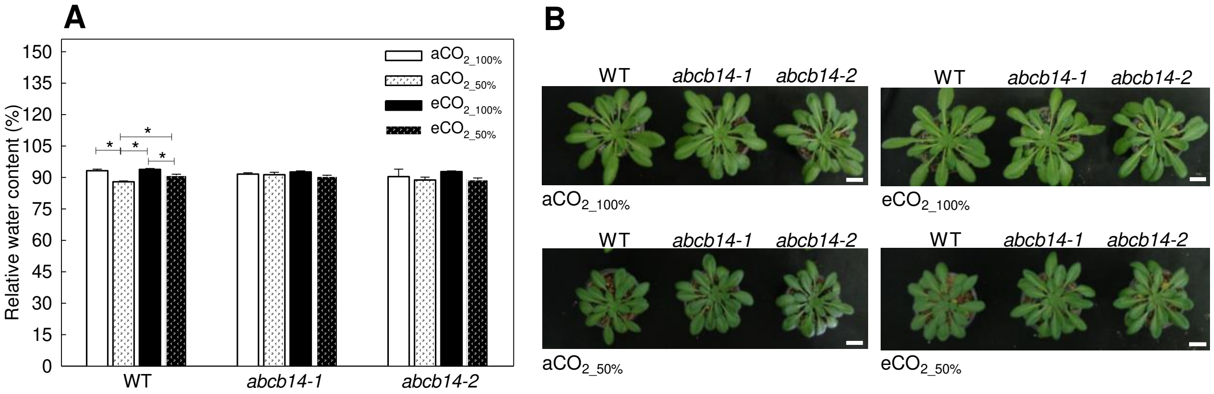

Figure 1. Water status and growth phenotype of *abcb14* mutant plants in response to isolated or combination of water restriction and elevated [CO$_2$]. Relative water content (A) and phenotype (B) of 4,5-week-old, short-day-grown Arabidopsis mutants and wild-type (WT). Plants growing under either ambient (aCO$_2$) (A) or elevated [CO$_2$] (eCO$_2$) after water limitation. Water suspension was imposed on 2-week-old plants after transplanting. The parameters were analyzed 10 days after the plants reached 50% of water in the soil. The water was replenished daily in order to maintain 50 and 100% of water in the soil. aCO$_{2\_100\%}$, plants were grown at ambient [CO$_2$] and with 100% water content replenished daily; aCO$_{2\_50\%}$, plants were grown at ambient [CO$_2$] and with 50% water content replenished daily; eCO$_{2\_100\%}$, plants were grown at elevated [CO$_2$] and with 100% water content replenished daily; eCO$_{2\_50\%}$, plants were grown at ambient [CO$_2$] and with 50% water content replenished daily. Values are presented as means ± SE (n = 5). Means followed by the same letter are not different by a one-way ANOVA followed by the Tukey test between genotypes or treatments. Dashed line compares the three genotypes under the same condition. Continuous line compares a genotype under different conditions. An asterisk (*) indicates a significant difference ($P<0.05$). White bar = 2 cm.

Table 1. Response of the photosynthesis parameters to CO_2 curve. aCO_2 and eCO_2 represent plants grown at ambient and elevated [CO_2], respectively. Values are presented as means ± SE (n = 4). Lowercase letters compare a genotype under different conditions of [CO_2] and uppercase letters compare the three genotypes under the same treatment condition. Means followed by the same letter not differentiated by a one-way ANOVA followed by Tukey test ($P< 0.05$) between genotypes or treatments.

Parameters*	WT		*abcb14-1*		*abcb14-2*	
	400 ppm	800 ppm	400 ppm	800 ppm	400 ppm	800 ppm
C_i (µmol CO_2 mol^{-1})	320.17 ± 7.37 Aa	630.74 ± 12.54 Ab	301.89 ± 7.76 Aa	661.26 ± 6.51 Ab	308.77 ± 4.59 Aa	639.64 ± 10.24 Ab
C_c (µmol CO_2 mol^{-1})	168.22 ± 5.80 Aa	504.92 ± 16.89 Ab	166.63 ± 3.78 Aa	549.16 ± 41.47 Ab	159.51 ± 4.83 Aa	542.67 ± 34.60 Ab
C_c/C_i	0.52 ± 0.01 Aa	0.80 ± 0.01 Ab	0.55 ± 0.02 Aa	0.82 ± 0.05 Ab	0.51 ± 0.01 Aa	0.84 ± 0.08 Ab
g_{m_Harley} (mol CO_2 m^{-2} s^{-1} bar^{-1})	0.095 ± 0.01 Aa	0.101 ± 0.025 Aa	0.086 ± 0.004 Aa	0.107 ± 0.035 Aa	0.077 ± 0.004 Aa	0.088 ± 0.014 Ab
g_{m_Ethier} (mol CO_2 m^{-2} s^{-1} bar^{-1})	0.063 ± 0.003 Aa	0.072 ± 0.007 Ab	0.054 ± 0.003 Aa	0.064 ± 0.005 Ab	0.051 ± 0.001 Aa	0.058 ± 0.011 Aa
V_{cmax_Ci} (µmol m^{-2} s^{-1})	44.28 ± 3.08 Aa	46.66 ± 3.09 Aa	44.38 ± 1.81 Aa	45.87 ± 2.13 Aa	44.53 ± 1.51 Aa	43.73 ± 1.23 Aa
V_{cmax_Cc} (µmol m^{-2} s^{-1})	67.44 ± 5.33 Aa	69.65 ± 2.20 Aa	76.08 ± 4.66 Aa	77.68 ± 3.14 Aa	78.13 ± 2.81 Aa	75.07 ± 4.27 Aa
J_{max_Ci} (µmol m^{-2} s^{-1})	94.41 ± 8.28 Aa	104.33 ± 2.89 Aa	98.29 ± 3.74 Aa	103.06 ± 3.79 Aa	96.21 ± 2.13 Aa	99.78 ± 4.37 Aa
J_{max_Cc} (µmol m^{-2} s^{-1})	118.74 ± 13.78 Aa	107.76 ± 3.61 Aa	108.47 ± 2.42 Aa	111.85 ± 2.74 Aa	108.31 ± 3.41 Aa	104.12 ± 4.81 Aa
$J_{maxCi} : V_{cmax\_Ci}$	2.12 ± 0.064 Aa	2.25 ± 0.105 Aa	2.22 ± 0.063 Aa	2.25 ± 0.025 Aa	2.16 ± 0.033 Aa	2.29 ± 0.123 Aa
$J_{max\_Cc} : V_{cmax\_Cc}$	1.77 ± 0.193 Aa	1.55 ± 0.04 Aa	1.44 ± 0.058 Aa	1.44 ± 0.039 ABa	1.39 ± 0.03 Aa	1.39 ± 0.031 Ba
Stomatal limitation	0.254 ± 0.024 Aa	0.179 ± 0.0177 Aa	0.217 ± 0.034 Aa	0.179 ± 0.0162 Aa	0.237 ± 0.012 Aa	0.185 ± 0.003 Aa
Mesophyll limitation	0.348 ± 0.023 Aa	0.229 ± 0.042 Ab	0.382 ± 0.005 ABa	0.239 ± 0.055 Ab	0.417 ± 0.007 Ba	0.205 ± 0.045 Ab
Biochemical limitation	0.369 ± 0.026 Aa	0.687 ± 0.031 Ab	0.395 ± 0.021 Aa	0.623 ± 0.0499 Ab	0.415 ± 0.031 Aa	0.609 ± 0.049 Ab

*C_i, Substomatal CO_2 concentration; C_c, chloroplastic CO_2 concentration; C_c/C_i, ratio between chloroplastic CO_2 concentration and substomatal CO_2 concentration; g_m, mesophyll conductance to CO_2 estimated according to the Harley or Ethier method; V_{cmax_Ci} or C_c, maximum carboxylation capacity based on C_i or C_c; $J_{max\_Ci\ or\ Cc}$, maximum capacity for electron transport rate based on C_i or C_c.

Despite of the changes in both RA and DWR, there was no significant difference in SLA between genotypes. Interestingly, *abcb14-1* under $eCO_{2\_100\%}$ had larger RA than WT (Fig. 2B), despite of reductions in g_s (Fig 4C).

High CO_2 concentration decreases leaf thickness and intercellular spaces more in WT than in *abcb14-1* plants

To further understand the effects of the functional lack of ABCB14 on *Arabidopsis* plants, a range of visual and anatomical parameters were analyzed (Fig. 3). Briefly, mesophyll thickness (MT) and palisade mesophyll thickness (PMT) significantly increased in *abcb14-1* mutant plants as compared to WT under $eCO_{2\_100\%}$ (Fig. 3 B and C). Likewise, spongy mesophyll thickness (SMT) tended to be larger in *abcb14-1* plants with significant differences between WT and *abcb14-1* under $aCO_{2\_50\%}$ (Fig. 3D). On the other hand, adaxial epidermis thickness (AdET) and abaxial epidermis thickness (AbET) decreased significantly only in *abcb14-1* mutant plants under $aCO_{2\_50\%}$ as compared to $aCO_{2\_100\%}$ whereas AbET was higher in *abcb14-1* than in WT under $eCO_{2\_50\%}$ (Fig. 3 E and F). By analyzing intercellular spaces (IS), strong reductions were observed in both *abcb14-1* and WT under $eCO_{2\_50\%}$ when compared to $aCO_{2\_100\%}$ (Fig. 3A). By comparing genotypes, it was observed that ISs were higher in *abcb14-1* mutant plants as compared to WT under $aCO_{2\_50\%}$. However, IS was higher in WT than in *abcb4-1* under $eCO_{2\_50\%}$ (Fig. 3A).

abcb14 plants exhibit higher photosynthetic capacity at elevated CO_2 concentration and water restriction

Gas exchange results indicates that *abcb14* plants at $eCO_{2\_50\%}$ showed higher A_N than WT plants (Fig. 4A). Significant changes in A_N were also observed at $eCO_{2\_100\%}$ as compared to the other treatments, for all genotypes. In addition, for all genotypes A_N had a compensatory response by the eCO_2 when $aCO_{2\_50\%}$ and $eCO_{2\_50\%}$ were compared (Fig. 4A). Although differences in A_N between conditions were observed, no changes in C_i/C_a ratio were identified (Fig. 4B). On the other hand, eCO_2 and water restriction led to significant reductions in g_s for all plants; nevertheless, only at $aCO_{2\_100\%}$ and $eCO_{2\_100\%}$ WT plants differed from the two mutant lines (Fig. 4C). Together, these results led to higher *WUE* at $eCO_{2\_50\%}$ compared to other conditions for all genotypes. Despite the similarity between genotypes in *WUE*, *abcb14-1* had higher *WUE* than WT at eCO2. In addition, *abcb14-2* plants had higher *WUE* at both eCO2 conditions (Fig. 4D).

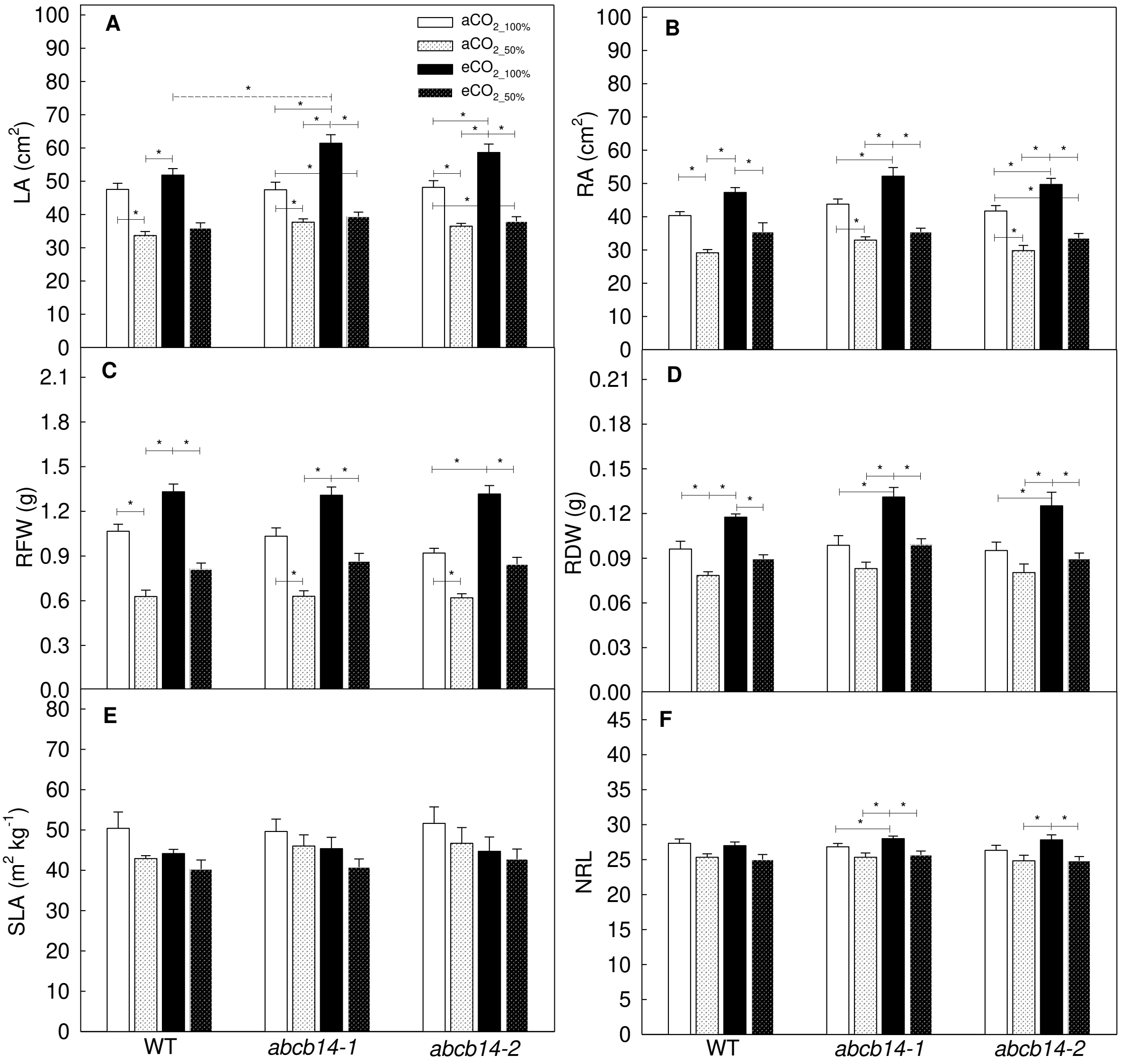

Figure 2. Differential responses of biomass accumulation and growth of *abcb14* mutant plants in response to isolated or combination of water restriction and elevated [CO2]. (A) RA, Rosette area; (B) LA, Leaf area; (C) RFW, Rosette fresh weight; (D) RDW, Rosette dry weight; (E) SLA, Specific leaf area; (F) NRL, Number of rosette leaves. Details as in Figure 1. Values are presented as means ± SE (n = 5-6). Dashed line compares the three genotypes under the same condition. Continuous line compares a genotype under different conditions.

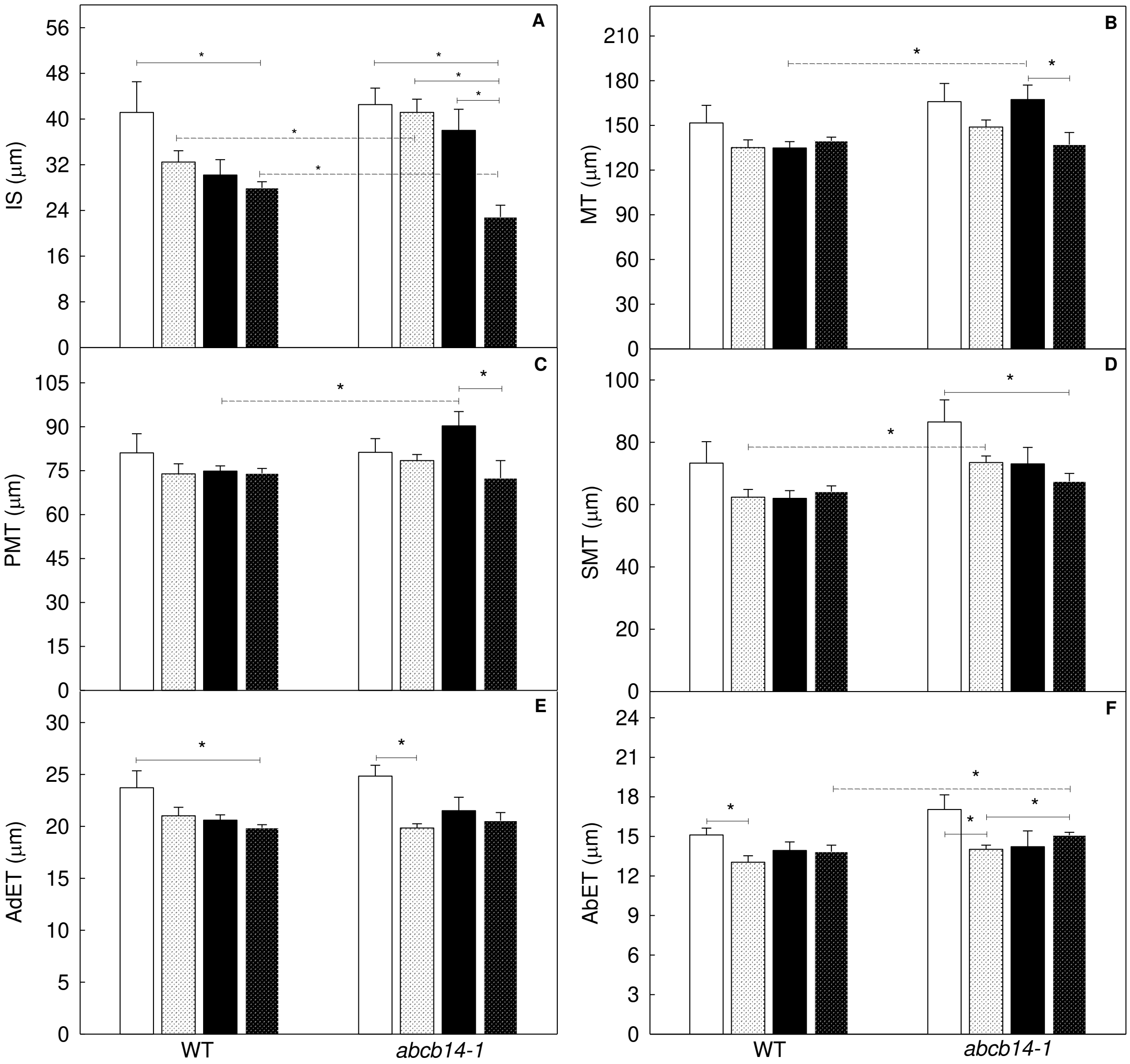

Figure 3. Differential responses of the leaf anatomy to the combination of water restriction under ambient and elevated CO_2 concentrations in both WT and *abcb14-1*. (A) IS, Intercellular space; (B) MT, Mesophyll thickness; (C) PMT, Palisade mesophyll thickness; (D) SMT, Spongy mesophyll thickness; (E) AdET, Adaxial epidermis thickness; (F) AbET, Abaxial epidermis thickness. Detail as in Figure 1. Values are presented as means ± SE (n = 5-6). Dashed line compares the three genotypes under the same treatment condition. Continuous line compares a genotype under different conditions.

Different behavior was observed for both R_d and R_p. While R_d decreased at $aCO_{2\_50\%}$, R_p was increased as compared to $aCO_{2\_100\%}$. On the other hand, R_d was maintained while R_p decreased in all genotypes at eCO_2. In general, there was no difference in R_d between genotypes; whereas R_p differed between WT and *abcb14-1* plants at $eCO_{2\_50\%}$ (Fig. 4, E and F). Despite the reduction of almost all parameters evaluated, ETR did not change in response to WR and CO_2. Furthermore, F_v/F_m differed in plants at eCO_2 and WR together (Fig. 4, G and H).

Metabolism of *abcb14* plants at elevated CO_2 concentration and water restriction

In order to evaluate the metabolic effects of functional lack in ABCB14 under eCO_2 and WR, we further explored the metabolic changes by conducting a detailed metabolic analysis in both entire leaves and guard cell-enriched epidermal fragments of the mutant and wild-type plants. First, the results obtained with leaf samples are described. Relatively minor changes in both total chlorophyll content and chlorophyll *a/b* ratio were observed (Supplemental Fig. S5, A and B). Glucose levels increased after 7 days under WR (7WR). After 17 days in WR (17WR), glucose levels increased significantly only in *abcb14* mutant lines at $aCO_{2\_50\%}$ in relation to $aCO_{2\_100\%}$. Additionally, fructose levels significantly increased in mutant lines at $eCO_{2\_100\%}$/17WR as compared to WT plants (Fig. 5 A and B). In most treatments, sucrose increased significantly in both mutant lines and WT, mainly under WR (Fig. 5C). Starch level decreased in both mutant lines at $eCO_{2\_100\%}$ when compared to WT, with significant differences only for *abcb14-1*. Finally, starch metabolism was not affected after 17WR (Supplemental Fig. S5 E). Malate levels increased significantly at the onset of WR at $aCO_{2\_100\%}$ for *abcb14-2* when compared to WT plants. An increased in malate was also observed levels at the end of 17WR when $eCO_{2\_100\%}$ and $aCO_{2\_100\%}$ were compared in both mutant lines (Supplemental Fig. S5 C). In addition, fumarate levels increased significantly at 7WR in all genotypes by comparing $aCO_{2\_50\%}$ and $eCO_{2\_100\%}$. Differences in fumarate levels were also observed for both *abcb14* mutant lines in comparison to WT at $eCO_{2\_50\%}$ after 17WR (Supplemental Fig. S5 D). Nitrate, amino acids, and proteins had major changes after 17WR in all genotypes. Thus, nitrate levels decreased in WR as compared to plants under 100% water, independently of the [CO_2] (Fig. 5F).

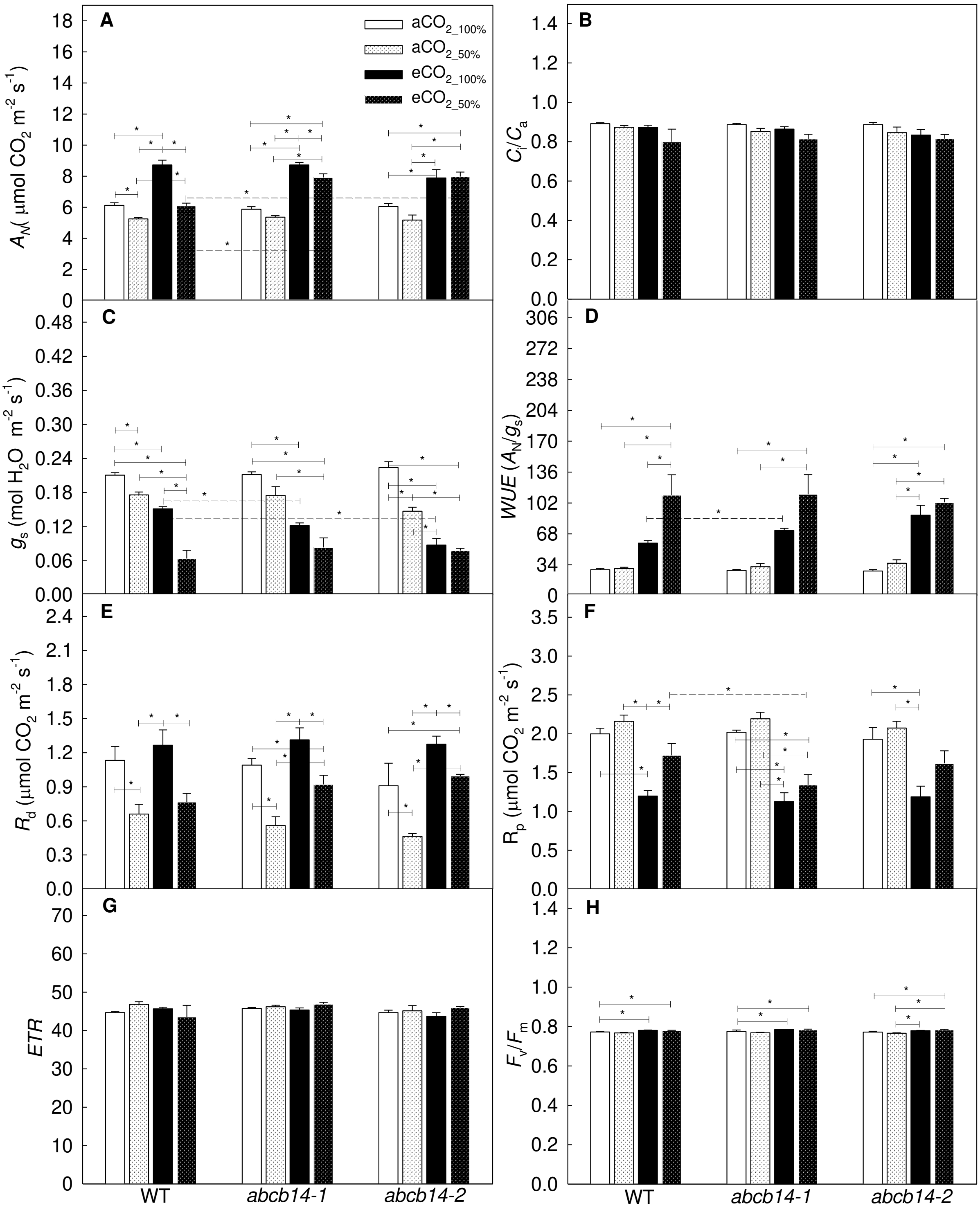

Figure 4. Photosynthetic characterization of *abcb14* mutant plants in response to isolated or combination of water restriction and elevated [CO_2]. (A) A_N, net photosynthesis rate; (B) C_i/C_a, ratio between concentration internal carbon and atmospheric carbon; (C) g_s, stomatal conductance; (D) WUE_i, intrinsic water use efficiency; (E) R_d, dark respiration; (F) R_p, photorespiration; (G) ETR, electron transport rate estimated by chlorophyll fluorescence parameters, and (H) F_v/F_m, maximum PSII photochemical efficiency. Gas exchange parameters were obtained in 4week-old-plants cultivated under either ambient (aCO_2) (A) or elevated [CO_2] (eCO_2) after water limitation. Detail as in Figure 1.

Although amino acids content was invariant after 17 days at $aCO_{2\_50\%}$ when compared to their respective controls, an increase in amino acid content was observed in mutant lines at $aCO_{2\_100\%}$ and $aCO_{2\_50\%}$ in comparison to WT (Fig. 5D). Finally, the protein content in both mutant lines was higher in $aCO_{2\_50\%}$ than in $aCO_{2\_100\%}$. The increase in protein content at both $eCO_{2\_100\%}$ and $eCO_{2\_50\%}$ was a general trend for all plants when compared to $aCO_{2\_100\%}$ plants (Fig. 5E). In addition, sugar content increased during the day; however, no significant alterations in response to eCO_2 were observed (Supplemental Fig. S4).

GC metabolism in *abcb14* plants at elevated [CO_2] and water restriction

Given the changes in both g_s and metabolic compounds previously observed in entire leaves of *abcb14* mutant exposed to eCO_2 and WR events, we next evaluate the metabolite profile in guard cell-enriched epidermal fragments of both WT and *abcb14-1* plants by using an established GC-MS approach (Lisec et al., 2006). Our metabolite analysis revealed that, among the 20 successfully annotated compounds, considerable changes in amino acids, as well as in both tricarboxylic acid cycle and photorespiratory intermediaries, were observed. All data were compared to the results obtained for samples from WT at $aCO_{2\_100\%}$. Increased levels of the most sugars and amino acids identified was observed at eCO_2 and WR (Fig. 6). The levels of organic acids had no significant difference between *abcb14-1* and WT at $aCO_{2\_100\%}$, with exception of myo-inositol that was higher in *abcb14-1* under the same conditions. Nevertheless, at $eCO_{2\_50\%}$ the levels of both fumarate and malate increased in GC of *abcb14* plants while myo-inositol increased at aCO_2 independent of WR (Fig. 6). On the other hand, fructose, mannitol, rhamnose increased in both *abcb14* and WT plants at both $eCO_{2\_100\%}$ and $eCO_{2\_50\%}$; otherwise, sucrose decreased at eCO_2 regardless of water availability. Glucose and galactinol increased in both genotypes under WR (Fig. 6). Finally, proline increased under all growth conditions and genotypes at eCO_2 and WR. The levels of threonate decreased in *abcb14* plants under $aCO_{2\_100\%}$; moreover, gamma-aminobutyric acid (GABA) and serine increased in *abcb14-1* plants at both $aCO_{2\_50\%}$ and $eCO_{2\_100\%}$. Despite the slight increase observed in most of the amino acids, no significant changes in the GC of WT at eCO_2 and WR were observed when compared to WT at $aCO_{2\_100\%}$, (Fig. 6).

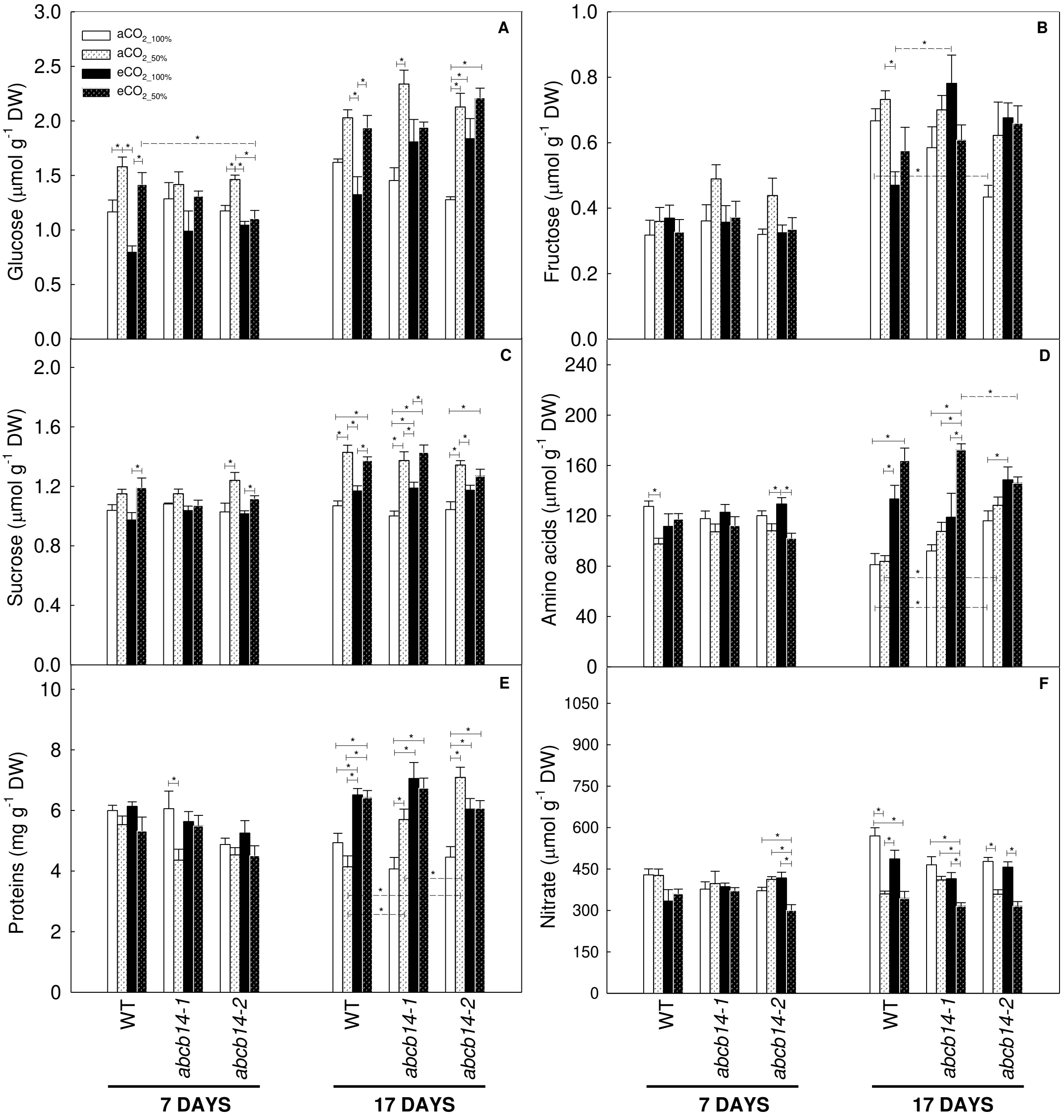

Figure 5. Metabolic responses of leaves of *abcb14* mutant plants in response to isolated or combination of water restriction and elevated [CO_2]. (A) Glucose; (B) Fructose; (C) Sucrose; (D) Nitrate; (E) Amino acids; (F) Proteins. 7 days: plants analyzed 7 days after reaching 50% of water in the soil; 10 days: plants analyzed 10 days after reaching 50% of water in the soil. Detail as in Figure 1. Values are presented as means ± SE (n = 5). Dashed line compares the three genotypes under the same condition. Continuous line compares a genotype under different conditions.

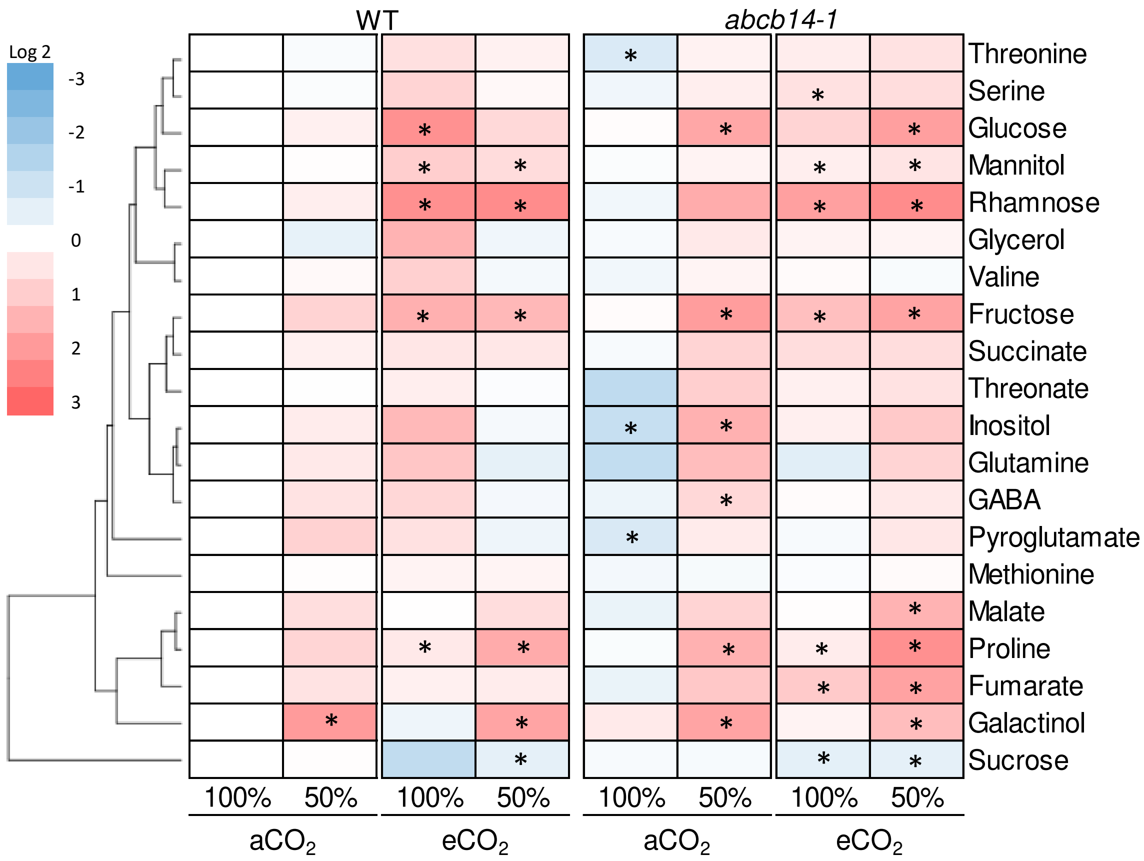

Figure 6. Changes in the relative metabolite content in guard cell-enriched epidermal fragments from *abcb14* mutant plants in response to isolated or combination of water restriction and elevated [CO_2]. The full data sets from these metabolic profiling studies are additionally available in Supplemental Table S3. Data are normalized with respect to the mean response calculated for the wild-type (WT) growing under ambient and fully available water ($aCO_{2\_100\%}$). To allow statistical assessment, individual plants from this set were normalized in the same way. Detail as in Figure 1. Values are presented as means ± SE (n = 4-5). The results from plants *abcb14-1 and* WT were compared with WT $aCO_{2\_100\%}$ by Student's *t*-test. An asterisk (*) indicate significantly different by the Student's *t* test (*P*<0.05).

The functional lack of ABCB14 effects on the expression of genes at elevated CO_2 concentration and water restriction

To better understand the interaction between eCO_2 and WR from a molecular perspective, the expression of stomatal related genes was evaluated in guard cell-enriched epidermal fragments (Figure 7 and Supplemental Table S2). All statistical comparisons were made in relation to the values obtained for WT samples at $aCO_{2\_100\%}$. Firstly, four genes (*AKT1*, *ALMT9*, *KAT2,* and *GORK*) showed altered expression at least in one of the conditions, independently of the genotype. Thus, the expression *of AKT1*, *ALMT9*, *KAT2,* and *GORK* were reduced in *abcb14-1* plants at $aCO_{2\_100\%}$ in comparison to WT under the same condition. On the other hand, *NCED*, *RD29A,* and *RHC1* expression were increased in at least two WR events ($aCO_{2\_50\%}$ and $eCO_{2\_50\%}$), independently of the genotype. Interestingly, genes involved with stomatal closure in response to eCO_2, namely *GORK*, *SLAC1*, *CA4*, *KC1*, had their expression reduced in *abcb14-1* plants at $aCO_{2\_100\%}$. In addition, reductions in the expression of stomatal closure related-genes which are associated to CO_2 and stress responses (*NCED5*, *RD29A*, *RHC1*, *TPC1*) were observed in *abcb14-1* plants at $eCO_{2\_50\%}$ (Fig. 7).

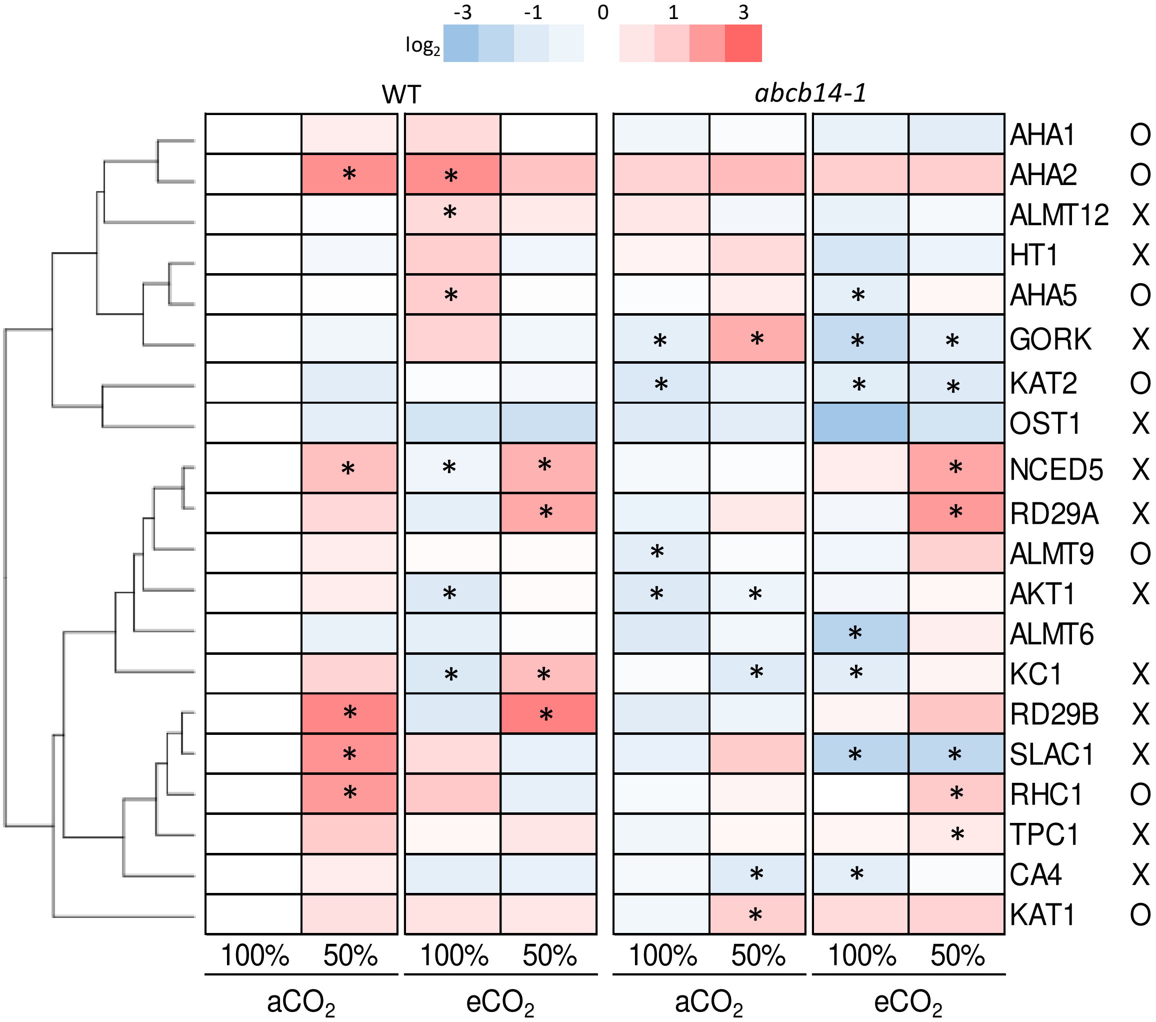

Figure 7. Changes in relative transcript levels of genes involved in stomatal responses in *abcb14-1* mutant plants. Selected genes are associated with the opening (O) or closing (X) stomatal responses. RNA was isolated from guard cell-enriched epidermal fragments isolated from 4-week-old plants from WT and *abcb14-1* mutant. Data are normalized with respect to the mean response calculated for the corresponding constitutively expressed *ACTIN* gene. In addition, data are normalized with respect to the mean response calculated for the corresponding WT of each growth condition. The full data sets from these gene studies are additionally available in Supplemental Table S4. Detail as in Figure 1. Values are presented as means ± SE (n = 4-5). The results from plants *abcb14-1* and WT were compared with WT $aCO_{2\_100\%}$ by Student's *t*-test. An asterisk (*) indicate significantly different by the Student's *t* test (P<0.05).

DISCUSSION

Historically speaking, the atmospheric CO_2 concentrations [CO_2] worldwide remained below 300 ppm for the vast majority of the last 800,000 years. This fact apart, the advent of the industrial revolution has led to a rapid rising of atmospheric [CO_2]. It is important to mention that increments of the atmospheric [CO_2] is not only associated with global warming, but it also affects the physiology and development of plants. Accordingly, it has been demonstrated that [CO_2] elevation triggers stomatal closure in leaves, a situation that might further impact leaf temperatures, plant growth, and water-use efficiency, ultimately impacting crop yield. Notably, the underlying mechanisms behind this coupled phenotype still remain unknown. Nevertheless, stomatal closure is usually mediated by anion efflux governed by anion channels localized in the plasma membrane of guard cells (Schroeder et al., 2001; Jezek and Blatt, 2017). This allows plants to continually balance the influx of CO_2 for photosynthesis against the loss of water vapor through stomatal pores in their leaves. This fine balance is usually achieved by regulating the aperture of the stomatal pores in response to several environmental stimuli, including [CO_2] and water limitation (Sirichandra et al., 2009; Xu et al., 2016). As such, to understand how guard cells adjust their physiology and metabolism in response to changes in [CO_2] and water restrictions is of paramount significance for the development of plants better adapted to the shifting climate condition.

In our attempts to further elucidate the physiological functions of ABCB14, a gene strongly expressed in guard cells (Lee et al., 2008), here we analyzed the responses of *abcb14* mutant plants to CO_2 and water restriction through gas exchange, growth and metabolic analyses. To this end, we first hypothesized that by applying a moderate and slow water restriction (50%) it should be enough to reduce stomatal closure, with minimal interference in RWC, no PSII damage, and no alteration in leaf turgor, as it indeed occurs (Fig. 1A and B; Fig. 4C and H). It has been previously demonstrated that stomatal closure is higher in *abcb14* mutants in response to elevated [CO_2] (Lee et al., 2008). By changing [CO_2] and restricting water availability in 2-week-olds plants and maintaining it for two extra weeks we could observe not only the metabolic alterations in plants with distinct g_s but also the long-term growth acclimation.

The functional absence of ABCB14 reduces stomatal response without affecting A_N

It was previously demonstrated that ABCB14 modulates stomatal movements by transporting malate from the apoplast into the guard cells during the transition to elevated [CO_2] (Lee et al., 2008). Here, we first confirmed that the functional absence of ABCB14 alters the stomatal response pattern under eCO_2 whereas it does not impact the ABA or light responses that display behaviour similar from that of the WT plants, independently of growth conditions (Supplemental Fig. S1; Fig. 4C). Overall, despite relatively few distinctions between genotypes, the water restriction leads to reduced biomass accumulation, growth, A_N, g_s, and R_d; by contrast, eCO_2 leads to general increases in growth, A_N and *WUE* with the reduction in gs in all evaluated genotipes (Figure 4). Further, it was also observed that the combination of elevated [CO_2] under water restriction conditions, eCO_2 mitigated the negative effects of the water restriction by decreasing g_s, R_p and increasing A_N and *WUE* with slight increases in growth between $aCO_{2\_50\%}$ and $eCO_{2\_50\%}$ (Fig. 4 and 5).

The main reason for the increase in photosynthesis in eCO_2 is likely the higher carboxylation efficiency of Rubisco coupled with the availability of N to additional photoassimilates and the reduction of the photorespiration rate (Figure 4 A and F; Fig. 5F; Bowes, 1991; Sims et al., 1998; Hymus et al. 2001). In addition, PSII efficiency was increased under eCO_2, leading to the production of more energy and reducing power which is necessary to activate photosynthetic enzymes (Fig. 4H; Van Heerden, Swanepoel end Krüger, 2007; Zhang et al., 2008). Altogether, the results obtained here coupled with evidence found in the literature (e.g., Proietti et al., 2013), it seems reasonable to suggest that improving photosynthesis under eCO_2 most likely occurs independently of light intensity (Supplemental Figure S3). Based on the maintenance of V_{cmax} and J_{max} (Table I) associated with the low carbohydrate accumulation (Fig. 5 A-C), it seems that there was neither photosynthetic acclimation (Tissue et al., 1993; Sage, 1994; Woodrow, 1994; Ghannoum et al., 1997; Sims et al., 1998) nor downregulation of photosynthesis (Fig 4A; Kramer, 1981; Mott, 1990; Stitt, 1991) in plants under eCO_2 as compared to aCO_2. These results are in good agreement with the relatively small response to high [CO_2] found in soybean plants (Bernacchi et al., 2005).

Although g_s varied by up to 60% between *abcb14* and WT plants under $eCO_{2\_100\%}$ (Fig. 4C), the intracellular and chloroplastic concentration of CO_2 varied much less by up to 8 and 6%, respectively (Table 1), showing that the reduction of g_s is not proportional to the reduction of both C_c and C_i. The tendency to increase C_c in *abcb14* plants may explain, at least partially, similar A_N and higher *WUE* in all growth conditions (Fig. 4A and D; Table 1). The maintenance of g_m (Table I) coupled with increased A_N (Fig 4A) is likely associated with anatomical trait responses, such as greater mesophyll thickness, palisade parenchyma and greater intercellular space (IS) and lacunar parenchyma (SMT) observed in *abcb14-1* plants when compared to WT under $eCO_{2\_100\%}$ (Fig. 3 A and D; Evans et al., 2009). Despite the lower photosynthesis, we observed significant increased growth in *abcb14* mutant plants under $eCO_{2\_100\%}$ compared to $aCO_{2\_100\%}$ (Fig 4A, B and D). By comparing genotypes, it was possible to observe that despite the higher LA in *abcb14* under $eCO_{2\_100\%}$, we did not observe a behavior different from that of WT for most of the growth and gas exchange parameters in any evaluated growth condition. When considered together, this most likely indicate a relatively minor influence of ABCB14 on growth of *Arabidopsis* plants and supports the notion that redundancy among guard cell transporter is likely in *Arabidopsis.*

Primary metabolism is more affected by moderate drought than by elevated [CO_2]

Given the lower g_s and higher *WUE* of the *abcb14* mutants under elevated [CO_2], we next decided to further analyze the metabolism of plants under combined or isolated water restriction and elevated [CO_2]. Metabolic analyses performed on both leaves and guard cells indicate that most of the modifications observed in *abcb14* and WT plants were apparently more affected by treatments than mutation (Fig. 5 and 6). In leaves, the content of the majority of sugars was affected by water restriction, especially glucose and sucrose, with no differences in starch content among genotypes (Fig. 5A-C; Supplemental Fig. S5 E). From the reduction in growth, the accumulation of sugar is important because it participates in the osmotic adjustment to maintain the hydraulic integrity in response to drought (Fig. 1B; Zhang et al., 1999; Sala et al., 2012). In addition, it appears that *abcb14* plants also induced the synthesis of both amino acids and proteins to a higher extent than WT under $aCO_{2\_50\%}$. Although there is only minor variation in leaf RWC (Fig. 1A), it is reasonable to suggest that plants that experienced water limitation were able to raise the levels of metabolites which was possibly related to osmoprotection and stress defense (Fig. 5; Tarczynski et al., 1993; Gomez-Ariza et al., 2007; Sanchez et al., 2012; Bonhomme et al., 2009; Obata and Fernie, 2012). In addition, low soil moisture may hinder nitrogen mineralization, and consequently, reduce the uptake of this element by roots. This reduction caused a modest decrease in the photosynthetic potential of plants, mainly in WT, as observed by Takatani et al. (2014). N limitation in soil is one of the main causes of acclimation that restricts the potential for yield increase in response to high CO_2 (Lou et al., 2004; et al., 2006; Reich et al., 2006). However, it seems that here there was no nitrogen limitation in $eCO_{2\_100\%}$ that have directly compromised rubisco biosynthesis (Fig. 5F; Woodrow, 1994). In guard cell-enriched epidermal fragments, the differences between the genotypes occurred mainly under water deficient conditions and at aCO_2 (Fig. 6). One conspicuous feature about the relatively high g_s in *abcb14* plants under $eCO_{2\_50\%}$ (Fig. 4C) is that it correlated well with higher levels of malate and fumarate in guard cells (Fig. 6), raising one intriguingly question: why do *abcb14* plants accumulate more malate and fumarate in guard cells than WT whether they actually stopped the transport of these metabolites caused by mutation? Although ABCB14 seems not to play an important role for stomatal opening under aCO_2, it clearly functions on overall guard cell metabolism as observed by the different levels of glucose, fructose, inositol, GABA and proline under $aCO_{2\_50\%}$. Moreover, under $aCO_{2\_100\%}$, there was a tendency in the reduction of several metabolites, with no great alterations in conditions of elevated CO_2. Collectively, these results indicated that under aCO_2 conditions the plants overcome the functional absence of ABCB14 by an extensive metabolic reprogramming. In the future, time-resolved live imaging of metabolites in guard cells (Bjarnhold et al., 2014) will likely advance our understanding of how and to which extent guard cells achieve their fine-tuned metabolic integration to ensure growth optimization.

Downregulation of stomatal closure related genes in *abcb14* under high [CO_2]

In this study, we were interested in establishing the physiological significance of the ABCB14, which is a malate importer that modulates stomatal response to CO_2, in the functioning of the illuminated leaf. Following the demonstrating that knockout mutant lines had an altered metabolism in both leaves and guard cells with no changes in photosynthetic rates, we concentrated our study in the expression of a range of genes involved on a stomatal function of the mutants. To this end, we further selected 20 genes related to stomatal functions and assessed their expression profile in guard cell enriched epidermal fragments under conditions of high [CO_2] and water limitation. Our analyze revealed little changes in expression levels of stomata related genes in *abcb14* mutant plants regardless of growth conditions. Thus, the majority of the genes showed similar patterns of transcript accumulation, and while some quantitative differences were apparent and significant, only those that were consistent within the genotypes evaluated here are briefly discussed below. As can be seen in Figure 7, *AHA5*, *GORK*, *HT1*, ALMT12, *AHA1*, *NCED5*, and *SLAC1* display an opposite behavior between *abcb14* and WT under $eCO_{2\_100\%}$ (Fig. 7), notably, the only condition where g_s differentiates between genotypes (Fig. 4C). Remarkably, the abovementioned genes are involved in the process of stomatal closure in response to high CO_2 (Hashimoto et al., 2006; Negi et al., 2008; Frey et al., 2012; Tian et al., 2015; Yamamoto et al., 2016) being mostly downregulated in *abcb14*. It seems reasonable to anticipate that this response is likely to prevent an extreme g_s reduction in *abcb14*, which would strongly limit photosynthesis under $aCO_{2\_100\%}$. Another interesting feature is that under $eCO_{2\_50\%}$ the expression of *GORK*, *AHA1*, *ALMT12,* and *SLAC1* all remain downregulated (Fig. 6), justifying the occurrence of higher g_s in WT than in *abcb14* plants (Fig 4C).

In summary, our results demonstrated that the reduction of g_s in *abcb14* plants does not affect photosynthesis, g_m, and growth. In addition, abcb14 stomata may be benefiting partially of a differential metabolic and genetic regulation in guard cells, probably to keep higher g_s, that compensates part of the functional of *abcb14*. Collectively, the results presented here indicated that although manipulation of stomatal function is a promising approach for crop yield improvement further studies, the complexity of the interconnected networks governing stomatal movements under varying conditions still requires further investigation, particularly field-grown crops.

REFERENCES

Ainsworth EA, Long SP (2005) What have we learned from 15 years of free-air CO_2 enrichment FACE? A meta-analytic review of the responses of photosynthesis, canopy properties and plant production to rising CO_2. New Phytologist 165: 351-371

Ameye M, Wertin TM, Bauweraerts I, Mcguire MA, Teskey RO, Steppe K (2012) The effect of induced heat waves on *Pinus taeda* and *Quercus rubra* seedlings in ambient and elevated CO_2 atmospheres. New Phytologist 196: 448-461

Araújo WL, Nunes-Nesi A, Osorio S, Usadel B, Fuentes D, Nagy R, Balbo I, Lehmann M, Studart-Witkowski C, Tohge T, Martinoia E, Jordana X, Damatta FM, Fernie AR (2011) Antisense inhibition of the iron-sulphur subunit of succinate dehydrogenase enhances photosynthesis and growth in tomato via an organic acid mediated effect on stomatal aperture. Plant Cell 23: 600-627

Arvidsson S, Kwasniewski M, Riaño-Pachón DM, Mueller-Roeber B (2008) QuantPrime - a flexible tool for reliable high-throughput primer design for quantitative PCR. Bmc Bioinformatics 9

Assmann, SM (1999) The cellular basis of guard cell sensing of rising CO_2. Plant Cell and Environment 22: 629-637

Azoulay-Shemer T, Palomares A, Bagheri A, Israelsson-Nordstrom M, Engineer CB, Bargmann BOR, Stephan AB, Schroeder JI (2015) Guard cell photosynthesis is critical for stomatal turgor production yet does not directly mediate CO_2- and ABA-induced stomatal closing. The Plant Journal 83: 567-581

Bauweraerts I, Wertin TM, Ameye M, Mcguire MA, Teskey RO, Steppe K (2013) The effect of heat waves, elevated CO_2 and low soil water availability on northern red oak (*Quercus rubra* L.) seedlings. Global Change Biology 19: 517-528

Bernacchi CJ, Morgan PB, Ort DR, Long SP (2005) The growth of soybean under free air [CO_2] enrichment (FACE) stimulates photosynthesis while decreasing in vivo rubisco capacity. Planta 220: 424-446

Bernacchi CJ, Portis AR, Nakano H, von Caemmerer S, Long SP (2002) Temperature response of mesophyll conductance. Implications for the determination of Rubisco enzyme kinetics and for limitations to photosynthesis in vivo. Plant Physiology 130: 1992-1998

Bjarnholt N, Li B, D'Alvise J, Janfelt C (2014) Mass spectrometry imaging of plant metabolites-principles and possibilities. Natural Product Reports 31: 818-837

Bonhomme L, Monclus R, Vincent D, Carpin S, Claverol S, Lomenech AM, Labas V, Plomion C, Brignolas F, Morabito D (2009) Genetic variation and drought response in two Populus x euramericana genotypes through 2-DE proteomic analysis of leaves from field and glasshouse cultivated plants. Phytochemistry 70: 988-1002

Bowes G (1991) Growth at elevated CO_2-Photosynthetic responses mediated through Rubisco. Plant Cell and Environment 14: 795-806

Bradford MM (1976) Rapid and Sensitive Method for the Quantitation of Microgram Quantities of Protein Utilizing the Principle of Protein-Dye Binding. Analytical Biochemistry 72: 248-254

Centritto M, Lauteri M, Monteverdi MC, Serraj R (2009) Leaf gas exchange, carbon isotope discrimination, and grain yield in contrasting rice genotypes subjected to water deficits during the reproductive stage. Journal of Experimental Botany 60: 2325-2339

Claeys H, Inze D (2013) The agony of choice: how plants balance growth and survival under water-limiting conditions. Plant Physiology 162: 1768-1779

Czechowski T, Stitt M, Altmann T, Udvardi MK, Scheible W-R (2005) Genome-wide identification and testing of superior reference genes for transcript normalization in *Arabidopsis*. Plant Physiology 139: 5-17

Daloso DM, Medeiros DB, Dos Anjos L, Yoshida T, Araújo WL, Fernie AR (2017) Metabolism within the specialized guard cells of plants. New Phytologist 16: 1018-1033

De Souza AP, Cocuron JC, Garcia AC, Alonso AP, Buckeridge MS (2015) Changes in Whole-Plant Metabolism during the Grain-Filling Stage in Sorghum Grown under Elevated CO_2 and Drought. Plant Physiology 169: 1755-65

Evans JR, Kaldenhoff R, Genty B, Terashima I (2009) Resistances along the CO_2 diffusion pathway inside leaves. Journal Experimental Botany 60: 2235-2248

Fang Y, Xiong L (2015) General mechanisms of drought response and their application in drought resistance improvement in plants. Cellular and Molecular Life Sciences 72: 673-689

Farfan-Vignolo ER, Asard H (2012) Effect of elevated CO_2 and temperature on the oxidative stress response to drought in *Lolium perenne* L. and Medicago sativa L. Plant Physiology and Biochemistry 59: 55-62

Farquhar GD, von Caemmerer S, Berry JA (1980) A biochemical model of photosynthetic CO_2 assimilation in leaves of C3 species. Planta 149: 78-90

Feng GQ, Li Y, Cheng ZM (2014) Plant molecular and genomic responses to stresses in projected future CO_2 environment. Critical Reviews in Plant Sciences 33: 238-249

Fernie AR, Aharoni A, Willmitzer L, Stitt M, Tohge T, Kopka J, Carroll AJ, Saito K, Fraser PD, DeLuca V (2011) Recommendations for Reporting Metabolite Data. The Plant Cell 23: 2477-2482

Fernie AR, Roscher A, Ratcliffe RG, Kruger NJ (2001) Fructose 2,6-bisphosphate activates pyrophosphate: fructose-6-phosphate 1-phosphotransferase and increases triose phosphate to hexose phosphate cycling in heterotrophic cells. Planta 212: 250-263

Frey A, Effroy D, Lefebvre V, Seo M, Perreau F, Berger A, Sechet J, To, A North HM, Marion-Poll A (2012) Epoxycarotenoid cleavage by NCED5 fine-tunes ABA accumulation and affects seed dormancy and drought tolerance with other NCED family members. Plant Journal 70: 501-12

Geissler N, Hussin S, Koyro HW (2009) Elevated atmospheric CO2 concentration ameliorates effects of NaCl salinity on photosynthesis and leaf structure of Aster tripolium L. Journal of Experimental Botany 60: 137-151

Genty B, Briantais JM, Baker NR (1989) The relationship between the quantum yield of photosynthetic electron transport and quenching of chlorophyll fluorescence. Biochimica Et Biophysica Acta (bba) - General Subjects 990: 87-92

Ghannoum O, von Caemmerer S, Barlow EWR, Control JP (1997) The effect of CO_2 enrichment and irradiance on the growth, morphology, and gas exchange of a C3 (*Panicum laxum*) and a C4 (*Panicum antidotale*) grass, Aust. Journal Plant Physiology 24: 227-237

Gomez-Ariza J, Campo S, Rufat M, Estopa M, Messeguer J, San Segundo B, Coca M (2007) Sucrose-mediated priming of plant defense responses and broad-spectrum disease resistance by overexpression of the maize pathogenesis-related PRms protein in rice plants. Molecular Plant-Microbe Interactions 20: 832-842

Grassi G, Magnani F (2005) Stomatal, mesophyll conductance and biochemical limitations to photosynthesis as affected by drought and leaf ontogeny in ash and oak trees. Plant, Cell and Environment 28: 834-849

Han J, Lei Z, Zhang Y, Yi X, Zhang W, Zhang Y (2018) Drought-introduced variability of mesophyll conductance in Gossypium and its relationship with leaf anatomy. Physiologia Plantarum

Hashimoto M, Negi J, Young J, Israelsson M, Schroeder JI, Iba K (2006) *Arabidopsis* HT1 kinase controls stomatal movements in response to CO_2. Nature Cell Biology 8: 391-397

Hedrich R, Marten I (1993) Malate-induced feedback regulation of plasma membrane anion channels could provide a CO_2 sensor to guard cells. EMBO Journal 12: 897-901

Hedrich R, Marten I, Lohse G, Dietrich P, Winter H, Lohaus G, Heldt HW (1994) Malate-sensitive anion channels enable guard cells to sense changes in the ambient CO_2 concentration. The Plant Journal 6: 741-748

Hedrich R, Neimanis S, Savchenko G, Felle HH, Kaiser WM, Heber U (2001) Changes in apoplastic pH and membrane potential in leaves in relation to stomatal responses to CO_2, malate, abscisic acid or interruption of water supply. Planta 213: 594-601

Hetherington AM, Woodward FI (2003) The role of stomata in sensing and driving environmental change. Nature 424: 901-908

Hunt R, Causton DR, Shipley B, Askew AP (2002) A modern tool for classical plant growth analysis. Annual Botany (Lond) 90: 485-488

Hymus GJ, Baker NR, Long SP (2001) Growth in elevated CO_2 can both increase and decrease photochemistry and photoinhibition of photosynthesis in a predictable manner. Dactylis glomerata grown in two levels of nitrogen nutrition. Plant Physiology 127: 1204-1211

IPCC. Climate change 2014: Mitigation of climate change. Contribution of Working Group III to the fifth assessment report of the Intergovernmental Panel on Climate Change. Cambridge University Press, Cambridge, UK and New York, NY, USA

Jezek M, Blatt MR (2017) The membrane transport system of the guard cell and its integration for stomatal dynamics. Plant Physiology 174: 487-519

Kang Y, Outlaw WH, Jr, Andersen PC, Fiore GB (2007) Guard-cell apoplastic sucrose concentration–a link between leaf photosynthesis and stomatal aperture size in the apoplastic phloem loader *Vicia faba* L. Plant Cell and Environment 30: 551-558

Kim TH, Böhmer M, Hu H, Nishimura N, Schroeder JI (2010) Guard cell signal transduction network: advances in understanding abscisic acid, CO_2, and Ca^{2+} signalling. Annual Review of Plant Biology 61: 561-591

Kollist H, Nuhkat M, Roelfsema MRG (2014) Closing gaps: linking elements that control stomatal movement. New Phytologist 203: 44-62

Kopka J, Schauer N, Krueger S, Birkemeyer C, Usadel B, Bergmuller E, Dormann P, Gibon Y, Stitt M, Willmitzer, L, Fernie AR, Steinhauser D (2005) GMD@CSBDB: The Golm Metabolome Database. Bioinformatics 21: 1635-1638

Kramer J (1981) Carbon dioxide concentration, photosynthesis and dry matter production. Bioscience 31: 29-33

Laanemets K, Wang YF, Lindgren O, Wu J, Nishimura N, Lee S, Caddell D, Merilo E, Brosche M, Kilk K, Soomets U, Kangasjärvi J, Schroeder JI, Kollist H (2013) Mutations in the SLAC1 anion channel slow stomatal opening and severely reduce K^+ uptake channel activity via enhanced cytosolic [Ca^{2+}] and increased Ca^{2+} sensitivity of K^+ uptake channels. New Phytologist 197: 88-98

Larionov A Krause A, Miller W (2005) A standard curve as ed method for relative real time PCR data processing. BMC Bioinformatics 6: 62

Lee M, Choi Y, Burla B, Kim YY, Jeon B, Maeshima M, Yoo JY, Martinoia E, Lee Y (2008) The ABC transporter *At*ABCB14 is a malate importer and modulates stomatal response to CO_2. Nature Cell Biology 10: 1217-1223

Lisec J, Schauer N, Kopka J, Willmitzer L, Fernie AR (2006) Gas chromatography mass spectrometry–based metabolite profiling in plants. Nature Protocols 1: 387-396

Liu XZ, Huang BR (2000) Heat stress injury in relation to membrane lipid peroxidation in creeping bentgrass. Crop Science 40: 503-510

Logan BA, Adams WIII, Demmig-Adams B (2007) Avoiding common pitfalls of chlorophyll fluorescence analysis under field conditions 34: 853-859

Lohaus G, Pennewiss K, Sattelmacher B, Hussmann M, Hermann Muehling K (2001) Is the infiltration-centrifugation technique appropriate for the isolation of apoplastic fluid? A critical evaluation with different plant species. Physiologia Plantarum 111: 457-465

Long SP, Ainsworth EA, Rogers A, Ort DR (2004) Rising atmospheric carbon dioxide: plants FACE the future. Annual Review of Plant Biology 55: 591-628

Long SP, Bernacchi CJ (2003) Gas exchange measurements, what can they tell us about the underlying limitations to photosynthesis? Procedures and sources of error. Journal Experimental Botany 54: 2393-2401

Luedemann A, Strassburg K, Erban A, Kopka J (2008) TagFinder for the quantitative analysis of gas chromatography-mass spectrometry (GC-MS)-based metabolite profiling experiments. Bioinformatics 24: 732-737

Luo Y, Su B, Currie WS, Dukes JS, Finzi Ad, Hartwig U, Hungate BA, McMurtrie RE, Oren R, Parton WJ, Pataki DE, Shaw MR, Zak DR, Field CB (2004) Progressive nitrogen limitation of ecosystem responses to rising atmospheric carbon dioxide. Bioscience 54: 731-739

Martinoia E (2018) Vacuolar transporters-companions on a longtime journey. Plant Physiology 176: 1384-1407

Martins SCV, Galmés J, Molins A, DaMatta FM (2013) Improving the estimation of mesophyll conductance to CO_2: on the role of electron transport rate correction and respiration. Journal Experimental Botany 64: 1-14

Medeiros DB, Martins SCV, Cavalcanti JHF, Daloso DM, Martinoia E, Nunes-Nesi A, DaMatta FM, Fernie AR, Araújo WL (2016) Enhanced Photosynthesis and Growth in *atquac1* Knockout Mutants Are Due to Altered Organic Acid Accumulation and an Increase in Both Stomatal and Mesophyll Conductance. Plant Physiology 170: 86-101

Meyer S, Mumm P, Imes D, Endler A, Weder B, Al-Rasheid KAS, Geiger D, Marten I, Martinoia E, Hedrich R (2010) *At*ALMT12 represents an R-type anion channel required for stomatal movement in *Arabidopsis* guard cells. The Plant Journal 63: 1054-1062

Mori H (2000) Direct determination of nitrate using nitrate reductase in a flow system. Journal of Health Sciences 46: 385-388

Mott KA (1988) Do stomata respond to CO_2 concentrations other than intercellular? Plant Physiology 86: 200-203

Mott KA (1990) Sensing of atmospheric CO_2 by plants. Plant Cell and Environment 13:731-737

Naudts K, Van Den Berge J, Farfan E, Rose P, AbdElgawad H, Ceulemans R, Janssens IA, Asard H, Nijs I (2014) Future climate alleviates stress impact on grassland productivity through altered antioxidant capacity. Environmental and Experimental Botany 99: 150-158

Naudts K, Van Den Berge J, Janssens IA, Nijs I, Ceulemans R (2013) Combined effects of warming and elevated CO_2 on the impact of drought in grassland species. Plant and Soil 369: 497-507

Negi J, Matsuda O, Nagasawa T, Oba Y, Takahashi H, Kawai-Yamada M, Uchimiya H, Hashimoto M, Iba K (2008) CO_2 regulator SLAC1 and its homologues are essential for anion homeostasis in plant cells. Nature 452: 483-486

Nunes-Nesi A, Carrari F, Gibon Y, Sulpice R, Lytovchenko A, Fisahn J, Graham J, Ratcliffe RG, Sweetlove LJ, Fernie AR (2007) Deficiency of mitochondrial fumarase activity in tomato plants impairs photosynthesis via an effect on stomatal function The Plant Journal 50: 1093-1106

O'Brien TP, Feder N, Mccully ME (1964) Polychromatic staining of plant cell walls by toluidine blue O. Protoplasma 59: 368-373

Obata T, Fernie AR (2012) The use of metabolomics to dissect plant responses to abiotic stresses. Cellular and Molecular Life Sciences 69: 3225-3243

Pandey S, Wang X-Q, Coursol SA, Assmann SM (2002) Preparation and applications of *Arabidopsis thaliana* guard cell protoplasts. New Phytologist 153: 517-526

Pandey S, Zhang W, Assmann SM (2007) Roles of ion channels and transporters in guard cell signal transduction. FEBS Lett 581: 2325-36

Peñuelas J, Sardans J, Estiarte M, Ogaya R, Carnicer J, Coll M, Barbeta A, Rivas-Ubach A, Llusià J, Garbulsky M, Filella I, Jump AS (2013) Evidence of current impact of climate change on life: a walk from genes to the biosphere. Global Change Biology 19: 2303-2338

Pinelli P, Loreto F (2003) $^{12}CO_2$ emission from different metabolic pathways measured in illuminated and darkened C3 and C4 leaves at low, atmospheric and elevated CO_2 concentration. Journal of Experimental Botany v. 54: 1761-1769

Porra R, Thompson W, Kriedemann P (1989) Determination of accurate extinction coefficients and simultaneous equations for assaying chlorophylls a and b extracted with four different solvents: verification of the concentration of chlorophyll standards by atomic absorption spectroscopy. Biochimica Et Biophysica Acta (BBA) - Bioenergetics 975: 384-394

Proietti S, Moscatello S, Giacomelli GA, Battistelli A (2013) Influence of the interaction between light intensity and CO_2 concentration on productivity and quality of spinach (Spinacia oleracea L.) grown in fully controlled environment. Advances in Space Research 52: 1193-1200

Reich PB, Hobbie SE, Lee T, Ellsworth DS, West JB, Tilman D, Knops JMH, Naeem S, Trost J (2006) Nitrogen limitation constrains sustainability of ecosystem response to CO_2. Nature 440: 922-925

Robredo A, Perez-López U, Miranda-Apodaca J, Lacuesta M, Mena-Petite A, Munoz-Rueda A (2011) Elevated CO_2 reduces the drought effect on nitrogen metabolism in barley plants during drought and subsequent recovery. Environmental and Experimental Botany 71: 399-408

Rodeghiero M, Niinemets U, Cescatti A (2007) Major diffusion leaks of clamp-on leaf cuvettes still unaccounted: how erroneous are the estimates of Farquhar et al. model parameters? Plant, Cell and Environment 30: 1006-1022

Roy J, Picon-Cochard C, Augusti A, Benot M-L, Thiery L, Darsonville O, Landais D, Piel C, Defossez M, Devidal S (2016) Elevated CO_2 maintains grassland net carbon uptake under a future heat and drought extreme. Proceedings of the National Academy of Sciences 113: 6224-6229

Ruiz-Vera UM, Siebers MH, Drag DW, Ort DR, Bernacchi CJ (2015) Canopy warming caused photosynthetic acclimation and reduced seed yield in maize grown at ambient and elevated [CO_2]. Global Change Biology 21: 4237-4249

Sage RF (1994) Acclimation of photosynthesis to increasing atmospheric CO_2: The gas-exchange perspective. Photosynthesis. Research 39: 351-368

Sala A, Woodruff DR, Meinzer FC (2012) Carbon dynamics in trees: feast or famine? Tree Physiology 32: 764-775

Salazar-Parra C, Aguirreolea J, Sanchez-Diaz M, Irigoyen JJ, Morales F (2012) Climate change (elevated CO_2, elevated temperature and moderate drought) triggers the antioxidant enzymes response of grapevine cv. Tempranillo, avoiding oxidative damage. Physiologia Plantarum 144: 99-110

Salvucci ME, Crafts-Brandner SJ (2004) Inhibition of photosynthesis by heat stress: the activation state of Rubisco as a limiting factor in photosynthesis. Physiologia Plant 120: 179-186

Sanchez DH, Schwabe F, Erban A, Udvardi MK, Kopka J (2012) Comparative metabolomics of drought acclimation in model and forage legumes. Plant Cell and Environment: 35: 149

Schindelin J, Rueden CT, Hiner MC, Eliceiri KW (2015) The ImageJ ecosystem: an open platform for biomedical image analysis. Molecular Reproduction and Development 82: 518-529

Schroeder JI, Allen GJ, Hugouvieux V, Kwak JM, Waner D (2001) Guard cell signal transduction. Annual Review of Plant Physiology and Plant Molecular Biology 52: 627-658

Sharkey TD, Bernacchi CJ, Farquhar GD, Singsaas EL (2007) Fitting photosynthetic carbon dioxide response curves for C3 leaves. Plant, Cell and Environment 30: 1035-1040

Sims DA, Luo Y, Seemann JR (1998) Comparison of photosynthetic acclimation to elevated CO_2 and limited nitrogen supply in soybean. Plant Cell and Environment 21: 945-952

Sirichandra C, Wasilewska A, Vlad F, Valon C, Leung J (2009) The guard cell as a single-cell model towards understanding drought tolerance and abscisic acid action. Journal Experimental Botany 60: 1439-63

Smirnoff N (1993) Tansley Review. 52. The role of active oxygen in the response of plants to water-deficit and desiccation. New Phytologist 125: 27-58

Stitt M (1991) Rising CO_2 levels and their potential significance for carbon flow in photosynthetic cells. Plant Cell Environment 14: 741-762

Takatani N, Ito T, Kiba T, Mori M, Miyamoto T, Maeda S, Omata T (2014) Effects of high CO_2 on growth and metabolism of *Arabidopsis* seedlings during growth with a constantly limited supply of nitrogen. Plant and Cell Physiology 55: 281-92

Tarczynski MC, Jensen RG, Bohnert HJ (1993) Stress protection of transgenic tobacco by production of the osmolyte mannitol. Science 259: 508-510

Terashima I, Yanagisawa S, Sakakibara H (2014) Plant responses to CO_2: background and perspectives. Plant and Cell Physiology. 55: 237-40

Tian W, Hou C, Ren Z, Pan Y, Jia J, Zhang H, Bai F, Zhang P, Zhu H, He Y, Luo S, Li L, Luan S (2015) A molecular pathway for CO_2 response in *Arabidopsis* guard cells. Nature Communications 6: 6057

Tissue DT, Thomas RB, Strain BR (1993) Long-term effects of elevated CO_2 and nutrients on photosynthesis and Rubisco in loblolly pine seedlings. Plant Cell Environment 16: 859-865

Valentini R, Epron D, De Angelis P, Matteucci G, Dreyer E (1995) In situ estimation of net CO_2 assimilation, photosynthetic electron flow and photorespiration in Turkey oak (*Quercus cerris* L.) leaves: diurnal cycles under different levels of water supply. Plant, Cell and Environment 18: 631-640

Van Den Berge J, Naudts K, Janssens IA, Ceulemans R, Nijs I (2011) Does the stress tolerance of mixed grassland communities change in a future climate? A test with heavy metal stress (zinc pollution). Environmental Pollution 159: 3294-3301

Van Heerden P, Swanepoel J, Krüger G (2007) Modulation of photosynthesis by drought in two desert scrub species exhibiting C3-mode CO_2 assimilation. Environmental and Experimental Botany 61: 124-136

Van Kirk CA, Raschke K (1978) Release of malate from epidermal strips during stomatal closure. Plant Physiology 61: 474-475

Walker B, Ariza LS, Kaines S, Badger MR, Cousins AB (2013) Temperature response of in vivo Rubisco kinetics and mesophyll conductance in *Arabidopsis thaliana*: comparisons to *Nicotiana tabacum*. Plant Cell Environ 36: 2108-2119

Wang W, Vinocur B, Altman A (2003) Plant responses to drought, salinity and extreme temperatures: towards genetic engineering for stress tolerance. Planta 218: 1-14

Wang WX, Barak T, Vinocur B, Shoseyov O, Altman A (2003) Abiotic resistance and chaperones: possible physiological role of SP1, a stable and stabilizing protein from Populus. Plant Biotechnology 2002 and Beyond 439-44

Woodrow IE (1994) Optimal acclimation of the C3 photosynthetic system under enhanced CO_2. Photosynthesis Research 39: 401-412

Xu Z, Jiang Y, Jia B, Zhou G (2016) Elevated-CO_2 Response of Stomata and Its Dependence on Environmental Factors. Frontier Plant Science 7: 657

Yamamoto Y, Negi J, Wang C, Isogai Y, Schroeder JI, Iba K (2016) The Transmembrane Region of Guard Cell SLAC1 Channels Perceives CO_2 Signals via an ABA-Independent Pathway in *Arabidopsis*. The Plant Cell 28: 557-567

Yemm EW, Cocking E, Ricketts RE (1955) The Determination of Amino-Acids with Ninhydrin. The Analyst 80: 209

Zhang D-Y, Chen G-Y, Gong Z-Y, Chen J, Yong Z-H., Zhu J-G, Xu D-Q (2008) Ribulose-1, 5-bisphosphate regeneration limitation in rice leaf photosynthetic acclimation to elevated CO_2. Plant Science 175: 348-355

Zhang J, Nguyen HT, Blum A (1999) Genetic analysis of osmotic adjustment in crop plants. Journal Experimental Botany 13: 291-302

Zinta G, AbdElgawad H, Domagalska MA, Vergauwen L, Knapen D, Nijs I, Janssens IA, Beemster GT, Asard H (2014) Physiological, biochemical, and genome-wide transcriptional analysis reveals that elevated CO_2 mitigates the impact of combined heat wave and drought stress in *Arabidopsis thaliana* at multiple organizational levels. Global Change Biology 20: 3670-3685

Zinta G, AbdElgawad H, Peshev D, Weedon JT, Van den Ende W, Nijs I, Janssens IA, Beemster GTS, Asard H (2018) Dynamics of metabolic responses to periods of combined heat and drought in *Arabidopsis thaliana* under ambient and elevated atmospheric CO_2. Journal of Experimental Botany 69: 2159-2170

SUPPLEMENTAL DATA

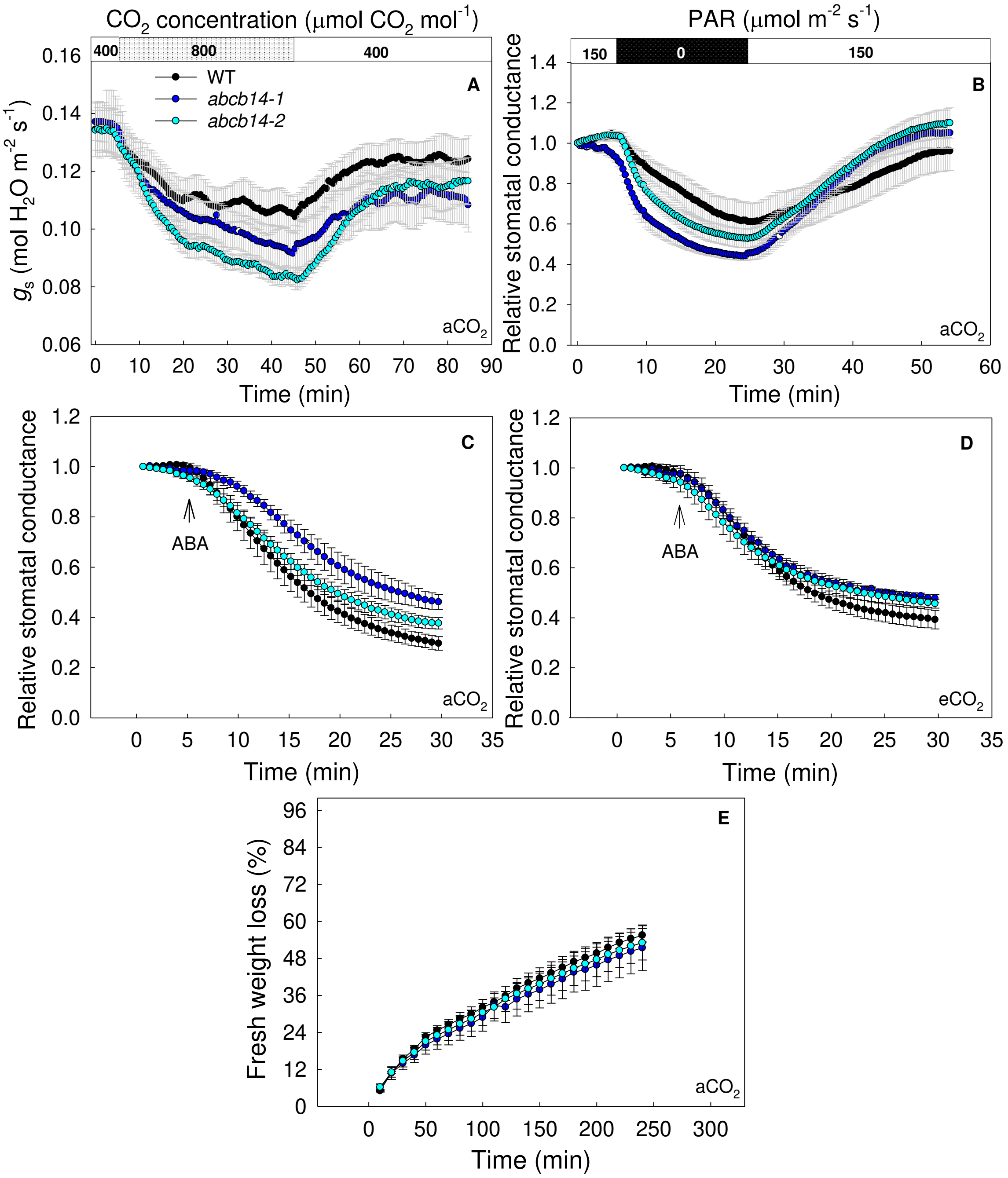

Supplemental Figure S1. CO_2-induced (A) conductance kinetics and transition light-dark-induced (B) conductance kinetics. Stomatal closing kinetics in response to exogenous ABA application in plants growing under either ambient [CO_2] (aCO_2) (C) or elevated [CO_2] (eCO_2) (D), and fresh weight loss from detached whole rosettes in WT (wild-type) and *abcb14* mutant plants growing under ambient [CO_2] (E). In A and B the arrow indicates the application of exogenous ABA 1 µm on petri dishes where the leaf petiole was immersed. During the first initial minutes, the petiole was immersed only in the opening buffer (see Material and Methods for details). Ambient and elevated CO_2 represents plants grown at 400 and 800 ppm, respectively. IRGA analyzes were performed with the respective CO_2 concentration in which the plants were cultivated. The means of each genotype was relativized by their respective initial conductance. The data were submitted an unpaired two-tailed Student *t*-test used for the comparison between WT and *abcb14*.

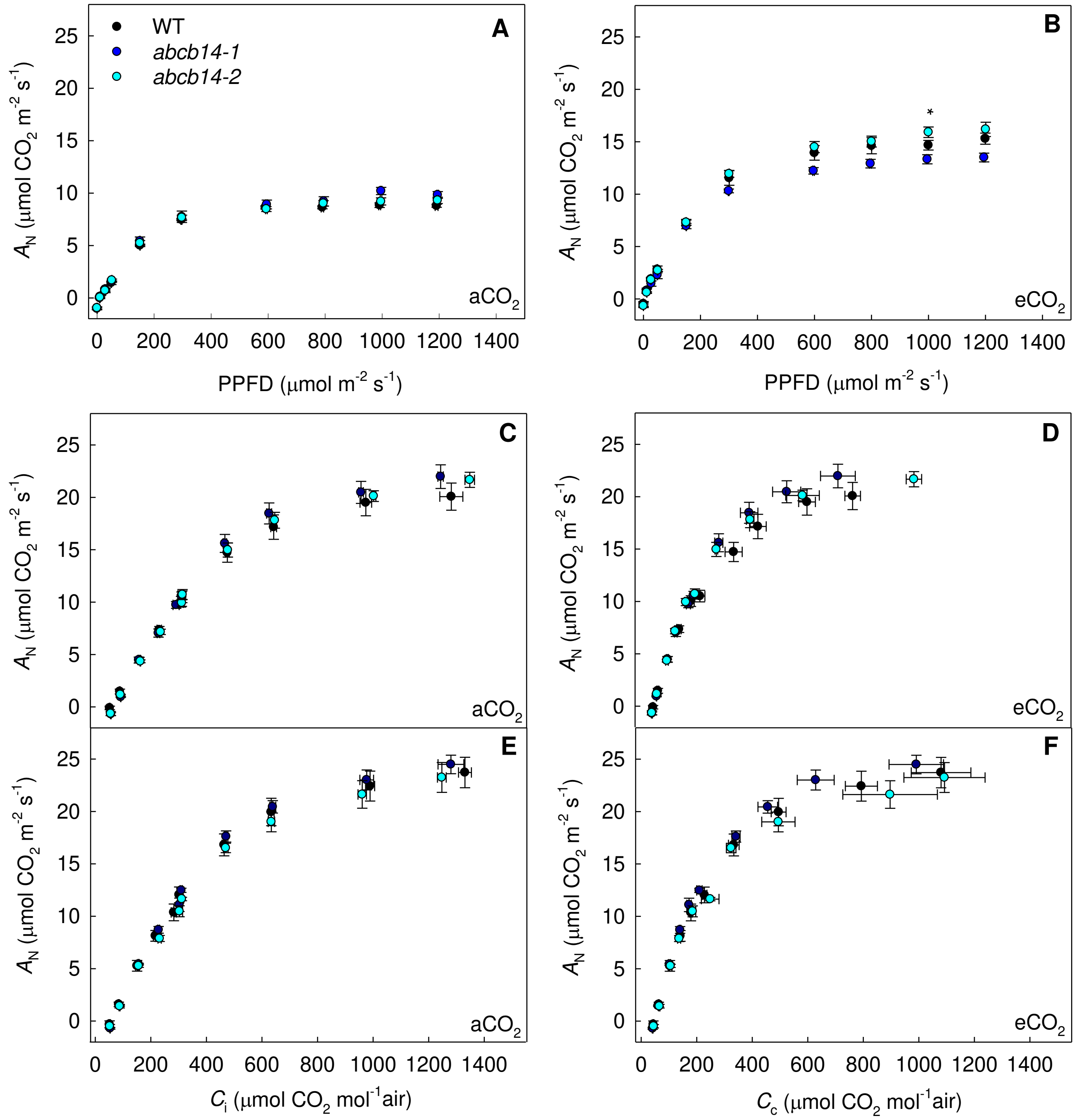

Supplemental Figure S2. Net photosynthesis (A_N) curves in response to changes in substomatal (C_i) or chloroplastic (C_c) CO$_2$ concentrations and photosynthetically active photon flux density (PPFD) of rosettes from at least 4-week-old. Ambient (aCO$_2$) or elevated (eCO$_2$) represents plants which were cultivated at either 400 and 800 ppm, respectively. Photosynthetic light-response curves *(A*/PPFD) were performed under growing ambient CO$_2$ concentration (C_a) of 400 or 800 μmol mol^{-1}. A_N /C_i curves were performed at saturated light of 1000 μmol m^{-2} s^{-1} at 25°C under ambient O$_2$ and started at ambient CO$_2$ concentration (C_a) of 400 μmol mol^{-1} independent of the growing conditions. Values were compared between WT (wild-type) and *abcb14* mutant plants by Student's *t*-test (P<0.05). Values are presented as means ± SE (n = 4) obtained using the ninth leaf totally expanded from different plants per genotype in two independent assays.

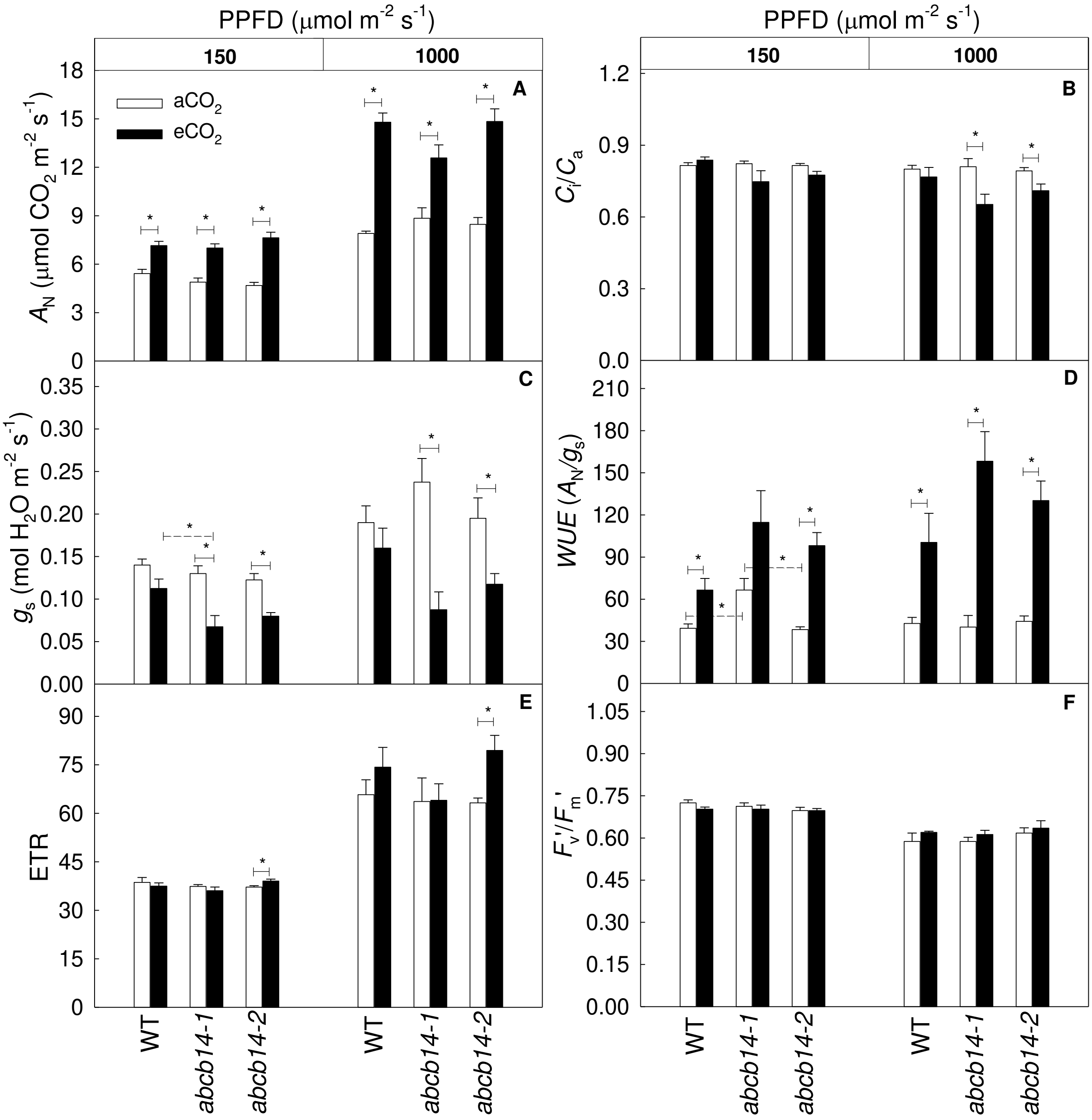

Supplemental Figure S3. Photosynthetic characterization of *abcb14* mutant plants. Gas exchange and chlorophyll fluorescence parameters were determined in plants under growth irradiance (150 µmol photons m^{-2} s^{-1}) and saturation, but not photoinhibitory, irradiance (1000 µmol photons m^{-2} s^{-1}). (A) A_N, net photosynthesis rate; (B) g_s, stomatal conductance; (C) C_i/C_a, ratio between concentration internal carbon and atmospheric carbon; (D) WUE_i, intrinsic water use efficiency; (E) F_v'/F_m', actual PSII photochemical efficiency; (F) ETR, electron transport rate estimated by chlorophyll fluorescence parameters. Values are presented as means ± SE (n = 5). Dashed lines compare the three genotypes under the same condition. Continuous line compares a genotype under different conditions. An asterisk (*) indicates a significant difference (*P*<0.05).

Supplemental Table S1. Photosynthetic parameters from light-response curves in WT and *abcb14* plants. Values are presented as means ± SE (n = 4-5). Lowercase letters compare a genotype under different conditions of [CO2] and uppercase letters compare the three genotypes under the same treatment condition. Means followed by the same letter not differentiated by a one-way ANOVA followed by Tukey test (P< 0.05) between genotypes or treatments.

Parameters*	WT		*abcb14-1*		*abcb14-2*	
	aCO_2	eCO_2	aCO_2	eCO_2	aCO_2	eCO_2
A_{max} (μmol CO_2 m^{-2} s^{-1})	9.81 ± 0.21 Aa	16.27 ± 0.62 Ab	11.32 ± 0.21 Aa	15.07 ± 0.67 Ab	10.82 ± 0.67 Aa	17.99 ± 1.13 Ab
I_c (μmol m^{-2} s^{-1})	11.59 ± 0.09 Aa	4.48 ± 1.74 Ab	13.74 ± 0.97 Aa	7.65 ± 1.84 Ab	14.43 ± 1.22 Aa	5.53 ± 1.70 Ab
I_s (μmol m^{-2} s^{-1})	358.3 ± 20.3 Aa	568.9 ± 66.0 Ab	350.4 ± 22.5 Aa	542.0 ± 40.6 Aa	331.9 ± 46.0 Aa	463.6 ± 61.8 Aa
$1/\phi$ (μmol photons mol^{-1} CO_2)	21.5 ± 0.84 Aa	15.36 ± 2.07 Ab	16.4 ± 0.62 Aa	16.84 ± 1.06 Aa	18.23 ± 1.58 Aa	15.10 ± 1.44 Aa

*A_{max}: Net CO_2 assimilation rate saturated by light; I_c: light compensation point; I_s: light saturation point;$1/\phi$: light use efficiency.

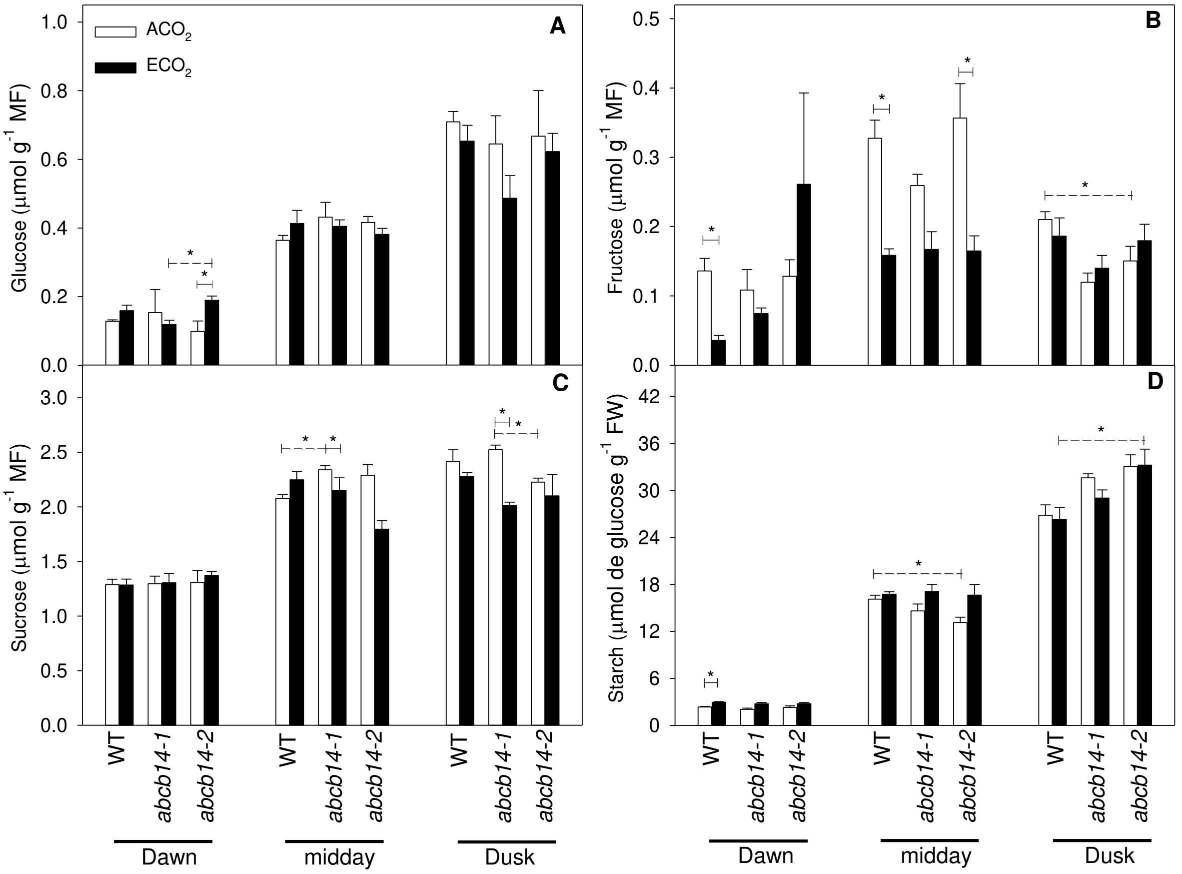

Supplemental Figure S4. Influence of $[CO_2]$ on the metabolism along the day in mutant plants 4,5-week-old. Dawn, midday, and dusk represent plants collected before, in the middle and end of the photoperiod. Values are presented as means ± SE (n = 5). The means comparison was performed through a one-way ANOVA followed by Tukey test. Dashed line compares the three genotypes under the same treatment condition. Continuous line compares a genotype under different conditions. * indicates a significant difference (*P*<0.05).

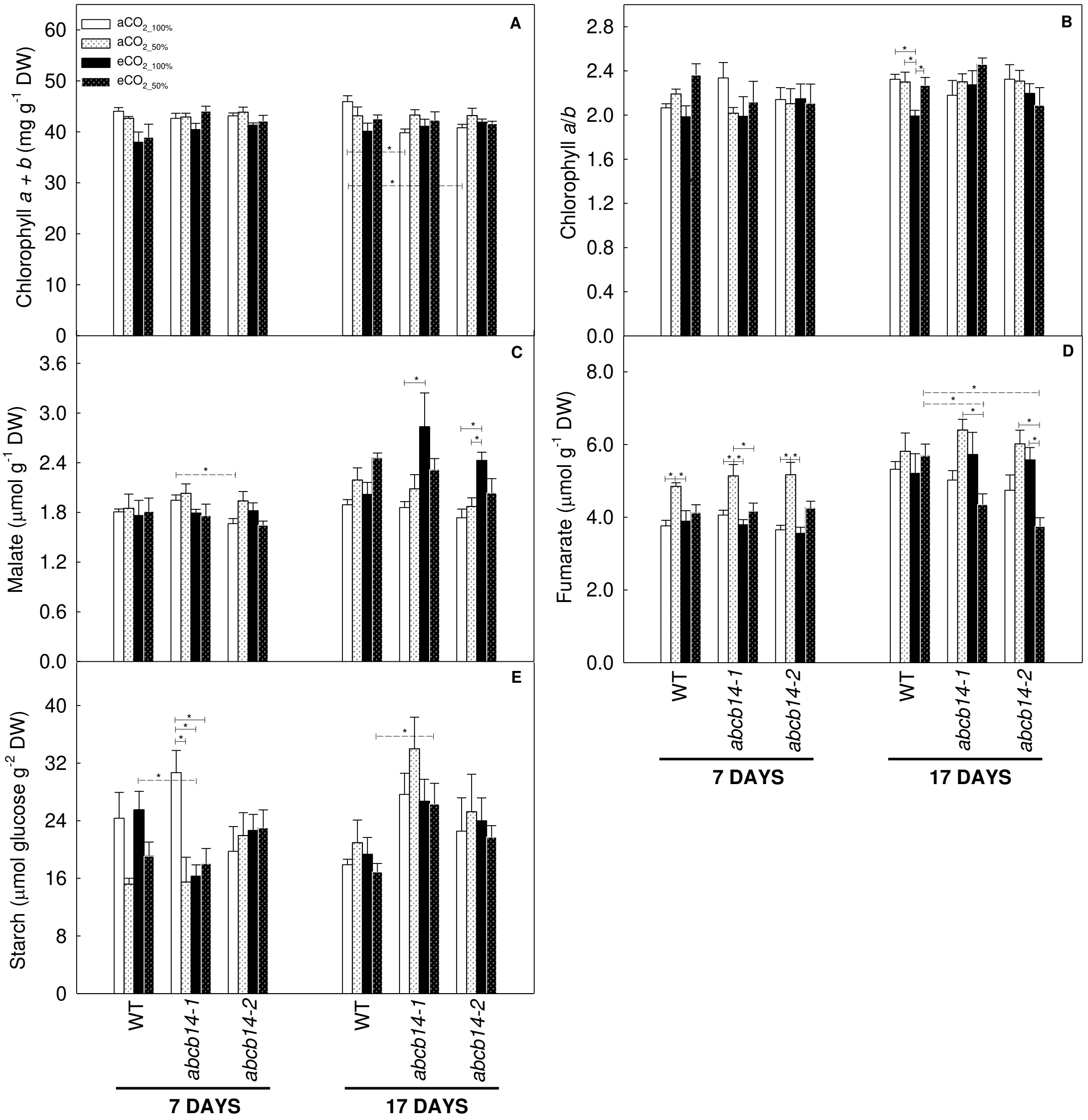

Supplemental Figure S5. Metabolic responses to a combination of water restriction under concentrations ambient and elevated of CO_2.Detail as in Figure 1. Values are presented as means ± SE (n = 5). Means followed by the same letter not differentiated by a one-way ANOVA followed by Tukey test between genotypes or treatments. Dashed line compares the three genotypes under the same treatment condition. Continuous line compares a genotype under different conditions. * indicates a significant difference (P<0.05).

Supplemental Table S2. Primers utilized to qRT-PCR

Gene	Locus	Efficiency	Sequence
Actina (control)	At2g37620	108.4	Forward 5' - CTTGCACCAAGCAGCATGAA - 3'
			Reverse 5' - CCGATCCAGACACTGTACTTCCTT - 3'
ABC14	At1g28010	113.35	Forward 5' - AGCTTTTCTACAGACCCGAATGCC - 3'
			Reverse 5' - TGCATCCAACAAGCAACTCCAATC - 3'
AHA1	At2g18960	103.89	Forward 5' - CTGGGAGGCTACCAAGCCA - 3'
			Reverse 5' - CTCACACCGAACTTGTCCGA - 3'
AHA2	At4g30190	107.49	Forward 5' - CCGGAGTCTTCCCAGGTT- 3'
			Reverse 5' - TTTAGAGCAGGGGCATCATT- 3'
AHA5	At2g24520	97.39	Forward 5' - GGCTGTTGCAAGACAGGAA - 3'
			Reverse 5' - CGGAGGATCAAAAAGAGGTAAA - 3'
AKT1	At2g26650	90.49	Forward 5' - ACATCCTTGTGAACGGAACC - 3'
			Reverse 5' - CCTCTCTCACAATGCTTTCTGTT - 3'
ALMT12	At4g17970	98.66	Forward 5' - CGGCAAAGTCCTTCGAGCTATC - 3'
			Reverse 5' - ATATAAGTAGCAGCCGCTCCAATG - 3'
ALMT6	At2g17470	140.83	Forward 5' - AGCCTCCACATGGACCTTACAG - 3'
			Reverse 5' - CGTTTCTCTGGAGCTGCCTGTATC - 3'
ALMT9	At3g18440	117.08	Forward 5' - TCTCTCAGAAATCCAGGCACCAG - 3'
			Reverse 5' - ACGCCCACTCTCTGAAGTTCTTG - 3'
BCA4	At1g70410	90.22	Forward 5' - TGGGTGAAGATAGGCGCATCAG - 3'
			Reverse 5' - AGCGATACGTTCACAGCTTCCTTC - 3'
GORK	At5g37500	102.21	Forward 5' - GCATCAATCCGCGCCAAGATT - 3'
			Reverse 5' - GTGGAGCAGCCTTTGAAGAGA - 3'
HT1	At1g62400	102.16	Forward 5' - AGTTTAAGTCCGAGGTTGCTCTGC - 3'
			Reverse 5' - CATTCGGAGGTTTCCTTGTGACA - 3'
KAT1	At5g46240	95.07	Forward 5' - AGCATGGGATGGGAAGAGTGGAG - 3'
			Reverse 5' - AGAGCAGTGTCGGAAGTCGGAT - 3'
KAT2	At4g18290	103.24	Forward 5' - TAGCTCGCTGTTTGCAAGG - 3'
			Reverse 5' - CAAACAGTGTCACCGAAATGA - 3'
KC1	At4g32650	115.09	Forward 5' - CTCAAGACATGAAAATGGACAGAT- 3'
			Reverse 5' - GAATCACCATTGTTTTTGTTATCTTG - 3'
NCED5	At1g30100	83.84	Forward 5' - ACGCCGTTACGTTGGAACTAGAAG - 3'
			Reverse 5' - AACATATCCGCCGAATTCACGAAA - 3'
OST1	At4g33950	157.15	Forward 5' - GACCCTGCAAAGAGGATATCAAT - 3'
			Reverse 5' - TTTGGCCCGGTTGATCCGATTC - 3'
RD29A	At5g52310	105.7	Forward 5' - TGGACAAAGCAATGAGCATGAGC - 3'
			Reverse 5' - AGGTTTACCTGTTACGCCTGGTG - 3'
RD29B	At5g52300	160.03	Forward 5' - ACTGATCCCACGCATAAAGGTG - 3'
			Reverse 5' - CTCGTCGGAAAGTCTTCTTCGC - 3'
RHC1	At4g22790	92.99	Forward 5' - TGCCTTGAATGGTGGTGCTACG - 3'
			Reverse 5' - AGCTTGCACCGGGTTTGGTAAC - 3'
SLAC1	At1g12480	118.71	Forward 5' - ATGGCCAATTCGACGGATGTTC - 3'
			Reverse 5' - ACCACGCCACTGAGAACTTAAATC - 3'
TPC1	At4g03560	86.45	Forward 5' - CGCTTGATATCGAAGAAAGCTC - 3'
			Reverse 5' - TCTCCAACACATATATCCAACCA - 3'

Supplemental Table S3. Relative abundance of primary metabolite levels in guard cell-enriched epidermal fragments from *abcb14-1* mutant plants in response to isolated or combination of water restriction and elevated [CO_2]. Data are normalized with respect to the mean response calculated for the wild-type (WT) growing under ambient and fully available water ($aCO_{2\_100\%}$). To allow statistical assessment, individual plants from this set were normalized in the same way. Detail as in Figure 1. Values are presented as means ± SE (n = 4-5).

METABOLITE	WT				*abcb14-1*			
	$aCO_{2\_100\%}$	$aCO_{2\_50\%}$	$eCO_{2\_100\%}$	$eCO_{2\_50\%}$	$aCO_{2\_100\%}$	$aCO_{2\_50\%}$	$eCO_{2\_100\%}$	$eCO_{2\_50\%}$
Threonine	1.00	0.93	1.54	1.21	0.61	1.20	1.29	1.50
Serine	1.00	0.94	1.81	1.11	0.82	1.27	1.50	1.61
Glucose	1.00	1.23	4.51	1.68	1.05	3.33	1.81	3.72
Mannitol	1.00	1.04	1.95	1.62	0.94	1.19	1.26	1.45
Rhamnose	1.00	1.27	4.54	4.78	0.83	3.13	3.65	4.81
Glycerol	1.00	0.73	2.84	0.82	0.90	1.37	1.18	1.16
Valine	1.00	1.09	1.91	0.87	0.84	1.17	1.08	0.92
Fructose	1.00	1.84	2.95	2.65	1.06	3.81	2.40	3.50
Succinate	1.00	1.23	1.42	1.40	0.90	1.81	1.60	1.59
Threonate	1.00	0.99	1.26	0.95	0.42	1.93	1.24	1.50
Inositol	1.00	1.30	2.62	0.87	0.46	2.89	1.26	2.10
Glutamine	1.00	1.35	2.19	0.72	0.44	2.47	0.67	1.82
GABA	1.00	1.47	1.73	0.86	0.79	1.71	1.06	1.35
Pyroglutamic acid	1.00	1.85	1.52	0.80	0.60	1.32	0.90	1.39
Methionine	1.00	1.03	1.19	1.17	0.86	0.90	0.95	1.07
Malate	1.00	1.58	1.03	1.60	0.76	1.80	1.03	2.84
Proline	1.00	1.78	1.36	3.15	0.93	2.91	1.31	4.56
Fumarate	1.00	1.48	1.24	1.31	0.75	2.12	2.07	3.55
Galactinol	1.00	3.93	0.80	3.48	1.34	3.47	1.19	2.46
Sucrose	1.00	1.03	0.44	0.71	0.91	0.90	0.70	0.71

Supplemental Table S4. Changes in relative transcript levels of genes involved in stomatal responses in *abcb14-1* mutant plants. Selected genes are associated with opening (O) or closing (X) stomatal responses. RNA was isolated from guard cell-enriched epidermal fragments isolated from 4-week-old plants from WT and *abcb14-1* mutant. Data are normalized with respect to the mean response calculated for the corresponding constitutively expressed *ACTIN* gene. In addition, data are normalized with respect to the mean response calculated for the corresponding WT of each growth condition. Detail as in Figure 1. Values are presented as means ± SE (n = 4-5).

GENE	WT				*abcb14-1*			
	aCO$_{2\_100\%}$	aCO$_{2\_50\%}$	eCO$_{2\_100\%}$	eCO$_{2\_50\%}$	aCO$_{2\_100\%}$	aCO$_{2\_50\%}$	eCO$_{2\_100\%}$	eCO$_{2\_50\%}$
AHA1	1.00	1.30	1.64	1.00	0.76	0.89	0.65	0.55
AHA2	1.00	**4.53**	**4.68**	2.26	1.82	2.53	1.96	1.93
ALMT12	1.00	0.96	**1.67**	1.36	1.40	0.78	0.63	0.82
HT1	1.00	0.81	1.96	0.74	1.18	1.65	0.43	0.67
AHA5	1.00	1.00	**1.98**	0.97	0.93	1.30	**0.59**	1.14
GORK	1.00	0.76	1.84	0.77	**0.58**	**3.03**	**0.29**	**0.56**
KAT2	1.00	0.55	0.91	0.81	**0.48**	0.61	**0.54**	**0.50**
OST1	1.00	0.57	0.40	0.35	0.51	0.54	0.14	0.40
NCED5	1.00	**2.36**	**0.72**	**2.85**	0.83	0.92	1.29	**3.32**
RD29A	1.00	1.69	0.58	**3.26**	0.67	1.37	0.78	**3.95**
ALMT9	1.00	1.30	1.07	1.07	**0.55**	0.90	0.74	1.87
AKT1	1.00	1.28	**0.49**	1.07	**0.50**	**0.69**	0.78	1.15
ALMT6	1.00	0.65	0.58	0.96	0.49	0.77	**0.22**	1.27
KC1	1.00	1.80	**0.47**	**2.43**	0.88	**0.52**	**0.55**	1.18
RD29B	1.00	**5.13**	0.49	**5.56**	0.53	0.69	1.17	2.18
SLAC1	1.00	**4.46**	1.64	0.62	0.63	2.02	**0.25**	0.26
RHC1	1.00	**3.97**	2.10	0.61	0.86	1.17	1.00	2.06
TPC1	1.00	2.03	1.14	1.41	0.75	1.14	1.15	1.36
CA4	1.00	1.28	0.58	0.63	0.83	**0.52**	**0.57**	0.89
KAT1	1.00	1.53	1.46	1.40	0.77	**1.91**	1.64	1.84

CHAPTER 3

GENERAL CONCLUSIONS

GENERAL CONCLUSIONS

Collectively the results of this study comprehensively increased our metabolic and molecular understanding of stomatal regulation in response to a future climate change scenario by using *slac1* and *abcb14* mutant plants which display opposite stomatal responses. Our results indicate that the constitutive increase of the stomatal opening observed in *slac-1* mutant plants is associated with an exquisite reorganization of primary metabolism, increasing mainly sugars, amino acids, and organic acids. Furthermore, it also represents another likely adaptive mechanism for maintaining the rate of respiration in guard cells of these mutant genotypes. Similarly, the reductions in a stomatal opening in plants with loss of functionality of the guard cell ABCB14 protein does not compromise overall photosynthetic activity and plant growth. We also observed that an exquisite metabolic and genetic regulations occur in guard cells in order to compensate, at least partially, the functional lack of ABCB14. When considered together, this most likely indicates a relatively minor influence of ABCB14 on the growth of Arabidopsis plants and supports the notion that there is redundancy among guard cell transporters in Arabidopsis. Together, the results presented here indicated that although manipulation of the stomatal function is a promising approach for crop yield improvement, the complexity of the interconnected networks governing stomatal movements under varying conditions still requires further investigation, particularly in field-grown crops.